Stable Locomotion Control of Bipedal Walking Robots: Synchronization with Neural Oscillators and Switching Control

by

Jianjuen J. Hu

E.E., Electrical Engineering and Computer Science (1998)
M.S., Electrical Engineering and Computer Science (1996)
M.S., Mechanical Engineering (1996)
Massachusetts Institute of Technology

Submitted to the Department of Electrical Engineering and Computer Science
in partial fulfillment of the requirements for the degree of

Doctor of Philosophy

at the

MASSCHUSETTS INSTITUTE OF TECHNOLOGY

September, 2000

Author.....
Department of Electrical Engineering and Computer Science
September 6, 2000

Certified by.....
Gill A. Pratt
Assistant Professor of Electrical Engineering and Computer Science, MIT
Thesis Supervisor

Accepted by.....
Arthur C. Smith
Chairman, Departmental Committee on Graduate Student

Stable Locomotion Control of Bipedal Walking Robots: Synchronization with Neural Oscillators and Switching Control

by

Jianjuen J. Hu

Submitted to the Department of Electrical Engineering and Computer Science
on September 6, 2000, in partial fulfillment of the
requirements for the degree of
Doctor of Philosophy

Abstract

Two novel approaches to stable legged locomotion control (neural-oscillator based control and switching control) are studied for achieving bipedal locomotion stability. Postural stability is realized by structural dynamics shaping, and gait stability is achieved by synchronization with neural oscillators and switching control.

A biologically inspired control with neural oscillators (central pattern generator, abbreviated as CPG) is used for global stable locomotion of bipeds based on a mutually inhibited neural oscillator model (Matsuoka, 1985). A systematic design approach is studied for the entrainment between the dynamics of neural oscillators and the natural dynamics of the plant (bipedal skeletal dynamics) in the neural oscillator driven rhythmic control. This design can guarantee global dynamic entrainment, bipedal gait stability and system robustness, which are explored and analyzed using nonlinear system theories.

The second control approach, called nonlinear switching control, is proposed to achieve stable locomotion control for a bipedal walking robot. This approach applies nonlinear switching control theory in the locomotion control system so as to ensure bipedal gait stability in the stable limit cycle sense. The switching surface is determined by means of the orbital contraction tuning technique. Both the structural dynamics stability and gait stability are analyzed. The convergence of the walking gait is proved based on nonlinear system theory.

Two common features for the above control approaches are that a global state machine based switching module and a closed-loop gait stabilization mechanism are used in both control systems. In neural oscillator driven locomotion control, the sensory feedback signals are switched according to the states of global state machine. However, in the switching control, the global state machine is used to select the appropriate control sub-systems in addition to a contraction tuning mechanism. In both approaches, an explicit closed-loop gait control mechanism is implemented to guarantee the bipedal gait stability.

Simulations of 2-D and 3-D bipedal walking robots demonstrate the effectiveness of the above locomotion control approaches. Different simulated experiments are given in the system analysis and evaluations. It has been shown that the above two bipedal locomotion control approaches can be further applied in the real-time control of bipedal walking robotic systems with proper locomotion stability and robustness.

Thesis Supervisor: Gill A. Pratt
Title: Assistant Professor of Electrical Engineering and Computer Science

Acknowledgements

I greatly acknowledge the support of my thesis advisor Professor Gill Pratt. Without his personal guidance and invaluable help, the study of this thesis would not be possible. He gave me freedom in choosing my interested research topics. The reported work represents an outcome of my research with his personal guidance and interaction, which reflects only partly the good memory of my four years' studying at the Leg Lab.

I would like to extend my special thanks to my thesis committee members, Professors Alex Megretski and Steve Massaguoi for their advices on the thesis. Alex has given me lots of help in the final stage of my thesis, particularly on the nonlinear system theory. I wish I could have had longer time in learning from him. Steve was a constant source in helping me to clarify my ambiguous concepts. The discussions between us were very constructive. I appreciate the precious time both of them spent in this summer serving as my committee members.

Jorge, as one of my new friends in LIDS, did teach me his new theory in Piece-wise Linear Analysis, which was quite useful while writing my thesis. His help and friendship were important support to this study.

Of course, I can never forget to thank my Leg Lab mates. I am indebted a lot to them. I will remember The Leg Lab in my lifetime. It was a fun place to stay and learn. Some of the lab mates have been my model colleagues at MIT. From them, I learned a lot. Thank you all. First, Jerry Pratt's help was priceless. Without his help in simulation and creature library, this thesis research could be much harder. I would like to thank Jerry Pratt, Allen Parseghian and Gregory Huang for proof reading my thesis draft. I also like to thank Dan Paluska, Peter Dilworth, Chee-Meng Chew, Hugh Herr, Olaf Bleck, David Robinson, Andreas Hoffman, Mike Wessler and the rest of lab members for their help and support during my staying at MIT. Former lab member, Dr. Robert Ringrose deserves the credit for setting up the creature library, which was the fundamental tool in my study.

I would like to thank my friend, Bruce Deffenbaugh. I am grateful for all his kind help he offered to me. His experience and knowledge beyond the academic areas are also tremendous resources and his encouragement was very important to my study and research. I appreciate the time he spent in correcting my English grammar and reading my papers and thesis through the years. Thank you.

Doctoral program was a long journey at MIT EECS Department. Professor George Verghese and Marilyn Pierce did give me many good advices and help in my study. I appreciate them very much.

Finally, I would like to thank my family members, my parents, my wife Sharon, my son Charles for their patience, full support and love. This thesis is dedicated to all my family members.

This research was supported in part by the Defense Advanced Research Projects Agency under contract number N39998-00-C-0656 and the National Science Foundation under contract numbers IBN-9873478 and IIS-9733740.

Contents

Chapter 1

Introduction

1.1 Study of Bipedal Walking Robot Systems

Engineers and scientists in the robotics field have been working on legged machines for decades [Todd (1985), Raibert (1986)]. There are two main reasons for studying legged robots: understanding the locomotion system of the biological counterparts and building walking machines for travel on rough terrain where existing wheeled vehicles cannot go.

There are a lot of potential applications for legged robots. Some day legged robots may explore Mars. Legged tanks may be able to maneuver in areas previously inaccessible to the current treaded variety. Scrambling robot soldiers may maneuver better than wheeled vehicles in urban landscapes designed for bipedal people. Walking robots may explore the bottoms of oceans. Bipedal robots of human dimensions will maneuver in the same areas as people. Artificial robotic legs may enable people with paralyzed or missing legs to walk and run.

Among legged walking machines, bipedal robots that mimic the bipedal animals represent an important locomotion system. Today, some researchers are focusing on understanding how bipedal animals walk, while others are trying to design physical systems to achieve certain walking tasks. In addition, a complete walking robot system should be integrated with almost all the technologies available in robotics, such as vision, arms, and navigation. Compared with other robotic branches, leg locomotion is in need of the most significant developments.

Many bipedal walking robots have been built since 1974, when the first powered biped was born [Kato (1974)]. Table 1-1 shows a list of major bipedal walking robots and their key technologies. Most of them were built for studying locomotion generation. The Honda humanoid robot [Hirai et al (1998)], which represents the state-of-the-arts in bipedal robotics, is integrated with modern technologies for vision, robot arms, remote control, and leg locomotion, and requires forty engineers ten years and tens of millions dollars to build [Menzel and D'Aluisio (2000)].

In general, research on bipedal walking robot systems can be classified as 1) physical-structure design and actuation, 2) locomotion control, 3) advanced performance enhancement and exploration of systematic behaviors.

- *Physical structure design and actuation*
  Research in this phase requires knowledge of the robot architecture, mechanical design skills, an understanding of dynamics, and proper actuation. It is now widely

acepted that the minimum number of joints for a bipedal walking robot with complete set of joints (in hip, knee and ankle) is 6 for a planar biped (*Spring Flamingo* etc.) and 12 for a 3-D biped (Honda robot *P3* and MIT *M2* etc.). Different types of actuators can be chosen for a given robot system, such as electrical actuators [Pratt 1995, Honda 1996], hydraulic actuators [Kato (1974)], and pneumatic actuators [Dunn & Howe (1994), Robinson (2000)].

- *Locomotion control*
  A bipedal locomotion control system is responsible for stable walking in a given environment. It should be capable of starting, stopping, and walking with variable speeds. Proper posture and stable walking gait are essential.

- *Advanced performance enhancement and exploration of system behaviors*
  Research in this phase targets complex walking tasks. High-level control involving vision feedback and navigation is studied in this stage. The Honda robot [Hirai (1998)], in which arms, vision and remote control are integrated with the legged lower body for possible complex tasks, is an example.

Table 1-1: Historical events of bipedal walking robot systems

When	Who	What
1974	Kato, Waseda Univ.	Wabot, a hydraulically powered biped with 11 d.o.f.
1984	Miura & Shimoyana, Tokyo Univ.	BIPER-4, Electrically powered biped with 7 d.o.f.
1985	Takanish et al, Waseda Univ.	WL-10RD, Electric actuators with 12 d.o.f.
1990	McGeer, Canada	Passive Walker, no actuators, 2-D
1990	Yuan F. Zheng et al, Ohio State Univ.	SD-2, Electrically powerd biped with 4 d.o.f.
1994	Dunn & Howe, Harvard Univ.	Timmy, 4 d.o.f. 2-D biped with electric actuators and pneumatic actuators.
1995	Kajita & Tani, Tsukuba, Japan	Meltran II, DC motor actuators with 6 d.o.f.
1996	Honda Motor Company	P2, a 12 d.o.f. biped with electric actuators. It has arms, head with vision, remote control
1996	Kun & Thomas, New Hampshire Univ.	Toddler, a 10 d.o.f. biped with DC motor actuators
1997	Pratt, MIT Leg Lab.	Spring Flamingo, a 2-D 6 d.o.f. biped with electrical actuators

This thesis concentrates on bipedal locomotion control. Our primary interest in bipedal locomotion control concerns the correct methodology for the control of "complex systems". It is difficult to provide a precise definition for this term; by "complex systems" we mean a system that has an intractable state space and severe nonlinearity. An intractable state space preludes the use of classic analytical analysis for control systems,

which are only suitable for problems of manageable scale. At the same time, methods of traditional linear control, which are applicable even when the state spaces are large, are ruled out by severe nonlinearity.

For a complex system like a bipedal robot, there are a few possible ways to achieve proper bipedal locomotion control: 1) control with model simplification, 2) control with distributed local controllers, or 3) complete model-free control assisted with efficient learning mechanisms. In this thesis the first two strategies are utilized.

- Control with a simplified dynamic model: by capturing the major features of the bipedal dynamics in different walking phases, a simplified model reduces the control complexity in practice and turns the original control problem into a new problem with lower order. However, there is always a trade-off between the degree of simplification and the system performance. It is not always true that the simpler, the better.
- Distributed local control: an overall self-organizing mechanism on top of the local controllers is required for local control. Neural oscillator control and trajectory control are two examples in this category. The former has a closed-loop self-organization mechanism, and the latter has the coordination moderated in the trajectory planning process.
- Model-free control with learning capability: The control complexity is shifted to the learning process. Complete model-free control approaches require a tremendous amount of learning time, which is usually impossible for real-time implementations.

1.2 Difficulties in Achieving Stable Bipedal Walking

Although stable bipedal locomotion is a difficult control task, it has been a research goal for about a century. Many successful attempts have been made so far. However, due to the difficulties in actuation and control, the robots developed thus far can execute some simple tasks, but their performance is still far below the level of their biological counterparts. Table 1-2 lists the difficulties in the research of bipedal walking robot.

Besides the difficulty in hardware, the extent of control difficulty is illustrated by the limited progress gained in bipedal control systems. A few approaches have been studied extensively in the bipedal walking robot area. The first approach, trajectory control, was used successfully in Honda's robot, where necessary modifications were made to the control on-line. Distributed local control and simplified dynamics based control approaches are also efficient ways to control biped walking. In the early days, the major goal of researchers was initially to understand how to generate bipedal locomotion with physical robotic systems, where system stability was partially achieved through some local adjustments inside the control systems.

The dynamics of bipedal locomotion is indeed difficult. The nonlinear dynamics, high dimensional dynamic state space, time variations, and impulse disturbances from environments (like ground contacts) make direct application of modern control theory extremely difficult. For example, a biped experiences two different dynamics phases (single support phase and double support phase) alternatively. In single support, the

biped dynamics are unstable and not entirely reachable (or controllable in a linearized form); in double support state, however the dynamics are constrained with redundant structures and fully controllable and stable. In order to achieve stable waling, the control method must merge the two alternatively changing walking phases together and stabilizes the walking sequences.

Table 1-2: Difficulties in the research of bipedal walking robot

Key Technologies	Difficulties in Research
Actuator	Limited bandwidth and transmission constraints
Robot structure	Rigid body, no flexibility
Sensory system	Limited sensory information used, i.e. velocity, position, force
Control system	Nonlinear, high dimensional, time varying dynamics; Not fully actuated in ankle joints

In practice, researchers usually mix the locomotion generation task with the locomotion stabilization process, which makes the control system very difficult to implement and makes the control problem ill-posed (i.e. not well defined in a standard framework). Separating the task into two steps (as shown in Figure 1-1) and conquering them separately maybe a better strategy.

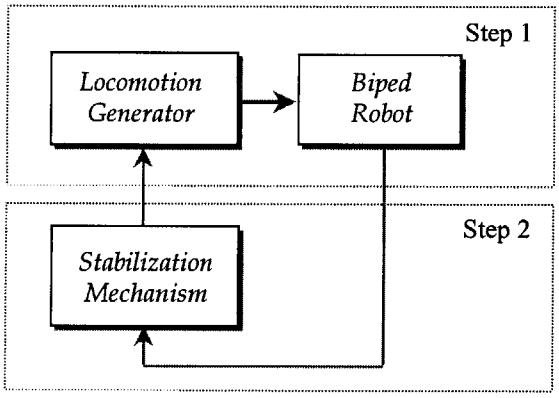

Figure 1-1: Bipedal locomotion control task decomposition

1.3 Closed-loop Locomotion Control

Feedback closed-loop control thrived in the 20th century, starting with Norbert Wiener's cybernetic study of control system mechanisms [Wiener 1948]. It has been clearly demonstrated that closed-loop control is better than open loop control not only in control accuracy but also in the robustness built into the closed-loop, which is capable of rejecting any noises and disturbances in the loop.

The same is true for bipedal locomotion control system. It has been observed that a bipedal walking robot controlled by distributed local controllers can walk stably under certain conditions if the control parameters are tuned well, which means that a good open

loop control system is made. However, the biped may fall down when disturbances occur or walking conditions change. This may be the reason why successful live demonstration of stable bipedal walking is so difficult to assure.

Limited success has been achieved in a number of bipedal walking robots, such as the Honda humanoid robot, Spring Flamingo and WABIAN etc. In those systems, local reactive control schemes are added to the control systems for enhancing the gait stability. Goswami et al (1996) demonstrated that with necessary additional control adjustments, a passive biped could achieve a stable gait, indicating that a closed-loop gait control mechanism can enhance bipedal locomotion stability.

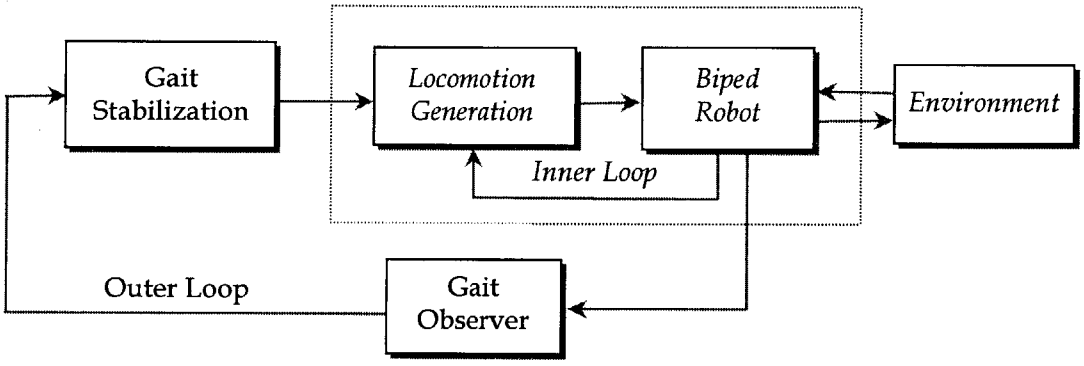

Figure 1-2: Diagram for closed-loop gait control of a bipedal walking robot.

Figure 1-2 shows a general closed-loop gait control system structure for stable bipedal walking control. In the inner loop, the structure dynamics are controlled so that postural stability is reached. In addition, the basic bipedal locomotion should be generated in the inner control loop using either distributed local control or overall trajectory control. The outer loop, i.e. the closed-loop, gait control is designed such that the gait stability is realized.

1.4 Approaches

Two control approaches are developed in the thesis: neural oscillator driven control and switching control. Both control approaches have an explicit closed-loop gait control in the system framework, which is intended to stabilize the bipedal locomotion.

1.4.1 Control with Neural Oscillators

With neural oscillators, the bipedal locomotion is generated by the oscillator outputs and the local impedance controllers and stabilized through the entrainment between the neural dynamics and the biped skeletal dynamics. The architecture of the neural oscillator modules and appropriate implementation of local joint control are crucial in the system.

There is no general framework or systematic control guidelines available to ensure the entrainment will take place. Therefore, the conditions of entrainment for essential neural oscillator modules, how to select sensory information to feedback to the neural oscillators, and how to establish locomotion, are important issues, and are investigated in this thesis.

Neural oscillator driven bipedal locomotion control is different from other applications of neural oscillators, such as arm control, where the dynamics are fixed and direct entrainment of neuro-dynamics and plant natural dynamics is easier to achieve [Williamson (199b)]. However, in the case of bipedal locomotion control, the neural oscillator control system is responsible for generating locomotion and stabilization as well. The dynamics changes in bipedal walking not only make the dynamic analysis difficult but also make the entrainment difficult to achieve.

This thesis starts from the fundamental analysis of a neural oscillator module (modified from Matsuoka's oscillator model) and a general rhythmic control system. A compensator based neural oscillator control scheme is proposed for general rhythmic motion control. A distributed neural oscillator network is formed, and the entrainment of neuro-dynamics and natural skeletal dynamics is demonstrated by means of a simulated bipedal walking robot.

Figure 1-3 shows a general structure for such a control system with closed-loop gait control. The details of the realization of the components described in the diagram (Figure 1-3) can be found in Chapter 6. In this system structure, the basic legged locomotion is generated by means of rhythmic controllers and local impedance control. The former governs the rhythmic motion, and the latter controls the robot posture. Closed-loop gait control is achieved through the sensory feedback and the entrainment of the neural dynamics and robot skeletal dynamics.

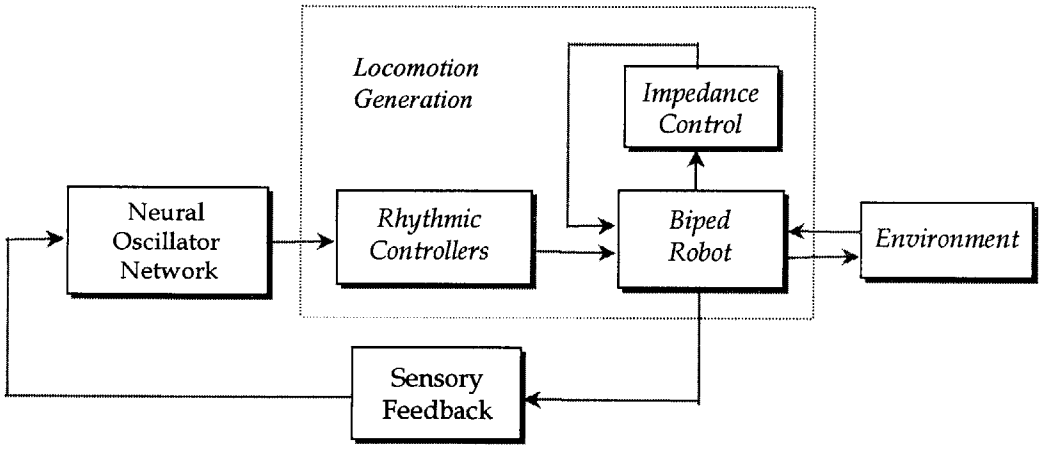

Figure 1-3: Neural oscillator based closed-loop control.

1.4.2 Switching Control

The second active locomotion control approach, i.e. nonlinear switching control, is Motivated by the switching nature of structural dynamics. It can be used to achieve gait stability. In this control approach, we used different control sub-systems for the double support and single support phases. An orbital contraction tuning technique is used to choose the state dependent switching surfaces. Using nonlinear control theory we prove that, with an appropriate switching control mechanism, stable rhythmic motion (or periodic gait stability) can be achieved by means of switching between stable local dynamics and unstable local dynamics.

With the switching control approach, the control target is divided into two parts: constructing bipedal locomotion with local controllers and stabilizing the bipedal locomotion. Separate local controllers are designed for the double support phase and the single support phase, and an outer closed-loop gait control is added to the system for stabilizing overall bipedal locomotion. This control approach is analyzed with nonlinear theory and the gait stability is proved by means of limit cycle analysis.

In the nonlinear switching control approach, the switching techniques are used to select control sub-systems and to realize the global synchronization of sub-dynamics. The switching modules are in the outer closed-loop (for the switching control approach). Figure 1-4 shows such a general closed loop gait control mechanism.

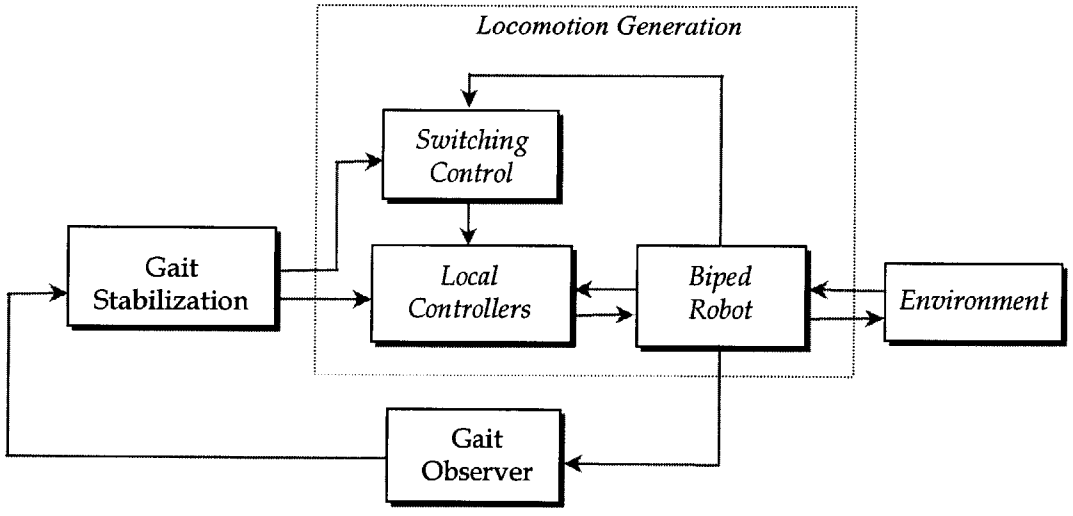

Figure 1-4: Closed-loop gait control with switching module.

1.5 Simulated Systems

To evaluate the experimental control performance of the two approaches, two bipedal robots are simulated. Different control approaches are applied in each robot. The robotic simulations are implemented using the Creature Library, a software package developed at the MIT Leg Lab, and based on the SD-FAST product of Symbolic Dynamics. Figure 1-5 shows the real robots and Figure 1-6 shows the simulated robots.

The first simulated robot is the simulation of an existing physical robot called *Spring Flamingo*, built by Jerry Pratt (Leg Lab., MIT) [Menzel and D'Aluisio (2000)]. This planar robot is constrained to the sagittal plane, i.e., no lateral motion is allowed. It has seven links: thigh, shin, and foot in each leg and a body link. There are six joint actuators for the hip, knee, and ankle in each leg. The robot has a height of 1.2 m and a weight of about 14 kg.

The second robot simulated is based on another 3-D bipedal walking robot, *M2*, which was assembled in the Spring of 2000 and is currently undergoing development of its control algorithms. M2 has a total of 12 degrees-of-freedom (d.o.f.): three d.o.f. at the hip joint (pitch, roll, yaw), one at the knee joint (pitch) and two at the ankle joint (pitch and roll) in each leg. It has a height of 1.5m and a weight of about 27 kg.

Both bipedal robots are designed mainly for studying bipedal locomotion control algorithms. There are no vision systems or arms on either robot. Hence the motion of the upper body is not included, and only blind walking is considered. A series of experiments are simulated for investigating legged locomotion stability and robustness under the new control approaches.

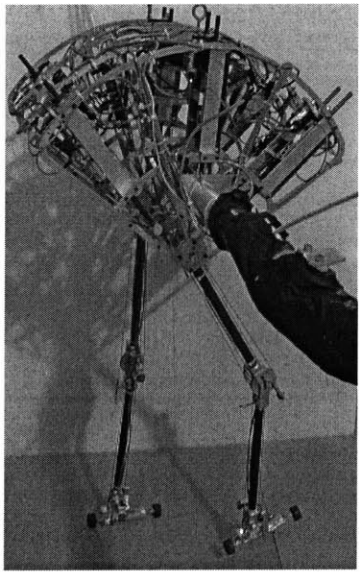

Spring Flamingo
(Courtesy of Jerry Pratt)

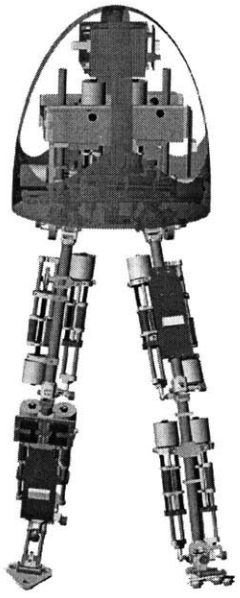

M2
(Courtesy of Daniel Paluska)

Figure 1-5: Bipedal Walking Robots: A planar biped, *Spring Flamingo*, on the left; a 3-D biped, *M2*, on the right.

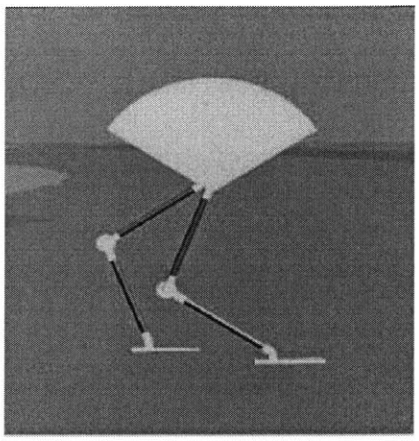

Simulated *Spring Flamingo*

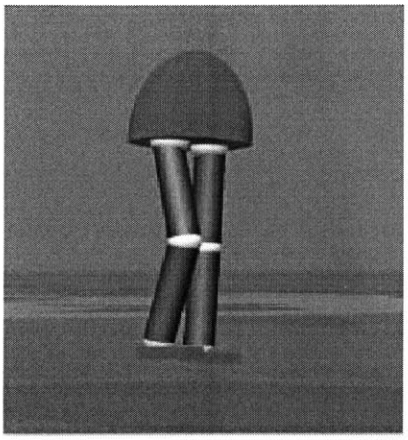

Simulated *M2*

Figure 1-4: Simulated robots: *Spring Flamingo*, on the left; Simulated *M2* on the right.

1.6 Thesis contributions

This thesis focuses on stable locomotion control of bipedal walking robots. The following contributions are made in stable bipedal locomotion control: 1) the stability and robustness of bipedal locomotion is studied with system theory, and 2) a few mechanisms are developed to achieve stable bipedal control.

The significance of this thesis is that the two control approaches developed will contribute to the understanding of bipedal locomotion and motor-sensory control, and also they can provide systematic control schemes for walking robotic system, in which the control design process is simplified.

(a) Neural oscillator based locomotion control. A design method for neural oscillators based locomotion control is developed with local dynamics shaping and appropriate sensory feedback. This is realized as a global state based switching scheme. A systematic analysis of neuro-skeletal dynamics in a bipedal walking robot is provided. The intrinsic robustness of neural dynamics is achieved by means of the dynamics entrainment in bipedal robots.

(b) Nonlinear switching control. A contraction tuning based switching control approach can achieve gait stability for a bipedal walking robot. The proof of the existence of a limit cycle is provided by means of nonlinear system theory, contraction control.

(c) Control applications in a simulated planar bipedal walking robot, *Spring Flamingo* and a 3-D biped, M2. Both neural-oscillator control and switching control approaches are applied in the simulated biped, *Spring Flamingo*. The switching control is also applied in the 3-D biped, *M2* in a task of stepping in place.

(d) Analytic tools have been applied to help the control design and analysis.

1.7 Organization of the Thesis

This rest of thesis is organized as follows: Chapter 2 reviews the methods previously developed for bipedal locomotion control, such as simplified model based control, passive dynamic control, trajectory planning based control, and biologically inspired control approach. A new concept of closed-loop gait control is proposed in this chapter. In Chapter 3, mathematical background for nonlinear system analysis is introduced. Preliminary theories, like linearization, limit cycle, piece-wise linear analysis, Poincar'e map, and orbital contraction theory are described. Chapter 4 defines stability and robustness in bipedal locomotion control and describes the guidelines for the control system design in the thesis. Dynamic models are introduced, and the controllability and observability are analyzed in this chapter. Chapter 5 presents and compares a few oscillator models. With Matsuoka's neural oscillator model, the general entrainment conditions for rhythmic motion control are discussed. Chapter 6 extends the study of neural oscillator control to bipedal locomotion. One global variable based switching scheme is proposed for the sensory information feedback during the entrainment process of the bipedal locomotion. Chapter 7 proposes a nonlinear switching control method for achieving stable bipedal walking. The proof of existence of a limit cycle is provided in this chapter. Chapter 8 describes the applications of switching control to 3-D bipedal walking robots. Methods for dealing with frontal plane dynamics and the synchronization of frontal dynamics and sagittal dynamics are given. The simulation results for a 3-D bipedal robot, M2, are presented. Chapter 9 summarizes the research in the thesis. A few discussions are also presented for further improvements. The perspectives of the future study in both neuro-dynamics of the bipedal walking robots and the switching control are described briefly.

Chapter 2

Review of Bipedal Locomotion Control

This chapter is devoted to a literature review of studies on bipedal locomotion control. Several main control approaches used in the past are reviewed and discussed, and the current status of bipedal locomotion control is addressed.

2.1 Control with Simplified Models

Since biped mechanical systems usually have high order and nonlinear, complex dynamics, it is a very hard task to design controllers for the joint actuators with full consideration of the entire biped system dynamics. In addition, from a mechanical point of view, a biped robot is inherently unstable because the center of mass extends beyond the base of support most of the time during walking.

For such a complex system, the control engineers' dilemma is how to make a suitable trade-off between the simplification of the system model and control precision. In walking machine design, there are two different approaches to controller design in current use. One approach is to design effective controllers based on some approximation of the dynamics of the bipedal mechanical system. The other approach, called model-free control design in this thesis, aims to make use of the control engineer's experience, intuition, as well as several learning techniques [Pratt (1996), Murakami (1995), Miller (1994), Hu (1998)].

One of the common features of the control approaches developed by researchers is that controllers of bipeds were designed based on approximations of the bipedal mechanical system. In the early days of 1970s, the simplest model used for the study of some of the characteristics of human walking was the inverted pendulum model. For example, Hemami et al used the inverted pendulum model to investigate biped stability in 1977 [Golliday & Hemami (1977)]. For control design, Golliday and Hemami used state feedback to decouple the high-order system of a biped into independent low-order subsystems. More complex models with more degrees of freedom were used mainly after 1980 for a more complete study of human walking (or other bipedal animals) as well as for the actual construction of biped robotic systems. Miyazaki and Arimoto (1980) used a singular perturbation technique and showed that bipedal locomotion can be divided into two modes, a fast mode and a slow mode, thus simplifying the controller design. Furusho

and Masubuchi (1987) derived a reduced order model as a dominant subsystem that approximates the original high-order model very well by applying local feedback control to each joint of a biped robot. Raibert (1986) used symmetry to analyze hopping robots controlled using "three part control". Miura and Shimoyama (1984) linearized the biped dynamics and designed stable controllers by means of linear feedback. Kajita and Tani (1995) developed their 6 d.o.f. bipedal robot "Meltran II" using a "Linear Inverted Pendulum Mode" successfully. In the above research, the dynamics of the biped robots were simplified so as to utilize the existing modern control theory in the controller design.

In contrast, the model-free control approach does not incorporate the complex intrinsic dynamics of the biped robot system in the controller design. This type of approach avoids dealing with the complex dynamics directly and, instead, tries to incorporate the control engineer's intuition, experience, and knowledge into the control system design. Pratt (1996, 1997) developed virtual model control, by which one can achieve good control capability for bipedal walking robots through appropriate choice of virtual components in virtual space. In addition, other researchers have made good progress in control of biped robots by means of learning techniques such as reinforcement learning [Benbrahim (1997), Chew (2000)] and neural network control (Miller 1994, Hu 1998, 1999). For robustness and adaptation enhancement, Radial Basis Function neural networks, CMAC neural networks and Multi-Layer Perceptrons with back propagation successfully improved the performance of bipedal walking in gait control [Salatian & Zheng (1992)], dynamics compensation [Hu (1998b)] and posture balance [Miller (1994)].

2.2 Passive Dynamic Walking

Studies of passive dynamic walking demonstrated the physical nature of bipedal locomotion with simplified mechanical structure. These studies gave insight into how powered bipedal walking robots can be improved in terms of energy efficiency and control stability [McGeer (1990), Goswami (1996), Van der linde (1999), Kuo (1999)]. McGeer (1990), a pioneer in passive bipedal walking, explored the important features of passive bipeds. His simple kneeless passive biped robot, which moved passively on an inclined plane, attained a stable periodic motion, following a linearized mathematical model.

With a simplified bipedal dynamic model, Goswami (1996) analyzed and demonstrated numerically that gait stability for a passive walking robot can be achieved in terms of a limit cycle with some control adjustments. Similarly, Van der Linde (1999) demonstrated that a limit cycle can be constructed by means of a simple passive parameter adjustment in the structure. In their analysis, both researchers assumed a special case, in which the robot only experiences single support states. The work in Kuo's group presented a simple control scheme in stabilizing the lateral dynamics of a 3-D passive biped model.

The above studies on passive walking inspired the idea of an active switching control approach for the powered robot in this thesis. An explicit closed loop control scheme is proposed to achieve bipedal gait stability in the limit cycle sense, which is described in Chapter 7.

2.3 Trajectory Planning Based Control

Trajectory planning based control was an early approach to bipedal locomotion control which started in 1980s (Vukobratovic, 1990). Basically this approach assumed that the nominal trajectories of the joints are well generated for proper bipedal locomotion. Then the control task was simplified in a multi-input-multi-output (MIMO) control framework so that some modern control theory can be applied with further manipulations.

However this approach does not work successfully in practice for two reasons. First, the real dynamics are changing, and controller designs based on the nominal dynamics would have degraded performance when interacting with the environment. Second, this is open-loop control only. Real-time modifications are needed in order for this approach to succeed in a practical robot.

Honda's robots used this approach enhanced with Zero-moment-point (ZMP) modifications of the nominal trajectories, recorded from human walking. The control approach used in the Honda Humanoid robots is called a 'play-back' approach in the robotics field. Pre-recorded data is also used in Waseda univeristy's humanoid robot, WABIAN. Again the control is augmented with the ZMP approach. These robots achieved some success in stable walking. However, in the above robot systems, there is no explicit closed loop control mechanism for gait stability. Local modifications to the trajectories turned out to be an indirect adjustment, but not to guarantee stability. A stronger control mechanism is needed for stable walking.

2.4 Biologically Inspired Control Approach

A biologically inspired locomotion control approach, neural oscillator driven control, is now drawing the attention of researchers in bipedal walking with the promise of enhancing locomotion stability and robustness and reducing the difficulty of tuning system parameters. About two decades ago, biologists found evidence that both reactive control and central pattern generators exist in vertebrates, and the feedback loop that generates the motor patterns is closed by internal state variables and is interacted with the environment [Grillner (1976,1985)]. The lower level dynamic control is governed by the neural circuits in the spinal cord rather than in the brain. But these spinal cord neural circuits are also affected by inputs from higher level control systems. Katoh et al (1984) began applying stable limit cycles in bipedal locomotion. In studies of neural pattern generators, Matsuoka's mutually inhibited oscillators [Matsuoka (1985)] and Bay and Hemami's coupled nonlinear oscillators [Bay & Hemami (1987)] are two typical models from the 1980s. Based on Matsuoka's model, Taga (1995) studied the entrainment between the dynamics of a group of neural oscillators and investigated the rhythmic movements of a simulated musculo-skeletal system. Recently, Miyakoshi et al (1998) attempted to apply the neural oscillator approach to control the stepping motions of a simulated bipedal robot.

The approach used in the simulated human walking control by Taga (1995) is a biologically inspired control approach, which constructs the system synergy for a bipedal walking robot based on the biological motor-sensory control theory. Taga (1995) has

addressed this in his neural oscillator driven humanoid-legged locomotion simulations. With neural oscillators one can generate a nonlinear limit cycle oscillation process to accomplish bipedal walking [Miyakoshi (1998)].

The sensory feedback provides a closed-loop control for achieving the overall gait stability of the bipedal locomotion. Carefully selected sensory feedback signals are input to the neural oscillators, and the entrainment between the neural dynamics and the skeletal dynamics makes the bipedal gait stabilized in the sense of limit cycle.

To date, most research on the neural oscillator approach has focused on the neural oscillator models and simulation results. Yet, theoretical studies on how to systematically design locomotion control using neural oscillator models have not appeared, and a mechanical bipedal walking robot using neural oscillator models has not been produced. This thesis develops a neural oscillator driven control system for a bipedal walking robot.

2.5 Stabilizing Bipedal Locomotion

An important goal of bipedal locomotion is the control of a biped to achieve stable walking. The concept of system stability from conventional control theory needs to be extended in bipedal locomotion control since the desired tracking is no longer the primary control goal. To realize natural bipedal walking, a biped should not fall down, and it should walk at a stable pace. In other words, stable postural control and stable gait control should be achieved. Many researchers have studied postural control and how a stable posture can be realized. Zero Moment Point (ZMP) has become an important and useful criterion for postural stability in walking robot control. The ZMP control approach has been used to monitor postural stability during walking trajectory planning or trajectory modifications, as with the Honda humanoid robots [Hirai (1998), Ozawa (1995)] and the WABIAN robots [Yamaguchi (1999)]. On the other hand, stable periodic walking gait control was not the focus in the past years, and the systematic study of this topic is hardly found in the literature on biped control. Without an embedded mechanism to ensure gait stability, the biped may lose its walking pace or exhibit chaotic behavior when it encounters disturbances from environments. A few researchers have addressed this topic in passive walking [Goswami (1996), Van der Linde (1999)]. The majority of studies on gait control were on gait modification and implementation with different terrains [Kun & Miller (1999), Salatian & Zheng (1992)].

Gait stability is crucial for the global stability of locomotion. If the walking gait diverges or is not stabilized, bipedal walking will break down and stable locomotion will be lost. In his study of gait stability, Vukobratovic (1973, 1990) proposed a repeatability condition that is required for the stability of a periodic gait.

A closed-loop control system may enhance gait stability. Two such control systems, neural oscillator control and switching control, are described in Chapters 6 and 7, respectively.

2.6 Summary

In the above sections, previous locomotion control approaches are reviewed. As two of the most widely studied approaches, simplified dynamics model based control and trajectory planning based control, represent the early locomotion control research, which played an important role in bipedal locomotion study. Both approaches were used in control of the biped prototypes developed in 1980s and 1990s.

Passive dynamic walking helped researchers in understanding the necessary fundamental dynamic mechanism that is required for bipedal locomotion, which simplified the dynamics analysis and gave a lower bound in terms of energy consumption. The results in passive walking can help researchers in improving robot structure design and enhance powered robot control.

The neural oscillators driven control approach provides an elegant system control paradigm. It potentially has broad system capabilities, but further developments and studies are required in order to discover efficient mechanisms and to provide better analysis of its system behaviors.

A closed-loop gait stabilization approach is proposed in this chapter for the purpose of achieving stable locomotion. Two system frameworks are presented: neural oscillator driven control and switching control, which are rational options in control viewpoints. The use of these frameworks for control of bipedal walking, as presented in Chapters 6 and 7, is the major contributions of this thesis.

Chapter 3

Analysis of Nonlinear Systems

This chapter presents the necessary mathematics background for this thesis, including the linearization of nonlinear systems, orbital contraction, piece-wise linear analysis and the Poincare map. We will utilize these tools to analyze the control of the complex, nonlinear dynamics of bipedal robots. Additional references on these topics can be found in the literature [(Khalil (1996), Guckenheimer (1983), Hayashi (1985), Vidyasagar (1993)].

3.1 Linearization of Nonlinear Systems

3.1.1 Nonlinear dynamic systems

Consider a physical system with state variable x and input variable u defined as,

$$x(t) = \begin{pmatrix} x_1(t) & x_2(t) & \cdots & x_n(t) \end{pmatrix}^T,\ x \in \mathbb{R}^n.$$
$$u(t) = \begin{pmatrix} u_1(t) & u_2(t) & \cdots & u_p(t) \end{pmatrix}^T,\ u \in \mathbb{R}^p$$

We assume the system's behavior can be characterized by the coupled first-order ordinary differential equations

$$\dot{x}_i = f_i(x,u,t) \quad i = 1,2,\cdots,n \tag{3-1}$$

where $\dot{x}_i$ denotes the derivative of x_i with respect to the time variable t. The system starts at time $t = t_0$ with initial state $x(t_0)$. The system output equation is:

$$y = h(x,u,t) \tag{3-2}$$

which defines a q-dimensional output vector comprised of variables of particular interest in the analysis of the dynamic system, such as, variables which can be physically measured. Equations (3-1) and (3-2) are called the *state-space model* of the system. In general, $f = \begin{pmatrix} f_1 & f_2 & \cdots & f_n \end{pmatrix}^T$ and h are nonlinear functions of the state variable x and input u.

In a closed-loop system, a control law $u(t) = g(x(t),t)$ is chosen. Thus, the closed-loop dynamics can be written as

$$\dot{x} = f(x,t)\,. \tag{3-3}$$

A special case of (3-3) is when the function f does not depend explicitly on t, that is,

$$\dot{x} = f(x) \tag{3-4}$$

In this case, the system is said to be *autonomous* or *time-invariant.*

3.1.2 Equilibrium points

An *equilibrium point,* or *stationary solution* to a dynamic system, is a very important concept for analysis of the local properties of a nonlinear dynamic system. A point x^* in the state space is said to be an equilibrium point of (3-4) if it satisfies the equation $f(x^*) = 0$. An equilibrium point can be isolated (that is, there are no other equilibrium points in its vicinity) or can be part of a continuum of equilibrium points [Dahleh (1996)].

Equilibrium points can be characterized as stable, unstable, or asymptotically stable in the sense of Lyapunov (i.s.L.).

Definition 3.1 The equilibrium point x^* of (3-4) is

- *stable i.s.L.* if, for each $\varepsilon > 0$, there is a $\delta = \delta(\varepsilon) > 0$ such that

$$\| x(0) - x^* \| < \delta \;\Rightarrow\; \| x(t) - x^* \| < \varepsilon \;,\; \forall t \geq 0$$

- un*stable* if it is not stable;
- *asymptotically stable i.s.L.* if it is stable, and δ can be chosen such that

$$\| x(0) - x^* \| < \delta \;\Rightarrow\; \lim_{t\to\infty} x(t) = x^*$$

- globally *asymptotically stable i.s.L.* if it is stable and, for any $x(0)$,

$$\lim_{t\to\infty} x(t) = x^*$$

3.1.3 Linearization

Suppose we have an equilibrium point or an operating point $\bar{x}$ for the nonlinear system (3-4), such that $f(\bar{x}) = 0$. By linearizing (3-4) we can characterize the system behavior or the solutions near $\bar{x}$. The linearized system is expressed as

$$\dot{\tilde{x}} = Df(\bar{x})\tilde{x}\,,\; \tilde{x} \in \mathbb{R}^n \tag{3-5}$$

where $Df = [\partial f_i / \partial x_j]$ is the Jacobian matrix of first partial derivatives of the function $f = \begin{pmatrix} f_1 & f_2 & \cdots & f_n \end{pmatrix}^T$, and $x = \bar{x} + \tilde{x}$, $|\tilde{x}| << 1$. In particular, the linearized flow map $D\Phi_t(\bar{x})\tilde{x}$ at a fixed point $\bar{x}$ is obtained from (3-5) by integration:

$$D\Phi_t(\bar{x})\tilde{x} = e^{tDf(\bar{x})}\tilde{x} \tag{3-6}$$

In general, equations (3-1) and (3-2) can be linearized as

$$\dot{x} = Ax + Bu \tag{3-7}$$
$$y = Cx + Du \tag{3-8}$$

If A is *Hurwitz*, i.e. A has all eigenvalues in the left half plane *(LHP)*, the fixed point $\bar{x}$ is said to be stable. Otherwise, it is said to be unstable. If $\bar{x}$ is stable and there are no eigenvalues on the imaginary axis, $\bar{x}$ is asymptotically stable.

3.2 Periodic Behavior of Nonlinear Systems

The following sections introduce the concepts that are used in this thesis for nonlinear system analysis and system control design. More details can be found in books [Khalil, (1996), Guckenheim (1983)] and the literature [Gonçalves (2000)].

3.2.1 Piece-wise linear analysis

There is a class of nonlinear systems that is composed of linear sub-systems and nonlinear components, such as saturation, threshold, relay feedback, etc, where the nonlinearity is in fact piece-wise linear. We call those systems *piece-wise linear systems*. The obvious advantage of this type of system is that the linear system theory can be applied in local regions where the dynamics equations of the system are linear.

A piece-wise linear system can have periodic solutions; these are called limit cycles. Piece-wise linear analysis will be used in the neural oscillator control of Chapter 5.

Definition 3.2 A piece-wise linear system (PLS) is characterized by a set of affine linear systems

$$\dot{x} = A_\alpha x + B_\alpha u \tag{3-9}$$

where $x \in \mathbb{R}^n$ is the state, and

$$\alpha(x) \in \{1,...,M\} \tag{3-10}$$

which indicates the switching rules used in the system.

$\alpha(x)$ usually is a piece-wise constant which depends on the state x and possibly on the past values of x. We defining t as a *switching time* of a solution of (3-9) and (3-10) if α is discontinuous at t. Equivalently, we say that a trajectory of (3-9) and (3-10) *switches* at some time t if t is a switching time.

In the state space, switching occurs at switching surfaces consisting of hyperplanes of dimension $n-1$

$$S_j = \{x \mid C_j x + d_j = 0\} \tag{3-11}$$

where $j = \{1,...,N\}$.

The switching rule may or may not be memory-less. In some cases, the value of α depends only on the current state, as in linear systems with saturating inputs. In other

cases, the value of α also depends on the past values of the state (or on past values of α), as with relays having hysteresis.

When the switching rule has no memory, where the switching depends only on the present state x, the state space $\mathbb{R}^n$ is partitioned into M (possibly unbounded) sets called cells. In each cell i, given by $\{x \mid \alpha(x) = i\}$, the system dynamics are governed by the affine system $\dot{x} = A_i x + B_i u$. Figure 3-1 shows a piece-wise linear system with two switching surfaces and four partitioned sets or cells.

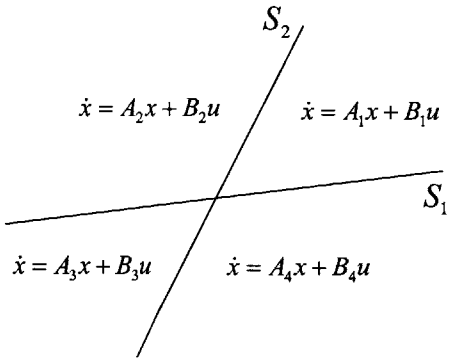

Figure 3-1: A piece-wise linear system with a memoryless switching rule

3.2.2 Limit Cycle

Periodic *oscillation* is one of the most important phenomena that occur in nonlinear dynamic systems. A system oscillates when it has a nontrivial *periodic solution*

$$x(t + t^*) = x(t), \text{ for all } t \geq 0, \tag{3-12}$$

for some $t^* \geq 0$ (the period of the oscillation). The word "nontrivial" is used to exclude constant solutions corresponding to isolated equilibrium points. The image set of a periodic solution in the state space is a closed trajectory that is usually called a periodic orbit or a closed orbit. Limit cycles are special cases of the closed trajectories of system. A *limit cycle* is defined as an isolated closed curve. That is, the trajectory has to be both closed (indicating the periodic nature of the motion) and isolated (indicating the limiting nature of the cycle that attracts and/or repels nearby trajectories). Thus, while there may exist many closed trajectories in the state space, only those that are isolated are called limit cycles.

Although linear systems may have closed trajectories, these trajectories are never isolated. Limit cycles are inherent properties of nonlinear systems. The analysis of limit cycles is difficult since no linear theory can be applied directly. Recent results in limit cycles analysis [Gonçalves (2000), Johansson (1996)], which are based on piece-wise linear systems have been applied in the nonlinear analysis of bipedal locomotion control and neural oscillators.

As continuum equilibrium points, limit cycles can be characterized as stable, unstable, or asymptotically stable. Let $\phi(t)$ be a nontrivial periodic solution of the autonomous system (3-4) with period t^*, and let γ be the closed orbit (limit cycle) given by the image set of $\phi(t)$ in the state space, that is,

$$\gamma = \{x \in \mathbb{R}^n \mid x = \phi(t), 0 \le t \le t^*\} \tag{3-13}$$

We define a ε-neighborhood of limit cycle γ as,

$$U_\varepsilon = \{x \in \mathbb{R}^n \mid dist(x,\gamma) < \varepsilon\} \tag{3-14}$$

where $dist(x,\gamma)$ is the minimum distance from x to a point in γ, that is,

$$dist(x,\gamma) = \inf_{y \in \gamma} \| x - y \| \tag{3-15}$$

Then the stability of a limit cycle can be defined as follows.

Definition 3.3 The limit cycle γ of system (3-4) is

- *stable* if, for ε>0, there is a δ>0 such that

$$x(0) \in U_\delta \Rightarrow x(t) \in U_\varepsilon, \ \forall t \ge 0.$$

- *asymptotically stable* if it is stable and δ can be chosen such that

$$x(0) \in U_\delta \Rightarrow \lim_{t \to \infty} dist(x(t),\gamma) = 0.$$

- *globally asymptotically stable* if it is stable and, for any $x(0)$

$$\lim_{t \to \infty} dist(x(t),\gamma) = 0.$$

We now wish to discuss the existence of limit cycles. Suppose a nonlinear system (3-1) can be formulated as a piece-wise linear system as (3-9) and (3-10), and it has a limit cycle γ with period t^*, and that this limit cycle crosses k switching surfaces (S_i, $i \in \{1,2,\cdots,k\}$) per cycle. For simplicity, assume the trajectory of the limit cycle evolves consecutively from system *1* to system 2, and so on until it reaches system *k*, and finally, after completing one cycle, returns to system *1*. Assume also that the switching surfaces are ordered the same way (see Figure 3-2). Then the trajectory $\phi(t)$ of the limit cycle starting at $x_0^* \in S_k$ satisfies $\phi(t_1^*) = x_1^* \in S_1$. System *2* is switched on until $\phi(t_1^* + t_2^*) = x_2^* \in S_2$, and so on. The k^{th} linear system takes the trajectory $\phi(t)$ from $x_{k-1}^* \in S_{k-1}$ to the point $x_k^* \in S_k$, i.e., $\phi(t_1^* + t_2^* + \cdots + t_k^*) = x_k^* = x_0^* \in S_k$. Note that $t^* = t_1^* + t_2^* + \cdots + t_k^*$. Then the existence condition of a limit cycle can be derived in the following way: first considering every switching surface (S_i), and computing the state $x_i^* \in S_i$ (by expressing it with the transition time t_1^*, t_2^*,...,t_k^*), then using the switching surface equation to find the condition on S_i, which can be formulated as

$g_i(t_1^*, t_2^*, ..., t_k^*) = 0$. For more details, the reader can refer to [Astrom (1995), Gonçalves (1999)].

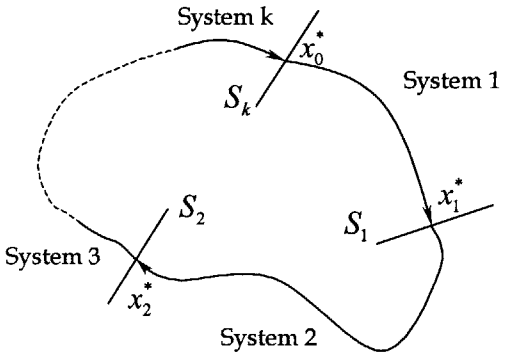

Figure 3-2: Limit cycle γ

The local stability of limit cycle for a PLS (3-9) and (3-10) can be analyzed in the following way. Assume there exists a periodic solution γ with period t^*. Let $x_0^* \in S_k$ be the initial state that generates the periodic motion. Consider the map T from a point in a small neighborhood of x_0^* in S_k to the point where the trajectory returns to S_k. The local stability of a limit cycle can be checked by looking at the poles of the linear part of map T. Stability follows if the poles are inside the unit disk. The following proposition gives conditions for the local stability of a limit cycle of the PLS (Amstrom 1998, Goncal 1999).

Proposition 3.1 *Consider the PLS (3-9)~(3-10). Assume there exists a limit cycle γ with period t^* as described above. Assume also that the limit cycle is transversal to the switching surfaces S_1, ..., S_k at x_1^*, ..., x_k^*, respectively. The Jacobian of the map T defined above is given by $W = W_k W_{k-1} \cdots W_2 W_1$ where*

$$W_i = (I - \frac{v_i C_i}{C_i v_i}) e^{A_i t_i^*}, \tag{3-16}$$

with $v_i = A_i x_i^* + B_i u$, $i = 1, ..., k$. The limit cycle γ *is locally stable if W has all its eigenvalues inside the unit disk. It is unstable if at least one of the eigenvalues of W is outside the unit disk.*

3.2.3 Poincare map

A Poincare map can be applied to prove that system trajectories converge to a limit cycle. We assume that a hyperplane H (H is n-1 dimensional provided that the system is n dimensional) is transversal to a periodic orbit γ (see Figure 3-3). Let p be a point on γ and H.

$$H = \{x \mid a^T(x-p) = 0\},\ a \in \mathbb{R}^n \tag{3-17}$$

Nonlinear system: $\dot{x} = f(x,t),\ x \in \mathbb{R}^n$. (3-18)

Let $W, S \subset H$ and $p \in W \subset S$. The Poincare map $g: S \to W$ is defined for a point $x \in S \subset H$ by

$$g(x) = \Phi(\tau, x) \tag{3-19}$$

where $\Phi(\tau, x)$ is the solution of (3-18) that starts at x at time $t = 0$ and $\tau = \tau(x)$ is the time taken for the trajectory starting at x to first return to W. Suppose we start at $x(0)$ on S, with a Poincare map, we can have a sequence, $x^{(0)}$, $x^{(1)}$, ... , $x^{(k)}$, ... Therefore, a discrete-time system is defined as,

$$x^{(k+1)} = g(x^{(k)}). \tag{3-20}$$

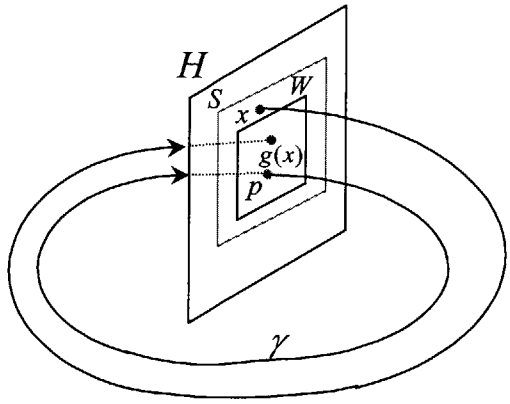

Figure 3-3: An example for Poincare map.

If we can prove the above discrete-time system has contraction mapping property [Khalil (1996)], we can say that p is a stable equilibrium point on H, and γ is a stable limit cycle.

3.3 Contraction Theory

We shall now extend the concepts of stability of limit cycles to the definitions of orbital stability of a nontrivial periodic solution $\phi(t)$ of system (3-4).

Definition 3.4 A nontrivial periodic solution $\phi(t)$ is

- *orbitally stable* if the limit cycle γ generated by $\phi(t)$ is stable.
- *asymptotically orbitally stable* if the limit cycle γ generated by $\phi(t)$ is asymptotically stable.

- *globally asymptotically orbitally stable* if the limit cycle γ generated by $\phi(t)$ is orbitally asymptotically stable, and it is also globally stable.

Since the above definitions of orbital stability of a nontrivial periodic solution of system (3-4) are based on the volume contraction of the ε-neighborhood of limit cycle γ, this concept is also referred to as, contraction of a steady orbit.

There is another way to prove the stability of a limit cycle or the orbital stability of a given system. If one can define a proper Poincare map between two hyperplanes and prove the Poincare map contracts in certain region of the state space hyperplane, then the system is said to be orbitally stable in that region.

Chapter 4

Stability of Bipedal Walking

The dynamics and locomotion stability of a bipedal walking robot are facilitated by first introducing some simplifications of the robot's dynamic models. The dynamics models are derived under some reasonable approximations and assumptions. The analysis of the dynamics uses nonlinear system theory. Foot strike, which enforces the dynamic switching of a bipedal walking robot, is also discussed.

4.1 Dynamic Modeling

Approximations are necessary in the dynamic modeling of a bipedal walking robot. To this end, the following assumptions are made:

(1) The legs of the biped are approximated as a lumped mass positioned a fixed distance from the hip, together with a linear slider joint capable of varying the leg length (Figure 4-1).

(2) There is no slipping between the feet and the ground.

(3) In single support phase, the length of the stance leg is fixed.

(4) In double support phase, the leading leg has a constant leg length, and the distance between two feet (step length) is also fixed.

(5) During walking, the step length in consecutive cycles is assumed to be constant.

Although (4) and (5) are admittedly bold assumptions, they have been found highly compatible with the simulation results.

4.1.1 Dynamic model in double support phase

Further simplification is made in the double support case. The leg mass (3~5% of body mass in *Spring Flamingo* shown in Figure 1-3) is ignored in the model of double support for simplicity of analysis. In Figure 4-1, the leg length of the leading leg is fixed. Only the trailing leg can be extended to propel the robot forward. Since the length of the leading leg is fixed in this control scheme, there is only one degree of freedom in the model. For

convenience, we choose θ as a state variable instead of x. The relationship between θ and x is expressed as,

$$\theta = \cos^{-1}\left(\frac{l^2 + \lambda^2 - x^2}{2l\lambda}\right) \tag{4-1}$$

where λ is the step length equal to the distance between two ankle positions (Figure 4-1) in double support phase.

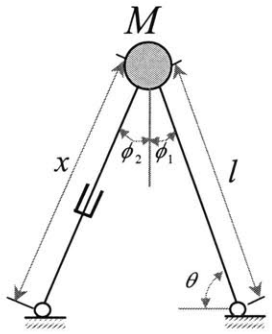

Figure 4-1: Diagram for the dynamic model in double support phase.

By means of Lagrangian equation, the system equation can be obtained, which is the same as an inverted pendulum except for the actuator force *f* exerted by the slider joint in the trailing leg. The derivation of this dynamic model is provided in Appendix A.

$$Ml^2\ddot{\theta} + Mgl\cos\theta = \tau \tag{4-2}$$

where the torque command is,

$$\tau = \vec{f} \times \vec{r} = f \cdot l\sin\alpha$$

$$\sin\alpha = \frac{\lambda}{x}\sin\theta$$

The linear slider joint command is expressed with τ,

$$f = \tau \cdot \frac{x}{\lambda l \sin\theta} \tag{4-3}$$

Substituting (4-3) into (4-2), we can derive the dynamic equation as a function of variable *x*:

$$m(x)\ddot{x} + n(x,\dot{x})\dot{x} + g(x) = c(x)\cdot f \tag{4-4}$$

We can also express the gait variables ϕ_1 and ϕ_2 in terms of θ:

$$\phi_1 = \frac{\pi}{2} - \theta \tag{4-5}$$

$$\phi_2 = tg^{-1}\frac{\lambda - l\cos\theta}{l\sin\theta} \tag{4-6}$$

4.1.2 Dynamic model in single support phase

We assume in single support, the leg length of the stance leg is constant in this model (Figure 4-2). Choosing variables θ_1, θ_2 and the gait variables ϕ_1 and ϕ_2 are expressed as:

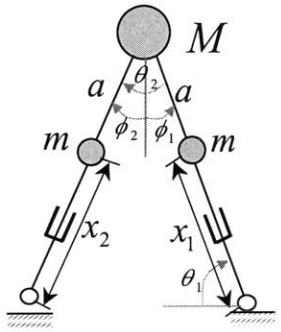

Figure 4-2: Diagram for a dynamic model in single support.

$$\begin{cases} \phi_1 = -(\frac{\pi}{2} - \theta_1) \\ \phi_2 = \theta_2 + \phi_1 = \theta_2 - \frac{\pi}{2} + \theta_1 \end{cases} \tag{4-7}$$

With the *Lagrangian* equation, we can derive the dynamic model for the single support phase below. The details of this derivation are provided in Appendix A.

$$[mx_1^2 + (M+m)l^2 + ma^2]\ddot{\theta}_1 + ma^2\ddot{\theta}_2 + mla\cdot\sin\theta_2\cdot\dot{\theta}_2 + [mgx_1 + (m+M)gl]\cos\theta_1 - mga\cdot\cos(\theta_1+\theta_2) = \tau_1 \tag{4-8}$$

$$ma^2\ddot{\theta}_1 + ma^2\ddot{\theta}_2 - mla\dot{\theta}_1\cdot\sin\theta_2 - mga\cdot\cos(\theta_1+\theta_2) = \tau_2 \tag{4-9}$$

Generally, the dynamics for any biped can be formulated as

$$M(\theta)\ddot{\theta} + N(\theta,\dot{\theta})\dot{\theta} + G(\theta) = u \tag{4-10}$$

where $M(\theta)$ is the inertia matrix, $N(\theta,\dot{\theta})$ is a matrix with the Coriolis and centrifugal coefficients, $G(\theta)$ is a vector of gravitational torques, θ is the state variable, and u is the torque commands.

4.2 Reachability and Stability in Local Dynamics

4.2.1 Reachability of nonlinear systems

When a nonlinear dynamic system is represented in the following state space form,

$$\dot{x} = f(x) + \sum_{i=1}^{m} u_i g_i(x), \tag{4-11}$$

where f, g_1, ..., g_m are given vector fields, and $x \in \mathbb{R}^n$, then we may define "system reachability" as follows:

Definition 4.1 The system (4-11) is said to be (locally) *reachable* around a state $x_0 \in X \subset \mathbb{R}^n$ if there exists a neighborhood U of x_0 such that for each $x_f \in U$, there exist a time $T > 0$ and a set of control inputs $\{u_i(t) \mid t \in [0,T], 1 \le i \le m\}$ such that, if the system starts in the state x_0 at time *0*, then it reaches the state x_f at time *T*.

The following theorem gives a simple sufficient condition for the system (4-11) to be locally reachable around an operating point x_0 by its linearized equation (Vidyasagar, 1991).

Proposition 4.1 *Consider the system (4-11), and suppose x_0 is an operating point, which satisfies the system equation (4-11). Define the linearized equation around x_0 as*

$$\dot{z} = A_0 z + \sum_{i}^{m} b_{i0} v_i \tag{4-12}$$

Then the system (4-11) is locally reachable, if the system (4-12) is reachable, i.e., if the following matrix

$$W_0 = \begin{bmatrix} B_0 & A_0 B_0 & \cdots & A_0^{n-1} B_0 \end{bmatrix} \tag{4-13}$$

has full rank, where $B_0 = [b_{10} \cdots b_{m0}]$.

Applying the above concepts, one can analyze the reachability of the dynamics in the double support phase and single support phase for a biped robot. We first convert the dynamics equations into a state space form then apply the above theorem to analyze the properties of the bipedal dynamics.

4.2.2 Dynamic analysis in double support

The biped dynamics equation (4-2) can be rearranged into a state space representation.

$$\begin{cases} \dot{x}_1 = x_2 \\ \dot{x}_2 = \dfrac{1}{Ml^2}(-Mgl\cos x_1 + \tau) \end{cases} \tag{4-14}$$

where $x_1 = \theta$, $x_2 = \dot{\theta}$. Using these in the control law, $\tau = K_p(\dot{\theta}^* - \dot{\theta}) = K_p(\omega - \dot{\theta})$, we have

$$\begin{cases} \dot{x}_1 = x_2 \\ \dot{x}_2 = \dfrac{1}{Ml^2}(K_p\omega - K_p x_2 - Mgl\cos x_1) \end{cases} \tag{4-15}$$

Since the time interval for double support phase (t_1) is usually very small, the state values do not change significantly, especially for the position variable $x_1 = \theta$. Therefore, local linearization allows us to find a closed form solution of the system dynamics during this period.

Let $x_1 = x_1(0) + \Delta x_1$, $x_2 = x_2(0) + \Delta x_2$. The linearized equation is

$$\begin{bmatrix} \Delta\dot{x}_1 \\ \Delta\dot{x}_2 \end{bmatrix} = \begin{bmatrix} 0 & 1 \\ -\frac{1}{l}g\sin x_1(0) & -\frac{K_p}{ml^2} \end{bmatrix} \begin{bmatrix} \Delta x_1 \\ \Delta x_2 \end{bmatrix} + \begin{bmatrix} x_2(0) \\ u_1 \end{bmatrix} \tag{4-16}$$

where $$u_1 = -\frac{g}{l}\cos x_1(0) + \frac{K_p\omega}{Ml^2} - \frac{K_p x_2(0)}{Ml^2}. \tag{4-17}$$

From the linearized equations (4-16) and (4-17), we can obtain,

$$A_0 = \begin{bmatrix} 0 & 1 \\ -\frac{1}{l}g\sin x_1(0) & -\frac{K_p}{ml^2} \end{bmatrix}, \quad B_0 = \begin{bmatrix} 1 & 0 \\ 0 & 1 \end{bmatrix}$$

Then, $W_0 = [B_0 \quad A_0B_0]$. We can easily check that W_0 has full rank. We may then conclude from Proposition 4.1 that the dynamics in double support are reachable. Also we can easily verify that the eigenvalues of the above dynamic system are both negative. Therefore we can conclude that this dynamic system is stable in double support phase.

4.2.3 Dynamic analysis in single support

From equations (4-8) and (4-9), the state space representation of the dynamics in single support phase is obtained:

$$\begin{cases} \dot{x}_1 = x_2 \\ \dot{x}_2 = \frac{1}{\gamma_0}[mla\sin x_3 \cdot x_2 - mla\sin x_3 \cdot x_4 - \gamma_2\cos x_1 + \tau_1 - \tau_2] \\ \dot{x}_3 = x_4 \\ \dot{x}_4 = \frac{1}{\gamma_0}[-\frac{l}{a}\gamma_1\sin x_3 \cdot x_2 + mla\sin x_3 \cdot x_4 + \frac{g}{a}\cos(x_1 + x_3)\cdot\gamma_1 + \gamma_2\cos x_1 \\ -mga\cos(x_1 + x_3) + \frac{\gamma_1}{ma^2}\tau_2 - \tau_1] \end{cases} \tag{4-18}$$

where $x_1 = \theta_1$, $x_2 = \dot{\theta}_1$, $x_3 = \theta_2$, $x_4 = \dot{\theta}_2$.

Distinct control schemes are used in the toe-off period ($\phi_2 \geq 0$) and the touch-down period ($\phi_2 < 0$). When $\phi_2 \geq 0$, i.e. $\theta_1 + \theta_2 \geq \frac{\pi}{2}$, the control commands are,

$$\tau_1 = 0 \tag{4-19}$$

$$\tau_2 = K_p(\tfrac{\pi}{2} - \theta_1 - \theta_2) - K_d(\dot{\theta}_1 + \dot{\theta}_2). \tag{4-20}$$

When $\phi_2 < 0$, i.e. $\theta_1 + \theta_2 < \frac{\pi}{2}$,

$$\tau_1 = 0 \tag{4-21}$$

$$\tau_2 = K_p(-\pi + 2\theta_1 - \theta_2) - K_d(\dot{\theta}_1 + \dot{\theta}_2). \tag{4-22}$$

In this case, for the double support dynamics (4-18), we cannot apply Proposition 4.1. Because the control signal τ_1 is always zero (for the half-actuated ankle joints in a biped), the Gramian matrix W_0 of the linearized system does not have full rank. However, we can use the reachability concept in definition 4.1 to analyze the dynamics.

Applying $\tau_1 = 0$ (since the ankle joint has very limited torque in actuation), we can analyze the local dynamics separately for θ_1 and θ_2 from equation (4-8) and (4-9). We can find the feature of the biped dynamics (in single support) in a similar way as we did for double support dynamics (by setting the other state variable as constants). The dynamics for θ_1 (stance leg), which is an inverted pendulum model, are unreachable and unstable, but the dynamics for θ_2 (swing leg) is reachable and stable.

4.3 Stability of Bipedal Locomotion Control

Whether it is rigorously proven or merely observed, stability is a critical requirement in the control of bipedal walking [Todd (1985), Vukobratovic (1993)]. But unlike conventional control system stability, a walking robot's stability is not a question of tracking some desired trajectory [Pratt (1999)]. To achieve the stability, a biped should not fall down and should walk at a steady pace. In other words, its posture (roll, pitch, yaw, height) should be bounded within some range of nominal values, and its gait should converge to a periodic orbit. We refer to these two ideas as *Postural Stability* and *Gait Stability*.

Figure 4-3 shows the relationship of gait stability and postural stability. Note that a robot may have postural stability and not have gait stability – for example its leg motion might be aperiodic or even chaotic [Vakakis (1990)] - but not the other way around. Ideal walking requires both gait stability and postural stability.

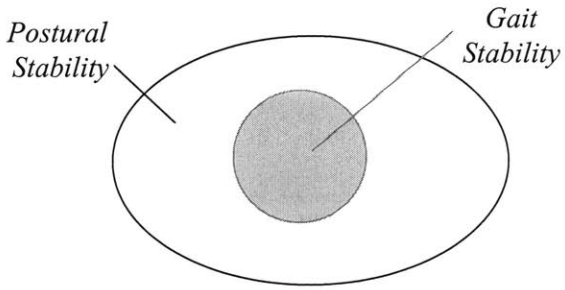

Figure 4-3: Description of relationship between gait stability and postural stability of a walking robot.

Many researchers have previously studied postural stability. Recently, Zero Moment Point (ZMP), which characterizes the zero moment point (the virtual turning point on the ground plane) of the biped structure, has been utilized to achieve postural stability, as with the Honda humanoid robots [Hirai (1998)] and the WABIAN robots [Li & Takanish (1992)]. ZMP control is used to maintain the zero moment point of the biped within the stance region, called a polygon area, such that the robot will not fall over. This approach is used in postural stability measurement, but it is extended to a walking control algorithm for trajectory planning [Hirai et al (1998)].

Gait stability has been much less studied. A few researchers have addressed this topic in passive walking [McGeer (1990), Goswami (1996)] and running [Vakakis (1990)], and in some neural models [Hu (1999), Taga (1995)]. McGeer (1990), a pioneer in passive bipedal walking [McGeer (1990)], demonstrated that a passive walker can attain a stable periodic motion, and he analyzed this behavior with a linearized mathematical model. Recently, Goswami (1996) studied the periodic behavior of a passive compass gait of a biped. Taga (1995) has addressed this in his neural oscillator driven humanoid-legged locomotion control. With neural oscillators one can generate a nonlinear limit cycle process to accomplish bipedal walking [Hu (1999)].

The majority of studies of gait control, however, have focused on gait modification and implementation for different terrains [Hirai (1998)] instead of stability. Despite this lack of work, gait stability is crucial for locomotion. Without gait stability, the leg motion and forces available to the robot to maintain postural stability become unpredictable, and postural control may fail despite a good postural control method.

In his study of stability, Vukobratovic (1973, 1990) proposed a repeatability condition, which is required for the stability of a periodic gait. In this thesis, an active locomotion control approach is developed by means of nonlinear switching control schemes that meet this condition. It can be used to achieve postural stability and gait stability. In this approach, we use different controllers for the double support and single support phases. An orbital contraction tuning technique is used to choose the state-dependent switching surfaces. Nonlinear control theory is then used to prove gait stability.

dependent switching surfaces. Nonlinear control theory is then used to prove gait stability.

Postural stability can be specified with indices like body pitch angle, roll angle and height. Figure 4-4 shows postural stability with height indices. Besides, the ZMP criterion is usually utilized for monitoring postural stability [Vokobratovic (1990), Li & Takanish (1992)], and it can also be used to specify the stability boundaries.

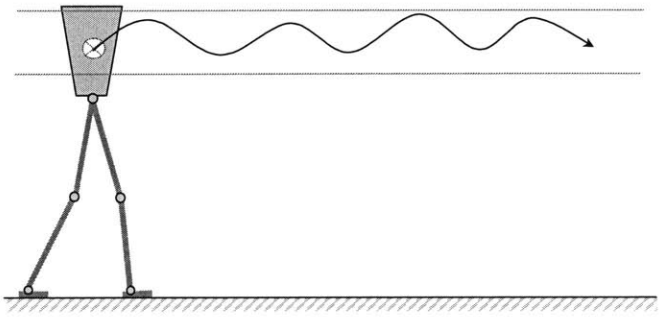

Figure 4-4: Postural stability with height index.

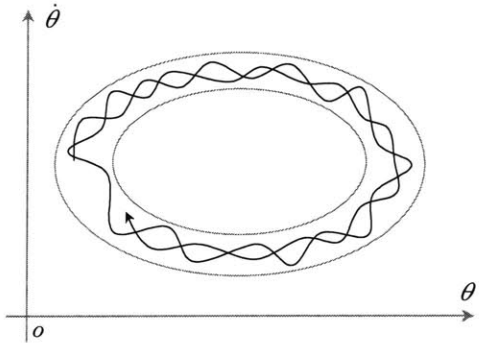

Figure 4-5: A description of approximate cyclic motions, which are confined a very narrow region. When the volume of the region shrinks to zero, a perfect limit cycle is achieved.

Gait stability requires a globally stable cyclic motion of the robot. That is, the global motion should be periodic. From Vukobratovic's definition [Vokobratovic (1990)], all the states and velocities should be repeated with a constant period and stride length. In this study, we create a global state variable that abstracts the state of the legs and enforce stability on this variable and its derivative to satisfy the repeatability condition. As a

Gait stability can be reached by appropriately switching between single support phases and double support phases. The switching point can be adjusted in the boundary area in order to balance the kinetic energy and the potential energy in the single support phase, which is described in details in Chapter 7. The goal is to enforce the repeatability condition (gait stability) while the constant stride length (step length) is guaranteed by means of controlling the swing leg. The repeatability condition with symmetry is expressed as:

$$\vec{x}_l(t_0) = \vec{x}_r(t_0 + T) \tag{4-23}$$

$$\vec{x}_r(t_0) = \vec{x}_l(t_0 + T) \tag{4-24}$$

$$\dot{\vec{x}}_l(t_0) = \dot{\vec{x}}_r(t_0 + T) \tag{4-25}$$

$$\dot{\vec{x}}_r(t_0) = \dot{\vec{x}}_l(t_0 + T) \tag{4-26}$$

where t_0 is the previous touch-down time of a foot, T is the period of one step, and $\vec{x}_l$ and $\vec{x}_r$ are the state variables for the left leg and right leg respectively.

4.4 Ground Impact

When the swing leg strikes the ground, there is a sharp change in the angular velocities, $\dot{\theta}_1$ and $\dot{\theta}_2$, while the angular positions, θ_1 and θ_2 will remain the same during the ground impact time interval. Assume that the ground surface is rigid, and that the angular momentum and energy will be conserved. When at high walking speed the double support phase vanishes, the stance leg leaves the ground as the swing leg simultaneously strikes the ground. Then conservation of angular momentum provides a deterministic linear function P [Goswami (1996)]:

$$\dot{\theta}(t_0^+) = P(\theta)\dot{\theta}(t_0^-) \text{ and } \dot{\theta}(t_2^+) = P(\theta)\dot{\theta}(t_2^-) \tag{4-27}$$

When the double support phase is of nonzero duration, the stance leg remains on the ground while the swing leg touches down. The relationship between $\dot{\theta}(t_0^+)$ and $\dot{\theta}(t_0^-)$ is non-linear and deterministic. This nonlinear mapping can be formulated as

$$\dot{\theta}(t_0^+) = P(\theta, \dot{\theta}(t_0^-)) \tag{4-28}$$

where P only depends on the robot geometry, θ and $\dot{\theta}(t_0^-)$.

Since the mapping from the state before striking the ground to the state after striking the ground is deterministic, linear, or nonlinear, the above Poincare map analysis will still be effective.

4.5 Summary

The simplified dynamics models that are presented in this chapter will be used in the switching control for illustrating the dynamic behaviors (Chapter 7). Nonlinear analysis of the biped dynamics was used to demonstrate that the dynamics in the double support phase is reachable and stable with redundant structure, and the dynamics in single support phase are not reachable and unstable. Locomotion stability, including postural stability and gait stability, is discussed. Also the discussion of ground strike gives dynamics constraint at the moment of ground strike.

Chapter 5

Rhythmic Control Driven by Neural Oscillators

This chapter introduces the neural oscillator model and the analysis of the general rhythmic control framework. The results of studying the basic oscillator module and its behavior within a closed loop feedback system provide the foundation for its application to bipedal legged-locomotion control (in Chapter 6).

5.1 Introduction

A growing number of researchers are using neural oscillators to control robots. The application domains include legged locomotion [Miyakoshi (1998)], locomotion of multi-segmented creatures [Orlovsky (1999), Lewis (1996)] and arm control [Williamson (1998)].

Oscillators are used in all these cases because they can entrain and adapt to the dynamics of the plant (system), giving robust behavior in the face of changing system parameters or perturbations. One drawback to these systems is that they are very difficult to tune. In spite of general analysis of oscillators [Matsuoka (1985)] and learning, there is a lack of practical knowledge of how the oscillators work and how to design systems using them. A general framework for designing neural oscillator driven control system with a compensator was proposed in the recent paper [Hu (1999a)]. However many reported results of neural oscillator rhythmic control are based only on experimental demonstrations or simulations. Theoretical study is needed in order to prove those results and to provide appropriate analysis for better control design.

In this chapter, nonlinear system theory is applied to neural oscillator driven rhythmic motion control [Hu (1999b)]. First, a neural oscillator unit is studied with nonlinear system theory. The existence and uniqueness of a solution to the oscillator unit equation is proved using the Lipschitz condition. Then, by proving the boundedness of the neural oscillator states, the condition of stable oscillation for a symmetric neural oscillator unit is given. Next, dynamic interaction (entrainment) with a passive plant is discussed with "describing functions". Finally a compensator based rhythmic control design approach is presented, in which a compensator is added to shape the plant dynamics. A sufficient condition has been derived for the entrainment of the neural oscillator driven control.

5.2 Neural Oscillator Models

Many different neural oscillator models have been inspired by biological research. Only a few of these can be analyzed mathematically. The two most populous models that have been used for pattern generators are introduced in the following sections.

5.2.1 Van der Pol oscillators

Van der Pol oscillators have been studied widely both in mathematics and engineering. Bay and Hemami (1987) and Zielinska (1996) applied this oscillator model in human locomotion rhythm generation. The equations describing the dynamical properties of the oscillators have the following general form:

$$\ddot{x} - \mu \cdot (p^2 - x^2) \cdot \dot{x} + g^2 \cdot x = s \tag{5-1}$$

where variables μ, p^2, g^2 are the parameters that influence the properties of the oscillators. q is the tonic input to the neural oscillator. The values of x as a function of time, resolving the coupled equations of these oscillators, describe the changes of states, which drive the plant in a synchronous rhythm.

Using the above general model, coupled oscillators can be formed. A four-oscillator system describing biped motion, which is formed in a ring, was proposed by Zielinska (1996).

$$\begin{cases} \ddot{x}_1 - \mu_1 \cdot (p_1^2 - x_a^2) \cdot \dot{x}_1 + g_1^2 \cdot x_a = s_1 \\ \ddot{x}_2 - \mu_2 \cdot (p_2^2 - x_b^2) \cdot \dot{x}_2 + g_2^2 \cdot x_b = s_2 \\ \ddot{x}_3 - \mu_3 \cdot (p_3^2 - x_c^2) \cdot \dot{x}_3 + g_3^2 \cdot x_c = s_3 \\ \ddot{x}_4 - \mu_4 \cdot (p_4^2 - x_d^2) \cdot \dot{x}_4 + g_4^2 \cdot x_d = s_4 \end{cases} \tag{5-2}$$

where

$$\begin{aligned} x_a &= x_1 - \lambda_{21} \cdot x_2 - \lambda_{31} \cdot x_3 \\ x_b &= x_2 - \lambda_{12} \cdot x_1 - \lambda_{42} \cdot x_4 \\ x_c &= x_3 - \lambda_{13} \cdot x_1 - \lambda 4_1 \cdot x_4 \\ x_a &= x_1 - \lambda_{21} \cdot x_2 - \lambda_{31} \cdot x_3 \end{aligned}$$

Here μ_i, p_i^2, g_i^2, s_i, $i \in \{1,2,3,4\}$ are the parameters which determine the properties of the oscillators. λ_{ij}s, $i \neq j$, $i, j \in \{1,2,3,4\}$ are the mutually-inhibited connections between the oscillators. The influence of the above parameters is very complex. An exact analytical solution describing the behavior of the coupled oscillators is not known.

5.2.2 Matsuoka's neural oscillators

A two dimensional recurrent neural oscillator can be described by the following coupled ordinary differential equations:

$$\begin{cases} \tau \cdot \dot{x}_i = -x_i - \beta v_i - \sum_{j=1}^{n} w_{ij} y_j + s_i \\ T \cdot \dot{v}_i = -v_i + y_i \end{cases} \tag{5-3}$$

$$y_i = f(x_i - \theta), \; f(x) = \max(0, x). \tag{5-4}$$

where i indicates the ith neuron in the neural oscillator, x_i is the membrane potential, y_i is the neuron output, v_i is the membrane current of the slow recovery component, $f(x)$ is a nonlinear output function of the neuron, and θ is the membrane potential threshold. Parameter τ is the membrane capacitance, β and T are the resistance and inductance associated with the slow current events, and s_i is the tonic input to the neuron.

Using this fundamental neuron model, Matsuoka (1985) studied the oscillation behavior of the mutually inhibiting neurons in general. Williamson (1998) successfully applied a modified two-neuron unit in the rhythmic arm movement control of a humanoid robot COG. In this study, we use a slightly modified two-neuron oscillator unit. The neural dynamics are expressed by the following differential equations:

$$\begin{cases} \tau_1 \dot{x}_1 = -x_1 - \beta v_1 - w_{12} y_2 + e + r \\ \tau_2 \dot{v}_1 = -v_1 + y_1 \\ \tau_1 \dot{x}_2 = -x_2 - \beta v_2 - w_{21} y_1 - e + r \\ \tau_2 \dot{v}_2 = -v_2 + y_2 \end{cases} \tag{5-5}$$

$$y_i = f(x_i) = \max\{x_i, 0\}, \; i = 1,2. \tag{5-6}$$

$$\text{Output: } y_o = k_1 y_1 - k_2 y_2, \; k_1, k_2 > 0. \tag{5-7}$$

where e is sensory signal feedback from the control plant, r is a tonic input, and k_1, k_2 are the constant coefficients of oscillator output. A structural diagram is shown below in Figure 5-1.

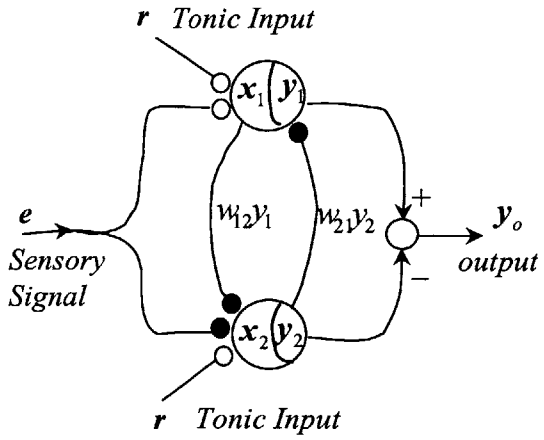

Figure 5.1: Diagram of a two-neuron oscillator. The recurrent links and the co-states of neurons are not shown in the diagram. Only visible are the exterior connections. Black circles correspond to inhibitory connections, open to excitatory.

From Matsuoka's analysis of neural oscillation networks [Matsuoka (1985)] and Williamson's later demonstration [Williamson (1999)], it is clear that mutually inhibitory neural oscillators have the following main features:

1) Amplitude of oscillation: The tonic input r determines the amplitude of the oscillation, with amplitude proportional to r.

2) Frequency of oscillation: The time constants τ_1 and τ_2 determine the frequency and shape of the oscillator output signal. Roughly, the frequency of oscillation output is proportional to $1/\tau_1$.

Example 5-1: Simulation results of neural oscillator (5-5). The parameters of this example are: $\tau_1 = 1/32$, $\tau_2 = 1/2.656$, $\beta = 2.5$, $w_{12} = w_{21} = 2.0$, $r = 6.0$, $e = 0$. The initial condition of the oscillator is, $x_1(0) = -3.9$, $x_2(0) = 5.5$, $v_1(0) = 0$, $v_2(0) = 0$. Figure 5-2 shows the dynamic responses of states, output and a typical limit cycle of the oscillator module (5-5).

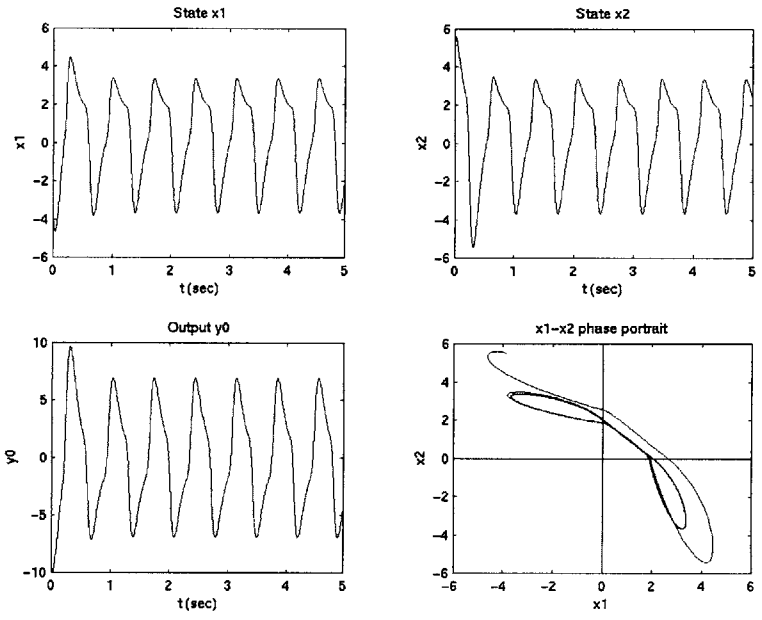

Figure 5-2: Simulation results of an example of oscillator (5-5).

5.3 Analysis of Neural Oscillator Unit

Although the properties of the mutually inhibited neural oscillator have been studied in general analyses and by simulations as well as experiments, a rigorous analysis of the modified neural oscillator is not available. The modified neural oscillator has been found very useful in robot control [Williamson (1999), Hu (1999)]. In this section, the

stable rhythmic behavior of the modified oscillator is studied and stated in the form of theorems. Theorem 1 states that the solution to the oscillator unit exists and is unique, and theorem 2 describes the boundedness of the neural oscillator circuit.

5.3.1 Existence and uniqueness of solution

Theorem 5.1: *There exists a unique solution for the modified neural oscillator circuit.*

Proof: Reorganizing the neural oscillator equation as,

$$\begin{cases} \dot{x}_1 = -\frac{1}{\tau_1}x_1 - \frac{\beta}{\tau_1}v_1 - \frac{w_{12}}{\tau_1}f(x_2) + r_1 = f_1 \\ \dot{v}_1 = -\frac{1}{\tau_2}v_1 - \frac{1}{\tau_2}f(x_1) = f_2 \\ \dot{x}_2 = -\frac{1}{\tau_1}x_2 - \frac{\beta}{\tau_1}v_2 - \frac{w_{21}}{\tau_1}f(x_1) + r_2 = f_3 \\ \dot{v}_2 = -\frac{1}{\tau_2}v_2 - \frac{1}{\tau_2}f(x_2) = f_4 \end{cases} \tag{5-8}$$

$r_1 = s_1/\tau_1$, $r_2 = s_2/\tau_1$.

Let $\underline{x} = [x_1 \quad v_1 \quad x_2 \quad v_2]^T$, $F(\underline{x},t) = [f_1 \quad f_2 \quad f_3 \quad f_4]^T$,

then, $\dot{\underline{x}} = F(\underline{x},t)$ (5-9)

$\forall t \in [0,T]$, $\forall \underline{x}, \underline{x}_0 \in D$ (an open region),

$$\|f(x) - f(x_0)\| \le \|x - x_0\| \quad \text{for } f(x) = \max\{x,0\}. \tag{5-10}$$

Then, we can derive

$$\|F(\underline{x},t) - F(\underline{x}_0,t)\| \le \tfrac{1}{\tau}\|\underline{x} - \underline{x}_0\| + \tfrac{\beta}{\tau}\|\underline{x} - \underline{x}_0\| + \alpha\|\underline{x} - \underline{x}_0\| \tag{5-11}$$

where $\tau = \min\{\tau_1, \tau_2\}$, $\alpha = \max\{\frac{w_{12}}{\tau_1} + \frac{1}{\tau_2}, \frac{w_{21}}{\tau_1} + \frac{1}{\tau_2}\}$.

By collecting terms, we get

$$\|F(\underline{x},t) - F(\underline{x}_0,t)\| \le L \cdot \|\underline{x} - \underline{x}_0\| \tag{5-12}$$

where $L = \frac{1}{\tau} + \frac{\beta}{\tau} + \alpha$. (5-13)

Therefore, we can conclude that $F(\underline{x},t)$ is locally Lipschitz on $[0,T]$. Since (5-12) holds for any $\underline{x}$ and $\underline{x}_0$, $F(\underline{x},t)$ is also globally Lipschitz on $[0,T]$. In summary, we know that $F(\underline{x},t)$ is piecewise continuous in $t \in [0,T]$, and $F(\underline{x},t)$ is Lipschitz on $[0,T] \times B$ with a constant L, where $B = \{\underline{x} \mid \|\underline{x} - \underline{x}_0\| \le \eta\}$ (closed ball).

From Theorem 2.6 [Nicola (1995), Khalil (1996)], we know that the equation $\dot{\underline{x}} = F(\underline{x},t)$, $\underline{x}(0) = \underline{x}_0$, has a unique solution in $C[0,\delta]$ for some $\delta > 0$. Hence the solution of equation (5-5) exists and is unique. *Q.E.D.*

5.3.2 Boundedness of the oscillator behavior

Theorem 5.2: *The solution of neural oscillator is bounded for a given input.*

Proof: To prove the boundedness of equation (5-8), let's consider variables x_1, v_1 first. Directly solving the co-state equation of v_1, we get,

$$v_1(t) = v_1(0)e^{-t/\tau_2} + \tfrac{1}{\tau_2}e^{-t/\tau_2}\int_0^t f(x_1(u))e^{u/\tau_2}du \tag{5-14}$$

$\because \quad f(x_1(u)) = \max\{x_1(u), 0\} \geq 0$

$$\Rightarrow \quad v_1(t) \geq -\left|v_1(0)\right| = -\alpha_1(v_1),\ (t \geq 0) \tag{5-15}$$

Solving for $x_1(t)$ from (5-8), we get,

$$x_1(t) = x_1(0)e^{-t/\tau_1} + r_1(1-e^{-t/\tau_1}) - \frac{\beta}{\tau_1}e^{-t/\tau_1}\int_0^t v_1(u)e^{u/\tau_1}du - \frac{w_{12}}{\tau_1}e^{-t/\tau_1}\int_0^t f(x_2(u))e^{u/\tau_1}du \tag{5-16}$$

Plug (5-15) into (5-16), we have

$$\begin{aligned} x_1(t) &\leq \left|x_1(0)\right| + r_1 + \frac{\beta}{\tau_1}e^{-t/\tau_1}\int_0^t v_1(0)e^{u/\tau_1}du \\ &= \left|x_1(0)\right| + r_1 + \beta\left|v_1(0)\right|(1-e^{-t/\tau_1}) \\ &\leq \left|x_1(0)\right| + r_1 + \beta\left|v_1(0)\right| \\ &= \alpha_2(x_1) \end{aligned} \tag{5-17}$$

Applying (5-17) to (5-14) and manipulating similarly gives

$$v_1(t) \leq \left|v_1(0)\right| + \left|x_1(0)\right| + r_1 + \beta\left|v_1(0)\right| = \alpha_2(v_1) \tag{5-18}$$

Then plugging (5-17) into (5-16), we obtain

$$x_1(t) \geq -\left|x_1(0)\right| - w_{12}[\left|x_1(0)\right| + r_1 + \beta\left|v_1(0)\right|] - \beta[\left|v_1(0)\right| + \left|x_1(0)\right| + r_1 + \beta\left|v_1(0)\right|] = -\alpha_1(x_1) \tag{5-19}$$

$$\Rightarrow \quad -\alpha_1(v_1) \leq v_1(t) \leq \alpha_2(v_1) \qquad \alpha_1(v_1), \alpha_2(v_1) > 0 \tag{5-20}$$

$$-\alpha_1(x_1) \leq x_1(t) \leq \alpha_2(x_1) \qquad \alpha_1(x_1), \alpha_2(x_1) > 0 \tag{5-21}$$

$\Rightarrow$ $v_1(t)$ and $x_1(t)$ are bounded.

In a similar way, we can prove that $v_2(t)$, $x_2(t)$ are also bounded.

Therefore, given that the inputs $|\, r_1 \,|$, $|\, r_2 \,|$ are bounded, we can conclude that the state variables $x_1(t)$, $v_1(t)$, $x_2(t)$, $v_2(t)$ are bounded.

Since $\quad y_o = y_1 - y_2 = f(x_1) - f(x_2)$,

the output of oscillator y_o is bounded. Hence the solution of the oscillator is bounded.

Q.E.D.

5.3.3 Analysis on stationary solution

From Matsuoka's analysis on the general form of the neural oscillator (equation (5-3), (5-4)), the following conclusion (in Lemma 5.1) for a symmetrically connected neural oscillator can be extended directly to the modified neural oscillator model.

From the definition in Chapter 3, a stationary solution of equation (5-5) must satisfy the following conditions:

$$y^0 = G(y^0) = [g_1(y^0) \quad g_2(y^0)]^T \tag{5-22}$$

where $y^0 = [y_1^0 \quad y_2^0]^T$ is the output,

$$g_1(y^0) = f(-w_{12}y_2^0 - \beta y_1^0 + s_1) \tag{5-23}$$

$$g_2(y^0) = f(-w_{21}y_1^0 - \beta y_2^0 + s_2) \tag{5-24}$$

$$s_1 = e + r,\ s_2 = -e + r.$$

Conversely, if y^0 satisfies (5-22), then there exists a stationary solution of equation (5-5):

$$\begin{cases} x_1 = -w_{12}y_2^0 - \beta y_1^0 + s_1 \\ v_1 = y_1^0 \\ x_2 = -w_{21}y_1^0 - \beta y_2^0 + s_2 \\ v_2 = y_2^0 \end{cases} \tag{5-25}$$

Lemma 5.1: *Oscillator equation (5-5) has at least one stationary solution.*

The above Lemma 5.1 can be proven by showing that G is a continuous, contractive mapping [Matsuoka (1985)].

Lemma 5.2: *For a symmetric, mutually inhibitory neural oscillator (equation (5-3)), i.e.* $w_{12} = w_{21} = w > 0$, *the above two-neuron oscillator unit (5-5) has no stable stationary solution if and only if the following hold*

$$w/(1+\beta) \le r_2 / r_1, \text{and } w > (1 + \tau/T) \tag{5-26}$$

Theorem 5.3: *The modified neural oscillator (equation (5-5)) with symmetric, mutually inhibitory connections has no stable stationary solution when the following conditions are satisfied*

$$w/(1+\beta) \le s_2 / s_1 \text{ and } w > (1 + \tau_1 / \tau_2) \tag{5-27}$$

The proof of this theorem is a straightforward application of the above Lemma 5.2 to equation (5-5).

In summary, from theorem 1 and theorem 2, we know the existence and uniqueness of the neural oscillator's dynamic solution and its boundedness. When the condition (5-26) holds, no stable stationary solution exists (Theorem 5.3). Therefore, the modified oscillator is guaranteed to have bounded oscillation.

5.3.4 Finding the limit cycle

Limit cycle is one of the bounded oscillation behaviors, which includes chaotic motion within certain bounds. However, using piece-wise linear analysis to find the limit cycle,

we can rule out the possibility of chaotic behavior. If a limit cycle exists for a given oscillator circuit, we say that it has periodic oscillation.

Considering the oscillator model of equation 5-5, we can use the piece-wise linear analysis technique described in Chapter 3 to find the conditions required for the existence of a limit cycle. First we formulate the model into piece-wise linear systems with several switching surfaces and then we derive the condition for the existence of a limit cycle.
The piece-wise linear system equations of model (5-5) are as follows,

Systems:

$$\dot{\underline{x}} = A_\alpha \underline{x} + B_\alpha \underline{u} \tag{5-28}$$

where $\underline{x} = (x_1 \quad x_2 \quad v_1 \quad v_2)^T$, $\underline{u} = (s_1 \quad s_2)^T$, $\alpha \in \{1,2,3,4\}$.
Switching surfaces:

$$\begin{aligned} S_1 &: x_1 = 0 \\ S_2 &: x_2 = 0 \end{aligned} \tag{5-29}$$

Two switching surfaces partition the state space into four different regions, where the local dynamics are linear. Figure 5-3 shows such partitions and a limit cycle of the oscillator. The limit cycle does not enter quadrant III for this oscillator model.

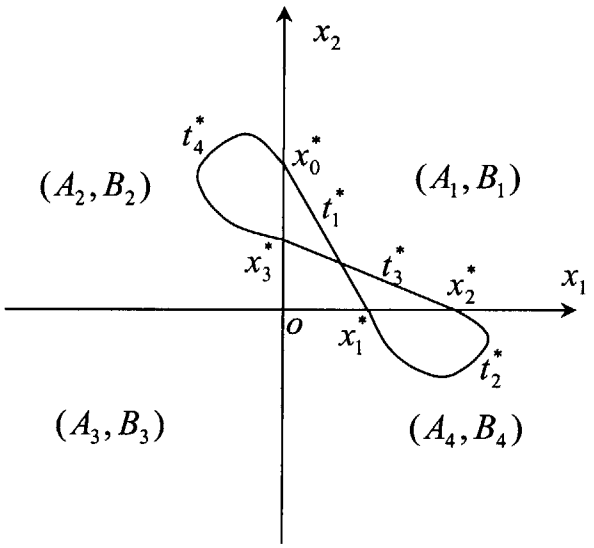

Figure 5-3: A limit cycle of the oscillator (5-5), and the piece-wise linear dydnamics.

System I: (A_1, B_1), $D = \{x_1 > 0, x_2 > 0\}$

$$A_1 = \begin{bmatrix} -\frac{1}{\tau_1} & -\frac{w_{12}}{\tau_1} & -\frac{\beta}{\tau_1} & 0 \\ -\frac{w_{21}}{\tau_1} & -\frac{1}{\tau_1} & 0 & -\frac{\beta}{\tau_1} \\ \frac{1}{\tau_2} & 0 & -\frac{1}{\tau_2} & 0 \\ 0 & \frac{1}{\tau_2} & 0 & -\frac{1}{\tau_2} \end{bmatrix}, \quad B_1 = \begin{bmatrix} \frac{1}{\tau_1} & 0 \\ 0 & \frac{1}{\tau_1} \\ 0 & 0 \\ 0 & 0 \end{bmatrix}$$

System II: (A_2, B_2), $D = \{x_1 < 0, x_2 > 0\}$

$$A_2 = \begin{bmatrix} -\frac{1}{\tau_1} & -\frac{w_{12}}{\tau_1} & -\frac{\beta}{\tau_1} & 0 \\ 0 & -\frac{1}{\tau_1} & 0 & -\frac{\beta}{\tau_1} \\ 0 & 0 & -\frac{1}{\tau_2} & 0 \\ 0 & \frac{1}{\tau_2} & 0 & -\frac{1}{\tau_2} \end{bmatrix}, \quad B_2 = \begin{bmatrix} \frac{1}{\tau_1} & 0 \\ 0 & \frac{1}{\tau_1} \\ 0 & 0 \\ 0 & 0 \end{bmatrix}$$

System III: (A_3, B_3), $D = \{x_1 < 0, x_2 < 0\}$

$$A_3 = \begin{bmatrix} -\frac{1}{\tau_1} & 0 & -\frac{\beta}{\tau_1} & 0 \\ 0 & -\frac{1}{\tau_1} & 0 & -\frac{\beta}{\tau_1} \\ 0 & 0 & -\frac{1}{\tau_2} & 0 \\ 0 & 0 & 0 & -\frac{1}{\tau_2} \end{bmatrix}, \quad B_3 = \begin{bmatrix} \frac{1}{\tau_1} & 0 \\ 0 & \frac{1}{\tau_1} \\ 0 & 0 \\ 0 & 0 \end{bmatrix}$$

System IV: (A_4, B_4), $D = \{x_1 > 0, x_2 < 0\}$

$$A_4 = \begin{bmatrix} -\frac{1}{\tau_1} & 0 & -\frac{\beta}{\tau_1} & 0 \\ -\frac{w_{21}}{\tau_1} & -\frac{1}{\tau_1} & 0 & -\frac{\beta}{\tau_1} \\ \frac{1}{\tau_2} & 0 & -\frac{1}{\tau_2} & 0 \\ 0 & 0 & 0 & -\frac{1}{\tau_2} \end{bmatrix}, \quad B_4 = \begin{bmatrix} \frac{1}{\tau_1} & 0 \\ 0 & \frac{1}{\tau_1} \\ 0 & 0 \\ 0 & 0 \end{bmatrix}$$

With respect to a symmetric neural oscillator unit in (5-5), we have $w_{12} = w_{21} = w$. The limit cycle is symmetric with respect to surface $x_1 = x_2$.

Assume there exists a limit cycle for the above neural oscillator. The conditions for the existence of a limit cycle are derived as follows. In Figure 5-3, we assume that x_i^*, $i \in \{0,1,2,3,4\}$, are the points where the limit cycle crosses switching surfaces S_1, S_2.
Let t_j^* be the transition time from x_{j-1}^* to x_j^*, $j \in \{1,2,3,4\}$.

Theorem 5.4: *Consider the oscillator model (5-5) as a piece-wise linear system. Assume there exists a periodic solution γ with four switches per cycle and with period $t^* = t_1^* + t_2^* + t_3^* + t_4^* > 0$, where t_j^*, $j \in \{1,2,3,4\}$ are defined as above. Define*

$$\begin{cases} g_1(t_1^*, t_2^*, t_3^*, t_4^*) = C_1 \underline{x}_0^* \\ g_2(t_1^*, t_2^*, t_3^*, t_4^*) = C_2 \underline{x}_1^* \\ g_3(t_1^*, t_2^*, t_3^*, t_4^*) = C_2 \underline{x}_2^* \\ g_4(t_1^*, t_2^*, t_3^*, t_4^*) = C_1 \underline{x}_3^* \end{cases} \tag{5-30}$$

$$C_1 = [1 \quad 0 \quad 0 \quad 0],\ C_2 = [0 \quad 1 \quad 0 \quad 0]$$

Then the following conditions hold

$$\begin{cases} g_1(t_1^*, t_2^*, t_3^*, t_4^*) = 0 \\ g_2(t_1^*, t_2^*, t_3^*, t_4^*) = 0 \\ g_3(t_1^*, t_2^*, t_3^*, t_4^*) = 0 \\ g_4(t_1^*, t_2^*, t_3^*, t_4^*) = 0 \end{cases} \tag{5-31}$$

and the periodic solution is governed by the linear sub-systems respectively as shown in figure 5-3. Furthermore the periodic solution γ is obtained with any of the following initial conditions:

$$\underline{x}(0) = \underline{x}_0^*, \text{ or } \underline{x}_1^*, \text{ or } \underline{x}_2^*, \text{ or } \underline{x}_3^*$$

where

$$\begin{aligned} x_0^* &= (1 - E_4E_3E_2E_1)^{-1} I_0 \\ x_1^* &= (1 - E_1E_4E_3E_2)^{-1} I_1 \\ x_2^* &= (1 - E_2E_1E_4E_3)^{-1} I_2 \\ x_3^* &= (1 - E_3E_2E_1E_4)^{-1} I_3 \end{aligned} \tag{5-32}$$

$$\begin{aligned} I_0 &= E_4Z_2 + E_4E_3Z_1 + E_4E_3E_2Z_4 + E_4E_3E_2E_1Z_1 - E_4E_3E_2Z_1 - E_4E_3Z_4 - E_4Z_1 - Z_2 \\ I_1 &= E_1Z_1 + E_1E_4Z_2 + E_1E_4E_3Z_1 + E_1E_4E_3E_2Z_4 - E_1E_4E_3Z_4 - E_1E_4Z_1 - E_1Z_2 - Z_1 \\ I_2 &= E_2Z_4 + E_2E_1Z_1 + E_2E_1E_4Z_2 + E_2E_1E_4E_3Z_1 - E_2E_1E_4Z_1 - E_2E_1Z_2 - E_1Z_1 - Z_4 \\ I_3 &= E_3Z_1 + E_3E_2Z_4 + E_3E_2E_1Z_1 + E_3E_2E_1E_4Z_2 - E_3E_2E_1Z_2 - E_3E_2Z_1 - E_3Z_4 - Z_1 \end{aligned} \tag{5-33}$$

$$E_1 = e^{A_1 t_1^*},\ E_2 = e^{A_4 t_2^*},\ E_3 = e^{A_1 t_3^*},\ E_4 = e^{A_2 t_4^*},\ Z_i = A_i^{-1} B u,\ i \in \{1,2,3,4\}.$$

The proof of the Theorem 5.4 is provided in Appendix B.

Example 5-2: Finding the limit cycle. For example 5-1, the limit cycle exists. It has following information:

$$\begin{aligned} x_0^* &= (0 \quad 0.7528 \quad 1.8679 \quad 1.6787)' \\ x_1^* &= (2.0693 \quad 0.7535 \quad 0 \quad 1.0645)' \\ x_2^* &= (1.8678 \quad 1.6792 \quad 0 \quad 0.7521)' \\ x_3^* &= (0 \quad 1.6053 \quad 2.0687 \quad 0.7530)' \\ t_1^* &= t_3^* = 0.0679 \\ t_2^* &= t_4^* = 0.2859. \end{aligned}$$

5.3.5 Local stability of a limit cycle

Assume there exists a periodic solution, i.e. limit cycle. A limit cycle is locally stable if states within a local neighborhood are attracted to the limit cycle. Consider the map T from some point in a small neighborhood of x_0^* in switching surface S_k, $k \in \{1,2\}$, to the point where the trajectory returns to S_k. Local stability of a limit cycle can be determined by looking at the poles of the linear part of the map T. Stability follows if the poles are inside the unit disk. The following theorem gives conditions for local stability of limit cycles of piece-wise linear systems.

Theorem 5.5: *Consider the above neural oscillator model (5-5). Assume that there exists a limit cycle γ with period $t^* = t_1^* + t_2^* + t_3^* + t_4^* > 0$ as described above. Assume also the limit cycle is transversal to (i.e. crossing) the switching surfaces S_1, S_2 at x_j^*, $j \in \{1,2,3,4\}$ as described in figure 5-3. The Jacobian of the map T defined above is given by $W = W_4 W_3 W_2 W_1$ where*

$$W_1 = (I - \frac{v_1 C_2}{C_2 v_1}) e^{A_1 t_1^*} \tag{5-34}$$

$$W_2 = (I - \frac{v_2 C_2}{C_2 v_2}) e^{A_4 t_2^*} \tag{5-35}$$

$$W_3 = (I - \frac{v_3 C_1}{C_1 v_3}) e^{A_1 t_3^*} \tag{5-36}$$

$$W_4 = (I - \frac{v_4 C_1}{C_1 v_4}) e^{A_2 t_4^*} \tag{5-37}$$

with $v_1 = A_1 x_1^* + Bu$, $v_2 = A_4 x_2^* + Bu$, $v_3 = A_1 x_3^* + Bu$, $v_4 = A_2 x_4^* + Bu$. *The limit cycle γ is locally stable if W has all its eigenvalues inside the unit disk. It is unstable if at least one of the eigenvalues of W is outside of unit disk.*

Proof: Assume there exists a limit cycle γ with period $t^* = t_1^* + t_2^* + t_3^* + t_4^* > 0$. The limit cycle is transversal to the switching surfaces S_1 and S_2 at x_0^*, x_1^*, x_2^*, x_3^*, x_4^* as described in figure 5-3. Consider a trajectory with initial condition $x(0) = x_0^*$.

$$\Rightarrow x(t_1^*) = x_1^* = e^{A_1 t_1^*}(x_0^* + A_1^{-1}Bu) - A_1^{-1}Bu$$

Now let $x(0) = x_0^* + \delta_1 x_0^* \in S_1$

$$\Rightarrow C_1 x(0) = C_1(x_0^* + \delta_1 x_0^*) = 0$$

$$\Rightarrow x(t) = e^{A_1 t}(x_0^* + \delta_1 x_0^* + A_1^{-1}Bu) - A_1^{-1}Bu$$

Assume the solution reaches the switching surface S_2 at time $t_1^* + \delta_1 t_1^*$.

$$\Rightarrow x(t_1^* + \delta_1 t_1^*) = e^{A_1(t_1^* + \delta_1 t_1^*)}(x_0^* + \delta_1 x_0^* + A_1^{-1}Bu) - A_1^{-1}Bu$$

Making a Taylor series expansion in $\delta_1 x_0^*$ and $\delta_1 t_1^*$, we get

$$x(t_1^* + \delta_1 t_1^*) = x_1^* + e^{A_1 t_1^*}\delta_1 x_0^* + e^{A_1 t_1^*}(A_1 x_0^* + Bu)\delta_1 t_1^* + o(\delta_1^2)$$

where $e^{A_1 t_1^*}(A_1 x_0^* + Bu) = A_1 x_1^* + Bu = v_1$.

$\because \quad x(t_1^* + \delta_1 t_1^*) \in S_1$

$\therefore \quad C_2 \cdot x(t_1^* + \delta_1 t_1^*) = 0$.

$\Rightarrow \quad C_2 \cdot x_1^* + C \cdot e^{A_1 t_1^*} \delta_1 x_0^* + C_1 v_1 \delta_1 t_1^* = 0$

$C_2 \cdot x_1^* = 0 \quad (\because \ x_1^* \in S_1)$

Assume that the limit cycle is transversal to S_1 at x_1^*, then $C_2 \cdot \dot{x}(t_1^*) \neq 0$.

$\Rightarrow C_2(A_1 x_1^* + Bu) \neq 0$, or $C_2 \cdot v_1 = 0$.

$$\Rightarrow \delta_1 t_1^* = -\frac{C_2 e^{A_1 t_1^*}}{C_2 v_1} \delta_1 x_0^*$$

$$\Rightarrow x(t_1^* + \delta_1 t_1^*) = x_1^* + (I - \frac{v_1 C_2}{C_2 v_1}) e^{A_1 t_1^*} \delta_1 x_0^* + o(\delta_1^2)$$

$$= x_1^* + W_1 \delta_1 x_0^* + o(\delta_1^2)$$

Similarly, we can derive

$$x(t_2^* + \delta_2 t_2^*) = x_2^* + W_2 \delta_2 x_1^* + o(\delta_2^2)$$

$$W_2 = (I - \frac{v_2 C_2}{C_2 v_2}) e^{A_4 t_2^*}$$

$$v_2 = e^{A_4 t_2^*}(A_4 x_1^* + Bu) = A_4 x_2^* + Bu$$

with initial condition $x_1^* + \delta_2 x_1^* = x_1^* + W_1 \delta_1 x_0^* + o(\delta_1^2)$.

Neglecting high order terms, we get

$$\delta_2 x_1^* = W_1 \delta_1 x_0^*$$

$$\Rightarrow \quad x(t_2^* + \delta_2 t_2^*) = x_2^* + W_2 W_1 \delta_1 x_0^* + o(\delta_1^2).$$

Repeat the above procedure until the solution reaches switching surface S_0 after time interval t_4^*. Then we get

$$x(t_4^* + \delta_4 t_4^*) = x_4^* + W_2 \delta_4 x_3^* + o(\delta_4^2)$$

$$= x_0^* + W_4 W_3 W_2 W_1 \delta_1 x_0^* + o(\delta_1^2)$$

where $x_4^* = x_0^*$,

$$W_3 = (I - \frac{v_3 C_1}{C_1 v_3}) e^{A_1 t_3^*}$$

$$W_4 = (I - \frac{v_4 C_1}{C_1 v_4}) e^{A_2 t_4^*}$$

$$v_3 = e^{A_1 t_3^*}(A_1 x_2^* + Bu) = A_1 x_3^* + Bu$$

$$v_4 = e^{A_2 t_4^*}(A_2 x_3^* + Bu) = A_2 x_3^* + Bu$$

This proves the theorem. *Q.E.D.*

Example 5-3: Local Stability. For example 5-1, the limit cycle of the neural oscillator is locally stable. The matrix $W = W_4 W_3 W_2 W_1$ has all the eigenvalues inside the unit disk:

{0.0033, 0.0003, 0, 0}. Figure 5-4 shows a limit cycle of oscillator example 5-1. The oscillator converges to the limit cycle from different quadrants.

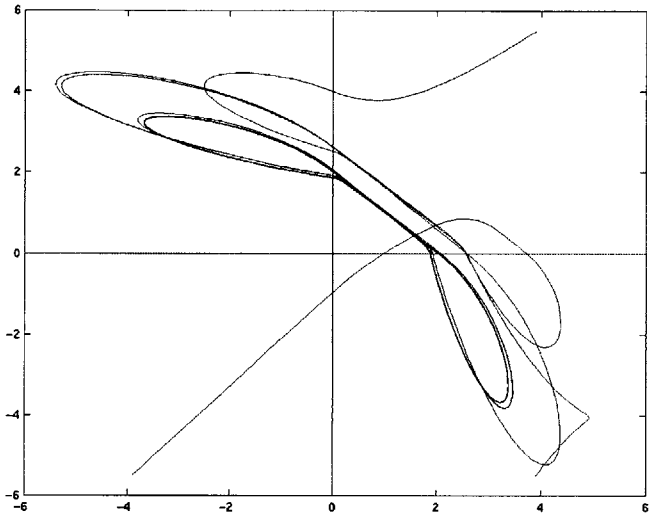

Figure 5-4: The limit cycle of example 5-1. The oscillator can converge to its limit cycle from four different quadrants.

5.3.6 Global stability of limit cycle

In the above analysis for Matsuoka's neural oscillator model, we have investigated the properties of the oscillator (5-5), have given the conditions for the existence of a limit cycle. The locally stability of a limit cycle has also been studied in an analytic way.

From our observations, when we have achieved a periodic oscillation with the neural oscillator model, we always have the properties, the local stability and global stability with the entrainment signal e not equal to zero. What conditions should be satisfied for an oscillator in order to have global stability of a limit cycle? If one can prove the global stability of a limit cycle for an given oscillator then the system analysis will become relatively simpler when the oscillator is applied to drive a plant for achieving periodic motion.

However, we observed a special case, in which the neural oscillator may not have periodic behavior. It may converge to a particular state. Figure 5-5 shows such an example. With a symmetric neural oscillator model (5-5), when the entrainment signal e is zero and the initial state for two neurons are identical the oscillator does not have a periodic behavior, instead it converges to a fixed point.

In general, it is very hard to characterize the region of stability of limit cycles. With the uniqueness and existence of a limit cycle, we can explore the global stability of a limit cycle for the neural oscillator. A surface Lyapunov function based method can be applied in the analysis, which Gonçalves et al (2000) have applied successfully in the relay feedback systems. This approach can be used for investigating the conditions for the global stability of limit cycle.

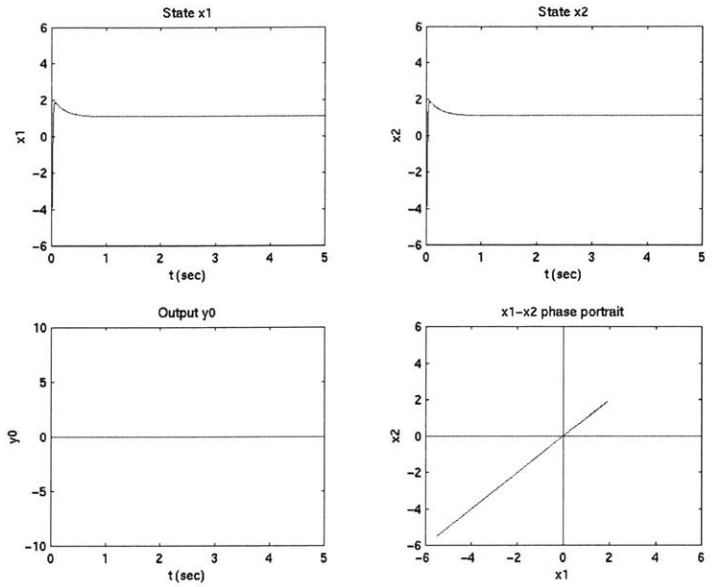

Figure 5-5: A special case: the oscillator converges to a fixed state.

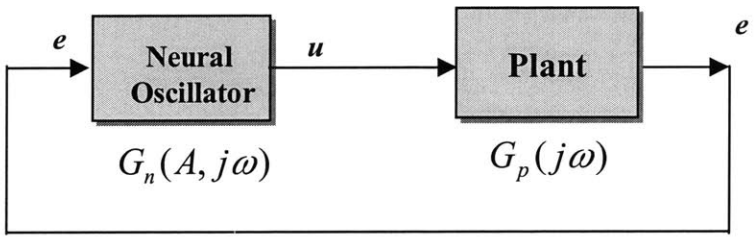

Figure 5-6: Diagram of an oscillator driven control system.

5.4 Rhythmic Control with Neural Oscillators

Use of neural oscillators to propel rhythmic motion of a plant was motivated by physiological research [Grillner (1985), Taga (1995)]. The general system structure of neural oscillator driven rhythmic control is shown in Figure 5-6. In this system, if we cut the sensory feedback loop, then the system becomes an open loop control structure, where the plant responds to the input without guaranteeing synchronous behavior with respect to the oscillator. Therefore, sensory feedback provides the possibility of achieving a synchronized rhythmic motion between the oscillator and the plant, called *entrainment*.

Under what condition, can the entrainment be insured for the above system? Several approaches are useful for the study of the entrainment behaviors, including piece-wise linear analysis in the time domain and analysis with describing functions in the frequency domain. Due to the non-linearity existing in the neural oscillator model, pursuing both a closed-form solution to the system parameters and an analytic design is extremely difficult.

Williamson (1998) used Nyquist plots to explain a graphical design approach in the frequency domain, using describing functions. This approach can be used to check the parameter selection of a neural rhythmic control system to some extent.

5.4.1 Study with a describing function in frequency domain

When a neural oscillator is used to control the rhythmic motion of a plant, like robot arms and legs, the global rhythmic movements are obtained through a process called "entrainment". Because of the nonlinearity in neural oscillator models, theoretical analysis and explainations for the entrainment phenomenon between the neural dynamics and the natural dynamics of the plant is very difficult to give. So far, only simulation reports on the entrainment are available although entrainment has been observed for many years. Taga (1995) used the entrainment concept and constructed neural oscillator driven human like locomotion successfully. The technique used by Williamson is Describing Function.

A common way to connect oscillators to systems is to tightly couple them, using the oscillator output to drive the system, and closing the loop by feeding back a signal from the system as the oscillator input (Figure 5-6). The transient analysis of this coupled system is complex but can easily be expressed in the frequency domain by the describing function method. If the frequency response of the linear plant is $G_p(j\omega)$, and the linearized response of the oscillator at frequency ω and input amplitude A is $G_n(A, j\omega)$, then the condition for a steady state oscillation is that the loop gain is unity:

$$G_n(A, j\omega) \cdot G_p(j\omega) = 1 \qquad (5\text{-}38)$$

Nyquist plots can be used to explain the graphical design approach in the frequency domain [Williamson (1999)], based on the describing function technique. It can be used to check the parameter selection of a neural rhythmic control system to some extent.

Since the frequency domain analysis by a describing function requires an assumption that the control plant has low pass filtering characteristics, only the first order (fundamental) component is considered. The prediction can offer an approximate result, only if the periodic responses of the overall system do not have much deformation, which means that the higher order harmonics are not severe [Slotine and Li (1991)]. In other words, the oscillator output is close to a pure sinusoidal waveform. In the case of robot arm control, this condition can be well satisfied. However, for a general control plant, the low pass filtering assumption may not hold. What if the control plant itself is unstable? We will approach this difficulty by shaping the dynamics of the plant in order to fascillitate the entrainment process.

5.4.2 General control framework

A compensator is added to modify the plant dynamics. Figure 5-7 shows the general diagram for a neural oscillator control system, where the plant dynamics can be linear, nonlinear, or unstable. Recent results for the periodic solution of a nonlinear system assumed that the dynamics beyond the nonlinear components are linear and stable

(Hurwitz) [Goncalves (2000)]. In our system, since the oscillator is nonlinear, we want the plant dynamics to be well shaped such that some existing results can be directly applied.

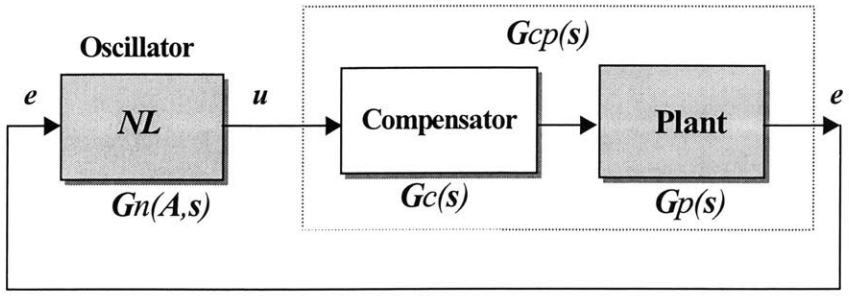

Figure 5-7: Block diagram of the general nonlinear System.

To facilitate analysis in the frequency domain, a compensator is inserted into the system to shape the dynamics of plant so that

a) a desired frequency response can be appropriately adjusted; for example, the pass range of the band-limited filter or the cutoff frequency of the low pass filter can be changed for certain purposes;
b) modifications can be made for an unstable system to be stabilized;
c) the following equality holds with the approximate transfer function $G_n(A, jw)$, which is a function of amplitude A and frequency ω [Slotine & Li (1991)].

$$G_n(A, j\omega) \cdot G_{cp}(j\omega) = 1 \tag{5-39}$$

The results of shaping dynamics are:

a) the describing function based frequency method will be appropriate, i.e. predicting the oscillation frequency and amplitude approximately,
b) entrainment can be guaranteed if a sufficient condition (proved in the following section) holds.

5.4.3 Nonlinear analysis in time domain

When the plant dynamics are linear, piece-wise linear analysis can be applied. Assume that the dynamics equation of the oscillator is formulated as

$$\begin{cases} \dot{\underline{x}} = A_\alpha \underline{x} + B_\alpha \underline{u} \\ y = C\underline{x} \end{cases} \tag{5-40}$$

where $\underline{x} = (x_1 \quad x_2 \quad v_1 \quad v_2)^T$, $\underline{u} = B_0 r + B_\alpha \tilde{y}$

$C = [1 \quad -1 \quad 0 \quad 0]$,

$$B_\alpha = \begin{bmatrix} 1 \\ -1 \\ 0 \\ 0 \end{bmatrix},\ B_0 = \begin{bmatrix} 1 \\ 1 \\ 0 \\ 0 \end{bmatrix},\ \alpha \in \{1,2,3,4\}$$

The dynamics of plant:

$$\begin{cases} \dot{\tilde{x}} = A_p \tilde{x} + B_p \tilde{u} \\ \tilde{y} = C_p \tilde{x} \end{cases} \tag{5-41}$$

Combining the above dynamics together, we get the following augmented dynamic equations:

$$\begin{bmatrix} \dot{\underline{x}} \\ \dot{\tilde{x}} \end{bmatrix} = \begin{bmatrix} A_\alpha & B_\alpha C_p \\ B_p C & A_p \end{bmatrix} \begin{bmatrix} \underline{x} \\ \tilde{x} \end{bmatrix} + \begin{bmatrix} B_0 \\ 0 \end{bmatrix} r \tag{5-42}$$

Based on this augmented dynamics equation, we can apply the piece-wise analysis with two switching surfaces S_1, S_2. The results are introduced in next section.

5.5 Entrainment between Neural Oscillator and Plant

5.5.1 Analysis in frequency domain

Considering the control system shown in Figure 5-7, a theorem can be derived as a sufficient condition for the entrainment of rhythmic dynamics in the frequency domain.

Theorem 5.6: *Boundedness of system. For a system as shown in Figure 5-7, if $G_{cp}(s)$ is stable and LTI, or is stabilized by $G_c(s)$, then the whole system is bounded.*

Proof: A periodic signal (oscillation) u is not a l^1 nor l^2 signal. It is a power signal,

$$pow(u) = (\lim_{T\to\infty} \frac{1}{T} \int_{-T}^{T} u^2(t)dt)^{\frac{1}{2}} < C \tag{5-43}$$

where C is a constant. Since both u (input to plant) and e (output of plant) are power signals, the induced norm for the plant is $\left\|\hat{G}_{cp}(jw)\right\|_\infty$. Assume $G_{cp}(s)$ is stabilized, i.e. no poles in RHP, then $\left\|\hat{G}_{cp}(jw)\right\|_\infty$ is bounded, and the output signal e is bounded. From theorem 5.5, given bounded input, the solution of the oscillator is bounded, hence it is also bounded for power signals.

$$\left\|\hat{G}_{cp}(jw)\cdot\hat{G}_n(A,jw)\right\|_\infty \le \left\|\hat{G}_{cp}(jw)\right\|_\infty \cdot \left\|\hat{G}_n(A,jw)\right\|_\infty \tag{5-43a}$$

Therefore, the whole system is bounded for power signals.

By using the describing-functions technique, a sufficient condition for entrainment is given in the frequency domain, which was analytically illustrated in a report [Hu (1999a)].

5.5.2 Piece-wise analysis in time domain

With the augmented system dynamics, we can apply the same approach used in section 5.4.3 in order to analyze the periodic behavior of the whole system and study the entrainment, i.e. synchronization.

Since the nonlinearity is only from the oscillator itself in this case (with linear plant), the switching surfaces are still the same, namely S_1, S_2. Therefore, the results from Theorem 5.4 and Theorem 5.5 can be directly applied with the augmented dynamic matrices.

Theorem 5.7: *Sufficient condition of entrainment. The system (in Figure 5-7) has a entrained oscillation if the followings are true:*

(a) $G_{cp}(s)$ *is LTI and stable;*

(b) the oscillator has symmetric connections and the inequality (5-26) holds;

(c) equation (5-31) holds;

(d) the augmented system (5-42) has no stable stationary solution.

Proof: From theorem 4, the overall system is bounded. Since equation (5-26) is satisfied, then by Theorem 5.3, there is no stable stationary solution of equation (5-5) (for the oscillator part). By Theorem 5.1, a solution of equation (5-5) with any initial states is unique.

As a closed-loop system, the stabilized LTI plant and the neural oscillator model both satisfy the Lipschitz condition separately, thus the composite system in (5-42) also satisfies the Lipschitz condition. Then the whole system consisting of neural oscillator and a compensated LTI plant has a unique solution. With condition (d), we know that there is no stable stationary solution for the composite system. Therefore, the system has an oscillation solution. Furthermore, with condition (c) satisfied, the limit cycle exists for the system. Hence entrainment is achieved.

For predicting the final frequency of the system, condition (5-31) or the Nyquist plot can be used. Also, harmonic analysis can be executed to predict the entrainment frequency [Williamson (1999)].

Design procedure for neural oscillator control:

From the above theory, a design procedure is presented for rhythmic control of a nonlinear plant with neural oscillators:

Step 1: use condition (5-26) to determine the oscillator parameters;

Step 2: use a compensator to stabilize the linearized (if nonlinear plant) plant model;

Step 3: check if condition (5-31) is satisfied with the composite system;

Step 4: check if the augmented piece-wise linear system (5-42) has no stable stationary solutions.

Step 5: Test the entrainment by simulation.

5.6 Examples

We use a pendulum model and an inverted pendulum model as examples for demonstrating the above theory.

5.6.1 Rhythmic control of a pendulum

The dynamic equation of a pendulum is given by

$$ml^2\ddot{\theta} + b\dot{\theta} + mgl\sin(\theta) = r \tag{5-44}$$

This pendulum model is stable, so no compensator is required for shaping the plant dynamics. A two-neuron oscillator controlled rhythmic movement is shown in Figure 5-8. Clearly, a limit cycle is reached.

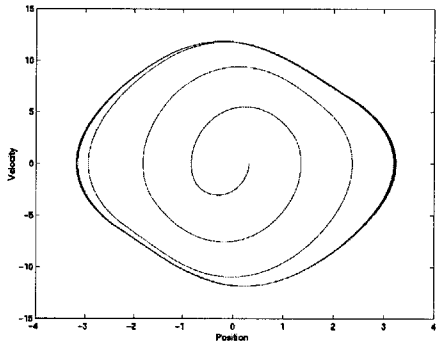

Figure 5-8: Phase plot of responses in pendulum control.

5.6.2 Rhythmic control of an inverted pendulum

The dynamic equation of an inverted pendulum model is,

$$ml^2\ddot{\theta} + b\dot{\theta} - mgl\sin(\theta) = r \tag{5-45}$$

This inverted pendulum model is unstable, but a compensator with state feedback can stabilize it. Equation (5-46) shows the dynamics of such a compensator.

$$\tau = -(k_1\dot{\theta} + k_2\theta) \tag{5-46}$$

Figure 5-9 shows the response of the neural oscillator controlled inverted pendulum without a compensator. The response shows that entrainment cannot exist in this case. But with compensation, entrainment can be achieved. A stable rhythmic response is shown in Figure 5-10. In this example, the compensator was designed based on the linearized model of inverted pendulum. The simulation results with the linearized model are very similar to those obtained with nonlinear model.

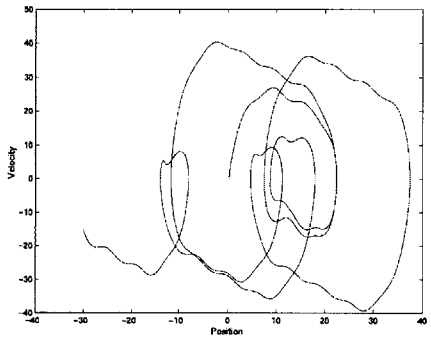

Figure 5-9: Phase plot of responses in inverted pendulum without compensator.

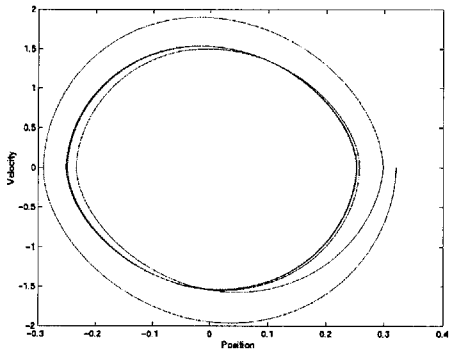

Figure 5-10: Phase plot of responses in inverted pendulum with compensator.

5.7 Conclusions

The existence and uniqueness of solution to the modified neural oscillator unit has been proved by means of Lipschitz condition. It has been shown that the neural oscillator can achieve stable rhythmic dynamic motion with certain conditions. The entrainment condition for a neural oscillator unit interacting under a passive plant is studied in time domain and frequency domain.

A compensator based design approach is presented for neural oscillator control systems. Using the sufficient condition of entrainment derived in this thesis, a design procedure is proposed for rhythmic control with neural oscillators. The concept and procedure have been demonstrated with simple examples such as pendulum and inverted pendulum models. The compensator based design approach can be used in dynamics shaping of the plant.

Chapter 6

Bipedal Locomotion Control with Neural Oscillators

The neural oscillator model studied in Chapter 5 can be directly applied to systems whose dynamics are fixed during the operating processes, such as robot arm control [Williamson (1999)]. For a bipedal walking robot, however, the dynamics are changing in different walking states, and proper coordination is required for generating locomotion. How to construct a neural oscillator network with the oscillator modules (described in previous chapter) for the joint control of a bipedal robot is the focus of this chapter. The goals in bipedal locomotion control with oscillators are two-fold: utilize the results developed in Chapter 5 for local joint control of the biped and construct the neural oscillator network with the local oscillator modules such that the biped can achieve a collectively synergetic skeletal motion (called synchronized coordination). The sensory feedback and organization of neural oscillator network are described here in details as follows.

6.1 Overall Structure of the Control System

Based the analytic results from the previous chapter, two things are important for controlling a bipedal walking robot with neural oscillator units. First, the local joint control should be designed properly so that the entrainment in the local control system is guaranteed. Second, the overall distributed neural control system should be able to generate a synergetic rhythmic motion for the bipedal skeletal system, called stable locomotion. A neural oscillator driven controller for a bipedal robot system is constructed based on these considerations.

Figure 6-1 shows a complete architecture of a bipedal locomotion control system driven by neural oscillators. There are five major components in this system: the neural oscillator module, the compensators, sensory feedback module, the state observer, and the impedance control module. The neural oscillator module generates and coordinates the rhythmic motion for robot joints. It takes the sensory feedback signals from the sensory feedback module and evolves to the common rhythm for the driven system and the oscillator with self-organization. The impedance control module provides the proper postural control and structure dynamics for the biped. The state observer detects the actually walking state and consequently adjusts the sensory feedback signals for

providing correct information to the neural oscillators. The neural oscillator driven control provides the bipedal control system with proper locomotion and a closed loop gait control mechanism through the sensory feedback and entrainment between the neural dynamics and the musculo-skeletal dynamics of the biped.

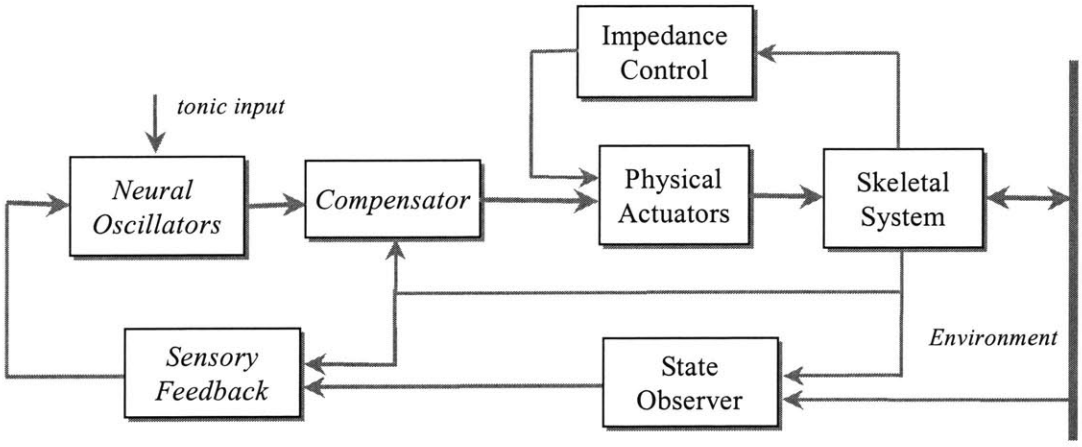

Figure 6-1: System Architecture for Neural Oscillator Control of a Bipedal Walking Robot.

6.2 Local Control with Neural Oscillators

A general framework is proposed for designing the nonlinear neural oscillator based rhythmic control. In Figure 6-2, a compensator is used to shape the dynamics of the plant. From the results of the previous chapter, we found out that the entrainment cannot be achieved with a Matsuoka's neural oscillator module if the plant is unstable (like an inverted pendulum) [Hu (1999b)]. Using a compensator, the sufficient condition for the entrainment between the neural dynamics and the natural dynamics of the plant can be used as a guideline for designing and tuning neural oscillator (CPG) based locomotion control.

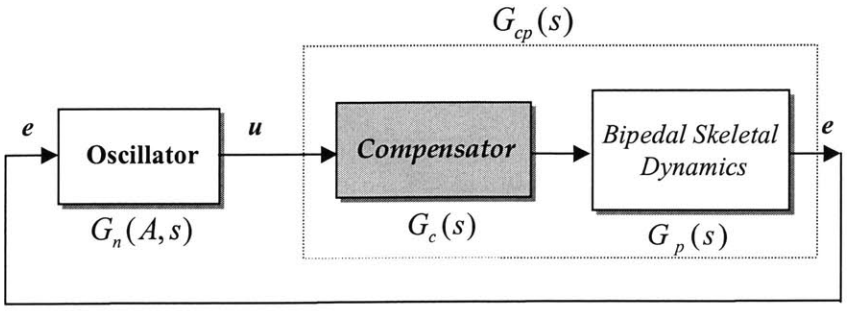

Figure 6-2: Block diagram of the general nonlinear System.

Figure 6-3 shows a neural oscillator driven control sub-system for one joint of a bipedal robot. The driving signals are generated by means of the neural oscillator module. The impedance control provides necessary local control for postural stability. A compensator is selected to modify the skeletal dynamics such that the dynamic entrainment can be achieved in the control. The sensory feedback link provides the closed loop coupling for the neural dynamic module with the bipedal natural dynamics (structural dynamics).

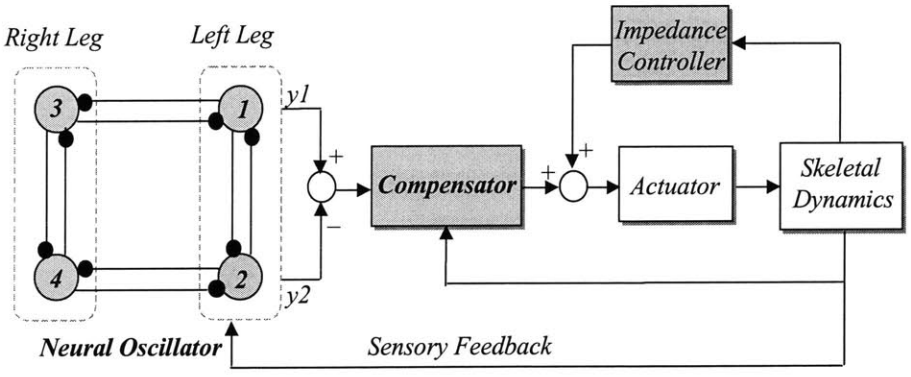

Figure 6-3: Neural oscillator based control of one joint in a bipedal walking robot.

The motion of two legs can be considered as similar to a pendulum and an inverted pendulum as analyzed in the previous section. For instance, the motion of a swing leg is similar to the motion of a pendulum, and the motion of a stance leg is similar to that of an inverted pendulum (Figure 6-4). A compensator is needed for the stance leg control since in that case the dynamic model of a joint in the stance leg is an inverted pendulum (an unstable system). In the following sections, we describe a control model for one joint in the bipedal walking robot.

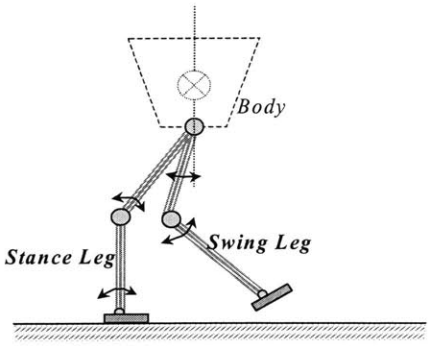

Figure 6-4: A bipedal walking robot with one stance leg and one swing leg.

6.2.1 Neural oscillator module

The rhythmic motion of a joint is driven by a neural oscillator module described in Figure 6-3. The neural oscillator module is composed of four neurons with symmetric mutually inhibitory connections. There are two sets of neural oscillator units, one for the joint in each leg. The mutually inhibitory connections establish a 180-degree out of phase in the motion of two respective joints in each leg. The output $y_1 - y_2$ is for a joint on the left leg, and $y_3 - y_4$ is for a right leg joint.

6.2.2 Local controller

The compensator dynamic equation is described as

$$\tau_{ci} = -(k_1\dot{\theta}_i + k_0\theta_i) \tag{6-1}$$

where k_1 and k_0 are constants, and θ_i is the angular position signal corresponding to joint i.
The impedance control is expressed as

$$\tau_{pi} = \alpha_1(\theta_{di} - \theta_i) - \alpha_2\dot{\theta}_i) \tag{6-2}$$

where α_1 and α_2 are constants and θ_{di} and θ_i are the desired position and actual position signals corresponding to joint i, respectively.
The oscillator control is

$$\tau_{oi} = k_3\theta_i^* \tag{6-3}$$

where θ_i^* is the output of the corresponding neural oscillator for joint i.

The total control signal for the joint actuator is the summation of the oscillator control, the compensator output, and the impedance control.

6.3 Sensory Feedback and Entrainment of Neuro-muscular-skeletal Dynamics

Sensory feedback plays a very important role in the motor-sensory dynamic control system (Figure 6-3). Since the dynamics change periodically during bipedal walking, the sensory feedback signals are selected appropriately according to a global state machine.

The global state variables and walking phases are illustrated in Figure 6-5. A variable ϕ is defined as the angular position of the leading stance leg (in double support) or the stance leg (in single support) with respect to the vertical plane crossing the hip joints. We use ϕ as a global gait variable in distinguishing two single support phases. When $\phi < 0$ the biped is in single support phase I, i.e. toe-off phase, while it is in single support phase II if $\phi \geq 0$. There are a total of six walking phases in a cycle: double support I, right single support I, right single support II, double support II, left single support I, left single support II (from left to right in Figure 6-5).

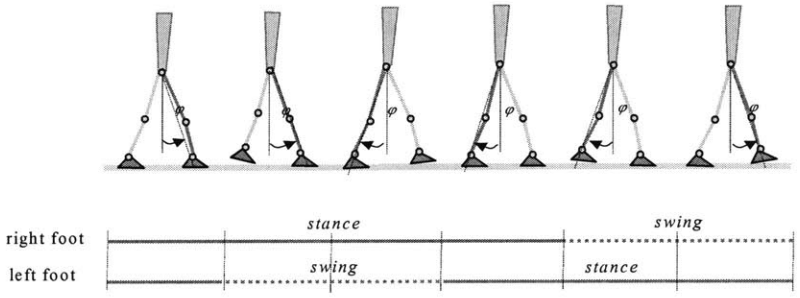

Figure 6-5: Diagram describing the global variable ϕ defined with respect to the right leg. The global states are also defined: double support I, right single support I, right single support II, double support II, left single support I, left single support II (from left to right).

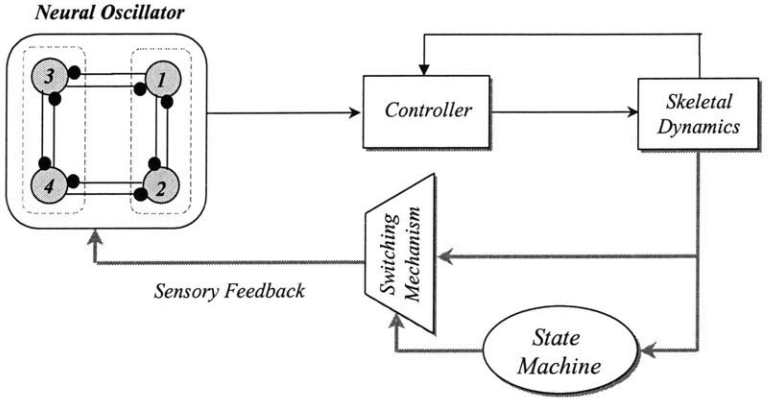

Figure 6-6: Switching in sensory feedback loop. The sensory feedback signal is selected based on the walking state.

The choice of sensory feedback is very crucial for dynamic entrainment. In this design, the angular position and velocity information of the corresponding joint is used for the entrainment feedback. Such a sensory feedback signal consists of the angular position and velocity signals of the connected lower link and the connected upper link with respect to the joint.

Figure 6-6 shows a switching mechanism, which is used to select the appropriate sensory feedback signals. The switching mechanism is dependent on a state machine, which observes the walking phases by means of global gait variable ϕ. The sensory feedback signal selection for knee joint is expressed as

$$f_{knee} = k_{sf}(S_{st} \cdot \theta_{th} + S_{sw} \cdot \theta_{sh}) \tag{6-4}$$

where k_{sf} is a feedback gain for the sensory signal, S_{st} and S_{sw} are the state indication functions for stance phase and swing phases respectively. S_{st} equals *1.0* when the leg is in stance phase and it is zero otherwise. S_{sw} is *1.0* when the leg is in swing phase and it is zero otherwise. θ_{th} and θ_{sh} are, respectively, the thigh angle and shin angle measured with respect to the vertical plane.

6.4 Distributed Neural Oscillator Network

To achieve synergy in the overall control system, connections are needed between the groups of neuron modules. The format and equations of compensators and impedance controller can be the same for each joint, except for the parameters.

A distributed neural oscillator module is required in order to control all the joints in a biped. Figure 6-7 shows a neural oscillator network for controlling a planar bipedal walking robot. There are couplings present between the local neural oscillator units.

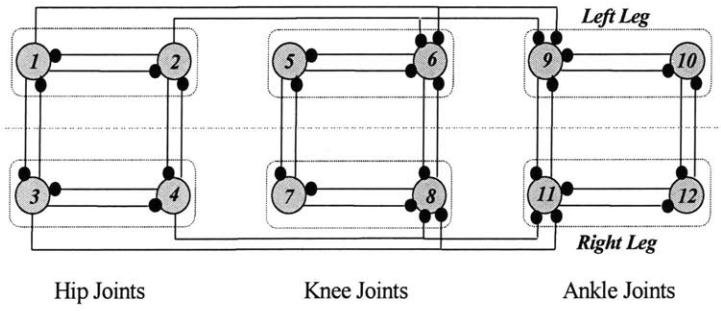

Figure 6-7: Distributed neural oscillator module for a bipedal walking robot.

In Figure 6-7, there are three neural oscillator modules. Each drives the corresponding control model, which includes compensator, and impedance control. The

actuator is commanded by the total effort of oscillator controller, compensator and impedance controller.

6.5 Self-organization

The above control implementation is accomplished through local controllers. Synchronization is achieved by the natural dynamic coupling (or called constraints) of the leg as well as the weighted connections (inhibitory connections) between neural oscillator modules for different joints in each leg. The neural oscillator network can define the phase relationship between the oscillator outputs for different joints. The local controller is the agent, which enforces the corresponding joint to follow the motion generated from oscillator module. The overall synchronous leg motion is realized through a process called *self-organization* of neural muscular skeletal system. Within the network constraints of the distributed neural oscillator modules and the dynamics constraints, the leg motion of the robot evolves into a synergetic motion as robot walks forward. This process can be viewed in the animation and the stick plots of bipedal walking.

6.6 Application in Bipedal Locomotion Control

We applied the neural oscillator driven locomotion control approach to a simulated 7 link planar bipedal walking robot, *Spring Flamingo*. The parameters of this robot are described in Chapter 1. This biped has six joint actuators for the hip, knee and ankle in each leg.

As described in section 6-4, we used distributed neural oscillator modules for bipedal locomotion control. Three neural oscillator modules are used for controlling hip joints, knee joints and ankle joints. Each oscillator module generates command signals for the corresponding joints on the left leg and right leg. Those three neural oscillator modules are connected globally to provide overall dynamic synergy.

In the simulation, the robot starts to walk from zero velocity and then achieves roughly constant walking speed. The entrainment between neural dynamics and the dynamics of the skeletal structure is achieved by means the control system. Figure 6-8 shows the dynamic responses for the angular position signals from left hip joint, left knee joint and left ankle joint, q-lh, q-lk, and q-la respectively on the left column. On the right column are the responses of joint angular velocities of left hip, knee and ankle, qd-lh, qd-lk and qd-la respectively.

Figure 6-9 shows the phase portraits of joint variables of hip, knee and ankle in the left leg. The overall walking gait behavior is shown in a phase plot of a global variable in Figure 6-10. A stick plot is shown in Figure 6-11 for the walking posture of the biped. From the above figures, it is shown that the biped has achieved a stable gait since the global variable reaches a limit cycle.

In the simulations, stable walking has been achieved, and the feasibility of our design method has been demonstrated.

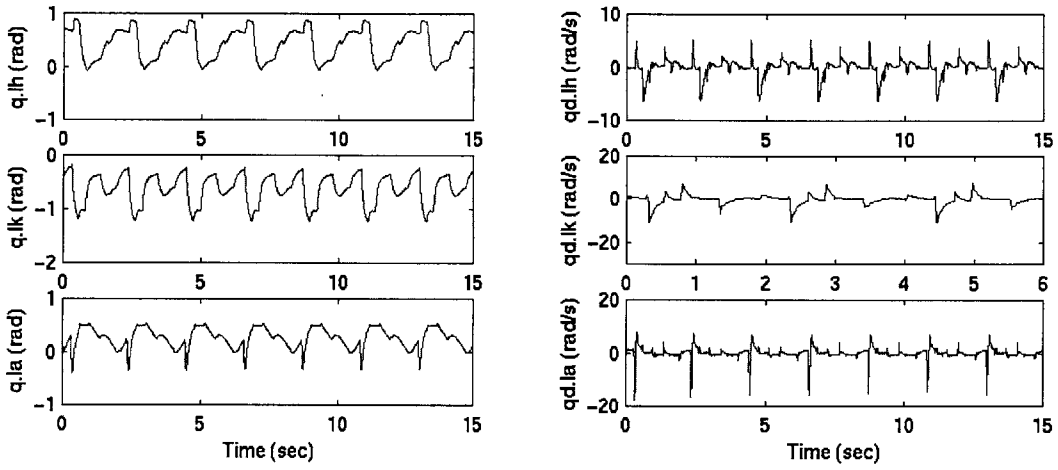

Figure 6-8: Dynamic responses of a bipedal walking robot controlled by neural oscillators.

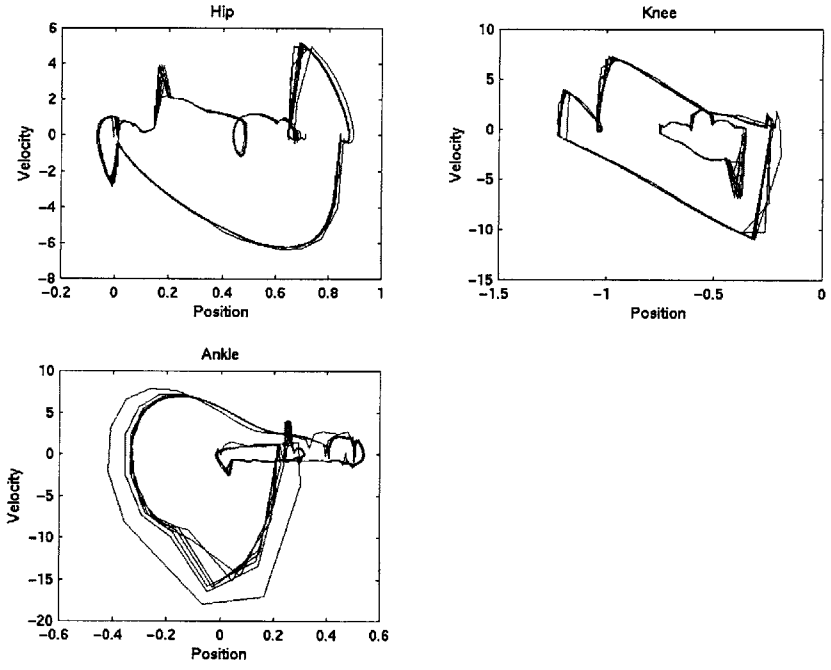

Figure 6-9: The phase portraits of the joint variables in left leg.

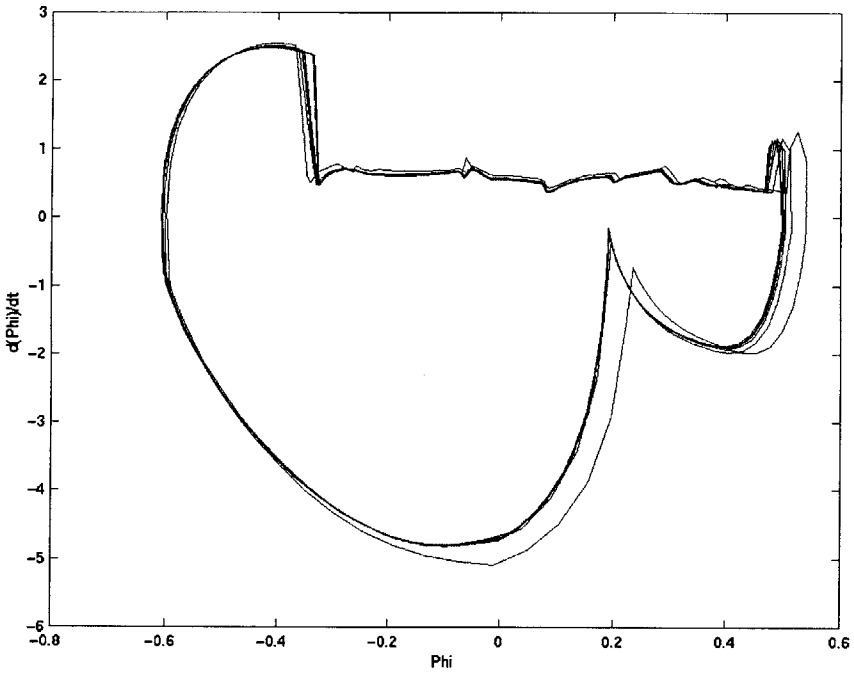

Figure 6-10: Phase portrait of the global variable ϕ in left leg.

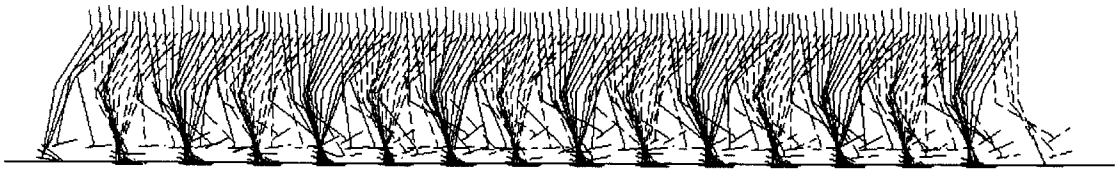

Figure 6-11: Stick plot of simulated bipedal walking.

6.7 Robustness

The robustness analysis for the above control system is very difficult and beyond the scope of this study. Instead we can perform some robustness tests for our system. Figure 6-12 shows the results of robustness test for the simulated biped (*Spring Flamingo*) controlled by neural oscillators. Two tests have been conducted: one is to push the robot in z-direction (vertical direction) with an external force (10 lbs) exerted on the robot body for 0.5 seconds; the other is to apply an external force (10 lbs) in forward (x-direction) for 0.5 seconds. Figure 6-12 shows the results of latter test, in which the robot was pushed forward. The results have shown that the robot has good robustness. It can recover quickly after the disturbance. From the simulations, we observed that the robot had better performance when rejecting external disturbances in z-direction.

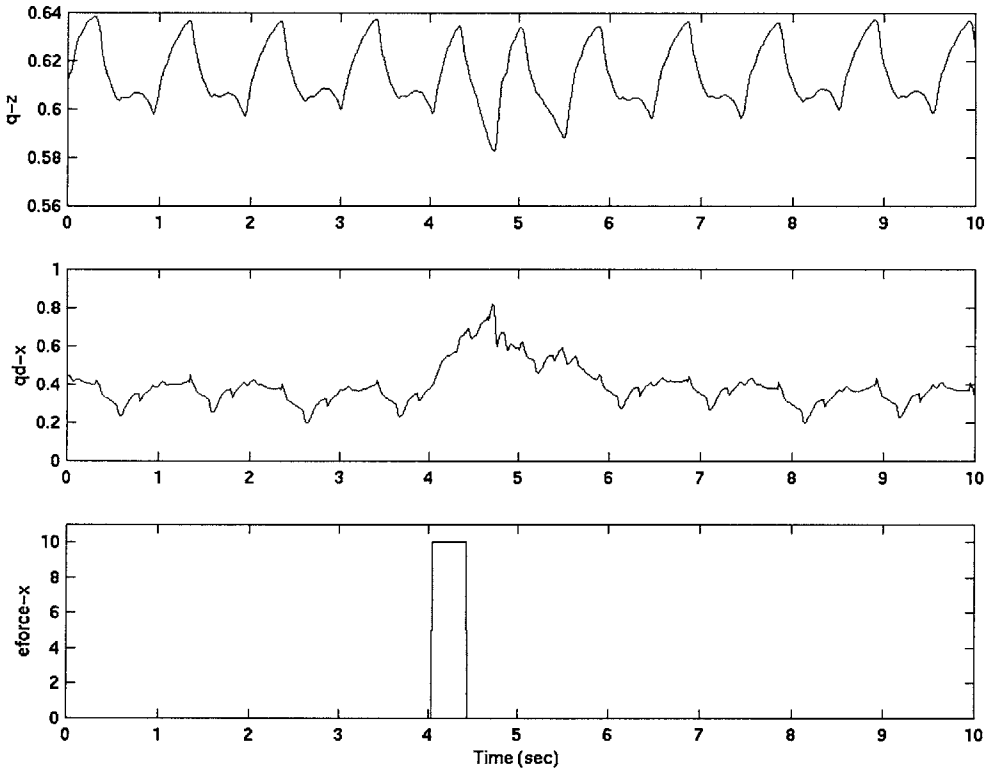

Figure 6-12: Responses of a simulated biped controlled by neural oscillators with an external force disturbance (10 lbs).

6.8 Conclusion

Locomotion control of a bipedal walking robot with neural oscillators is also studied. With local dynamics compensation and impedance control for each joint, the neural oscillators can propel stable walking of the bipedal robot. The guidelines for control design proposed in Chapter 5 have been applied in the local neural oscillator

control for robot joints.

A switching module based sensory feedback mechanism is developed for achieving entrainment between the neural dynamics and the robot's structure dynamics. The overall synergetic motion of the robot legs is achieved by means of a neural oscillator network, which facilitates the neural oscillator modules for hip joints, knee joints and ankle joints of the bipedal robot. A self-organization process is established by the neural dynamics of the oscillator network and the natural dynamics of the robot while bipedal walking proceeds.

Simulation results demonstrated the effectiveness of this design approach. With the robustness tests, it has been shown that this method has good robustness in rejecting external disturbances from the environments.

Chapter 7

Switching Control of Bipedal Locomotion

7.1 Introduction

In previous chapters, it was demonstrated that a neural oscillator based control approach can be utilized to build stable locomotion for a bipedal walking robot, which unifies both postural control and gait control. In this chapter, a new approach, active switching control is proposed to achieve gait stability in bipedal locomotion control. This approach applies nonlinear switching control theory to the locomotion control system so as to ensure bipedal gait stability in the stable limit cycle sense. Half of the switching surfaces are determined by means of the orbital contraction-tuning requirement.

Compared with the limit cycle analysis in passive dynamics of a biped by McGeer (1990) and Goswami (1996), this active switching control takes advantages of the powered joints in a biped robot and applies a feedback mechanism to tune the sub-control systems (refer to Figure 1-4). There are two parts in this system: fundamental locomotion control sub-systems, which generate bipedal locomotion in an open loop and switching control, which basically adds a closed loop to the control system. With the above two parts, the locomotion control system can achieve both postural stability and gait stability.

The dynamics derived in Chapter 4 are used in the nonlinear analysis, and the Poincare map theory is applied in setting the multiple-switching surfaces. Section 7.2 addresses the overall control system structure. The system formulation and fundamental and switching control is described in sections 7.3 and 7.4. In section 7.5, Poincare map theory is used to show that gait stability is achieved in the sense of limit cycle. An application of this control approach is presented for a bipedal walking robot, *Spring Flamingo*, in section 7.6. The final section will summarize the study of switching control in bipedal locomotion.

7.2 Control System Architecture of Bipedal Walking Robots

Figure 7-1 shows the overall control system. There are five main components: a state machine, a contraction tuning module, a state observer, control sub-systems, and a switching control module. The control sub-systems are provided for different walking

phases (single support, double support). The transition from one controller to another controller during walking is determined by the switching control module, which is based on the state machine, orbital gait contraction tuning.

The structural dynamics of a bipedal robot change with the different phases of a walking cycle. The dynamics are different between single support states (left single support, right single support) and double support states. Consequently, the corresponding controllers should change with respect to the states. A complete walking cycle can be broken down into five states, left single support I (left toe-off), left single support II (left leg touch-down), double support, right single support I (right toe-off), and right single support II (right leg touch-down).

We design control sub-systems for each state and then switch from one sub-system to another by observing the overall system state variables [Hu (2000)]. In our control system (Figure 7-1), the switching control is the top control sub-system and supervises the other control sub-systems. Figure 7-2 describes a state machine for five walking states and their transitions.

Single support I (toe-off) is the walking phase during which the swing leg leaves the ground and starts swinging forward until the swing leg passes the vertical plane above ankle point of the stance leg. Single support II (touch-down) specifies the rest of swing phase when the swing leg swings from the ankle position of the stance leg until it strikes the ground.

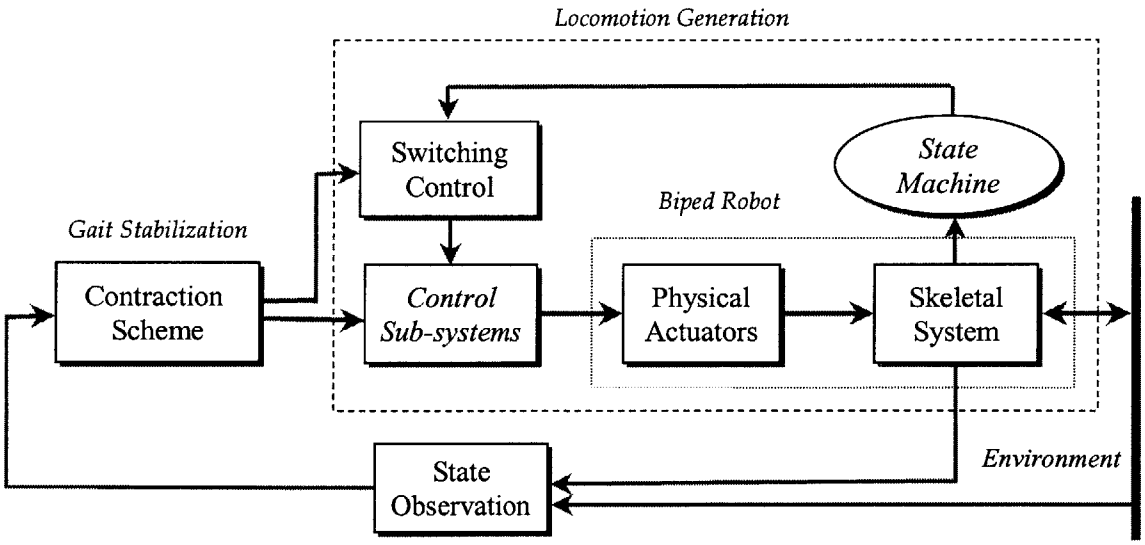

Figure 7-1: System structure of the switching control

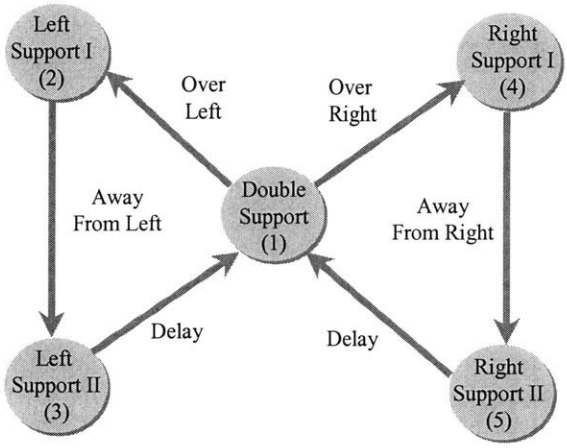

Figure 7-2: Diagram of a state machine.

7.3 Open Loop Control of Bipedal Locomotion

7.3.1 Description of dynamic system

The system dynamics are different in double support phase and single support phase, as we have seen in Chapter 4. We formulate the general system equations as follows:

$$M_\alpha(\theta,p)\ddot{\theta}+N_\alpha(\theta,\dot{\theta},p)\dot{\theta}+G_\alpha(\theta,p)=D_\alpha(\theta,p)U_\alpha \tag{7-1}$$

where $M_\alpha \in R^{n\times n}$, $N_\alpha \in R^{n\times n}$, $G_\alpha \in R^{n\times 1}$, $D_\alpha \in R^{n\times n}$, and n is the number of d.o.f. for the system. θ is the state vector, p is a parameter vector of step length λ and stance leg length l etc., and U is the control signal vector. Here, the switching rule is memory-less. Then

$$\alpha(\theta) \in \{1 \text{ (double support)}, 2 \text{ (single support)}\}$$

is a index function for walking states.
The system switching surfaces can be described as

$$H_\alpha(\theta,\dot{\theta},p)=0 \tag{7-2}$$

When $\alpha=1$, the system is in double support phase. The system dynamic equation is formulated in equation (2). When $\alpha=2$, the system is in single support phase. The system dynamic equations are shown in (9) and (10).

The switching surface that separates the double support phase from the single support phase (in toe-off period), S_1 is

$$\theta_1=d_1 \tag{7-3}$$

where d_1 is a constant.

The switching surface separating the double support phase from single support phase (in touch-down period), S_2 is,

$$\begin{cases} \theta_1 = c_0 \\ \theta_2 = c_1 \end{cases} \tag{7-4}$$

where c_0, c_1 are constants.

7.3.2 Control schemes for generating bipedal locomotion

In double support phase (Figure 4-1), if $\dot{\theta}$ is smaller than the desired value ω^*, the trailing leg of the robot can push the body forward while the leading leg maintains constant length l. Up to the limit point (a geometric constrain in the robot) $\theta = \theta_m$, the switching is enforced. Then the trailing leg lifts up and starts to swing. Consequently the single support phase begins.

The command torque τ is provided through the linear slider joint of trailing leg. The control command f for the slider actuator is

$$f = \tau \cdot \frac{x}{\lambda l \sin\theta} \tag{7-5}$$

$$\tau = K_p(\dot{\theta}^* - \dot{\theta}) \tag{7-6}$$

If the velocity $\dot{\theta}(t_0^+)$, i.e. the velocity after striking the ground, is larger than ω_m, then the dynamics is immediately switched to single support, in which case, the double support phase vanishes. When $\dot{\theta}(t_0^+) < \omega_m$, the switching surface $\theta = d_1$ can be adjusted,

$$\theta(t_0^+) < d_1 < \theta_m . \tag{7-7}$$

In the single support phase (Figure 4-2), there are two time-intervals: toe-off period and touch-down period. The control schemes are different in those cases. We illustrate the two control schemes below.

1) Toe-off period: the trailing leg leaves ground and swings forward until it is in a vertical position, $\phi_2^* = 0$, or $\theta_2^* = \frac{\pi}{2} - \theta_1$. The control in this period is

$$\begin{cases} \tau_1 = 0 \\ \tau_2 = K_p(\theta_2^* - \theta_2) - K_d\dot{\theta}_2 \end{cases} \tag{7-8}$$

2) Touch-down period: the trailing leg swings forward from the vertical position and maintains a mirror position of the stance leg with respect to the vertical plane, i.e. the set-point for the swing leg equals $\theta_2^* = \pi - 2\theta_1$. The corresponding control is the same as in 1) except the set-point value.

In this period, the swing leg extends the leg and maintains constant leg length l until

it strikes on the ground. Then the double support phase follows the ground striking instant.

The above control commands are called regular control efforts u (in the open loop). In order to achieve a stable walking pattern, the control signals are subject to adjustment Δu (in the closed-loop).
Total control output:

$$u_{total} = u + \Delta u . \tag{7-9}$$

7.4 Switching in Locomotion Control

From human and bipedal animals' walking, we observe that combining double support phases (reachable and stable dynamics) and single support phases (unreachable and unstable dynamics) can yield stable periodic bipedal walking. In this section we will show how a suitable switching control technique can combine stable double support and unstable single support subsystems to produce stable periodic motion, even at high speeds where the double support phase becomes very short.

7.4.1 Characteristics of steady gaits in phase plane

In Figure 7-3, ϕ is the global variable. It refers to the angular position of a leg measured from the straight line connecting the ankle and the hip of the leg to a vertical axis. There are two global variables, ϕ_l and ϕ_r, for the left leg and right leg, respectively. Given that the bipedal robot has symmetric structure, we assume that the dynamics for the global variables ϕ_l and ϕ_r are also symmetric.

With this global variable, ϕ, the characteristic of steady gait behavior can be viewed in the phase plane clearly. In Figure 7-4, a phase portrait of one complete walking cycle (for one leg) is shown. Since the two legs of a biped are symmetric, this phase portrait describes the motion of each leg. In the phase plane, we only refer to the global variable for the left leg. As shown in Figure 7-4, there are only four phases distinguishable and well defined in a walking cycle: double support with the left leg leading, single support with the left leg supporting, double support with the left leg behind, and single support with the left leg swinging.

The switching control model decides the switching points in the phase plane, t_i, $i = 0,1,2,3,4$. At t_4^-, the leg strikes the ground, then the angular velocity jumps from t_4^- to t_4^+ ($t_0 = t_4^+$). In Figure 7-4, at time t_0, t_2, when the swing leg strikes the ground, the control mode switching is immediately enforced. The switching points t_1 and t_3 can be appropriately selected by the switching control schemes (described in the following section).

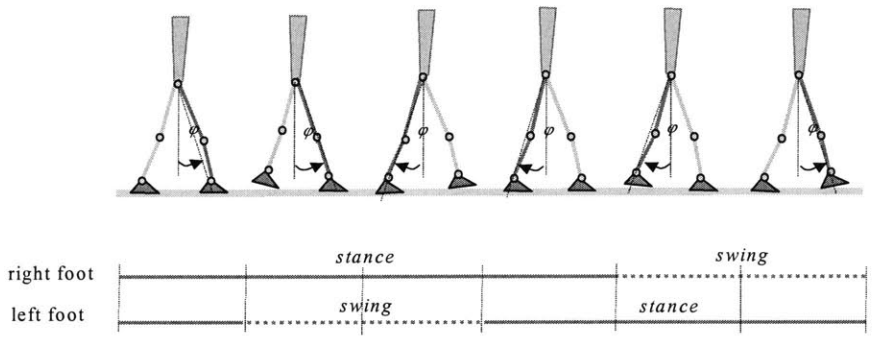

Figure 7-3: Diagram describing the global variable ϕ defined with respect to the right leg (dark shading).

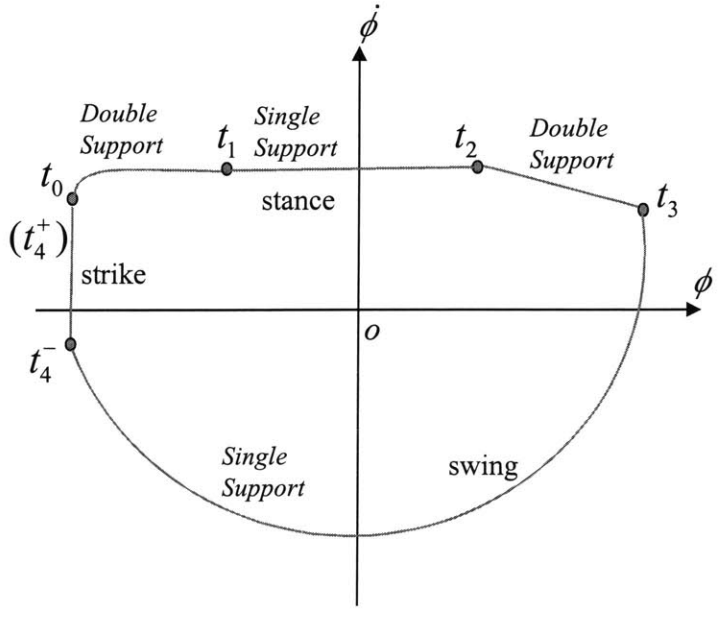

Figure 7-4: Switching control in phase plane of global variable ϕ. There are four switching points in this phase portrait: t_0, t_1, t_2 and t_3, where $t_4 = t_0$.

7.4.2 Switching surfaces and switching rules

There are two types of switching surfaces: one is for switching from double support to single support (like S_1 in Figure 7-5); the other is for switching from single support to double support (S_2).

The switching rules are the following:

1) S_1 is determined by the switching control so that the total energy on the switching surface converges. Therefore S_1 is adjustable. But there is a bound for the position of S_1.

$$\theta_{\min} \le \theta_1(S_1) \le \theta_{\max} \tag{7-10}$$

where $\theta_{\min}$ and $\theta_{\max}$ are determined by the geometric structure and geometric limitation in structure respectively. $\theta_{\min} = \cos^{-1}(\lambda/2l)$.

2) S_2 is determined by the step length and swing leg control. In our case, S_2 is fixed assuming that the leg length and step length is maintained constant when the leg touches down on the ground.

7.5 Contraction Tuning for Gait Stability

In order to achieve global gait stability, the switching control technique is used to enforce periodic global behaviors of the biped. Our strategy in dealing with the complex dynamics is to analyze the dynamics of global variables. If the motion of the global variables approaches a limit cycle, we assume that the behaviors of any joint variables are confined in the neighborhood of limit cycles. In our gait stability analysis, lateral control stability is assumed for a simplified illustration, and all the analysis is carried out in the sagittal plane.

We associate the periodic gait of an actuated bipedal robot with a limit cycle behavior of the piece-wise continuous non-linear system represented by the dynamics in single support and double support. With the help of a phase portrait of a global variable, the existence of a limit cycle and its convergence, i.e. gait stability, can be proved. The key point is to prove the contraction of the phase space volume as the system evolves in time.

A biped is in a stable walking gait if the behaviors of angles ϕ_1, ϕ_2 (see Figure 7-4) are periodic. In other words, the gait variables ϕ_1, ϕ_2 reach limit cycles. Since ϕ_1, ϕ_2 are functions of θ_1, θ_2, instead of analyzing the dynamics of ϕ_1, ϕ_2, we can indirectly consider proving the limit cycle of θ_1 and θ_2, with appropriate control and switching actions.

7.5.1 Poincare map

Poincare map can be applied to prove the existence of a limit cycle, as described in section 3.2.3. The process is as follows: first choose a switching surface, which is transversal to the

dynamic motion of the system. Then analyze the discrete sequence generated by the Poincare map. If we can prove that the above discrete-time system has the contraction property, then we say that the dynamic motion of the system converges to a stable limit cycle.

In a complete bipedal walking cycle (Figure 7-5), there are four switching surfaces, which separate different dynamics in four different phases: DS_1, SS_1, DS_2, SS_2. Here DS and SS denote double support and single support respectively.

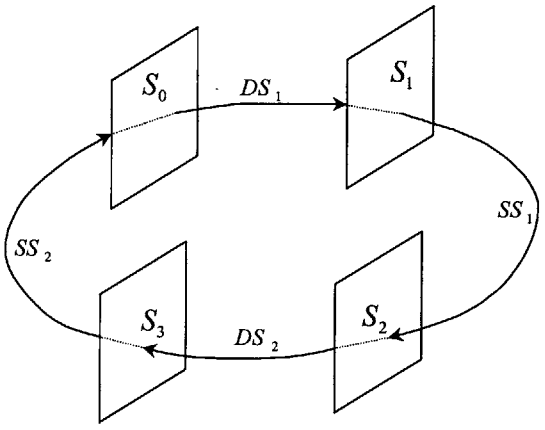

Figure 7-5: A complete cycle for bipedal walking.

Because of the symmetry in the bipedal robot, we only need to consider the Poincare Map in two switching surfaces, such as, S_0, S_2 (Figure 7-6). For a given biped with fixed geometric structure, in order for the biped to walk in a desired average velocity v_d, we can compute the desired angular velocity $\dot{\theta}_1^*$, $\dot{\theta}_2^*$ (or $\dot{\phi}_1^*$, $\dot{\phi}_2^*$) at the switching surfaces.

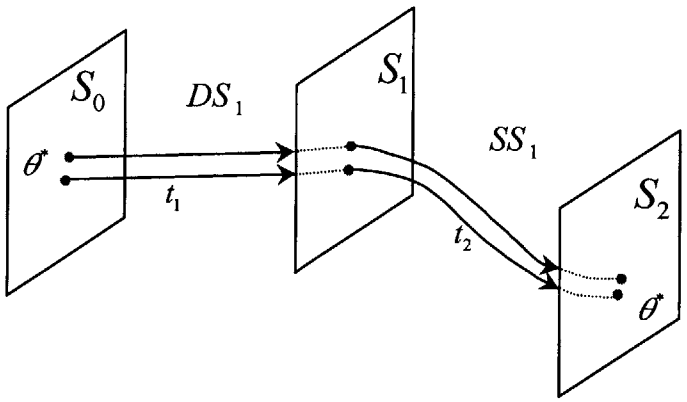

Figure 7-6: Diagram for the Poincare map of bipedal dynamics.

In Figure 7-6, we consider a Poincare map:

$$F : S_0 \rightarrow S_2 ,\ F = F_2 \cdot F_1$$

where $F_1 : S_0 \rightarrow S_1$, $F_2 : S_1 \rightarrow S_2$.

If we can prove that the Poincare map F is a contraction, we can say a periodic motion is achieved in the biped walking. In the following section, the contraction of F is proved by means of a switching surface Lyapunov function E (or called as energy function).

Define the Lyapunov function E as

$$E = \tfrac{1}{2}\dot{\theta}^T M \dot{\theta} \tag{7-11}$$

Lyapunov functions for desired state:

$$E^* = \tfrac{1}{2}\dot{\theta}_{S_0}^{*T} M \dot{\theta}_{S_0}^* \tag{7-12}$$

Lyapunov function on the switching surface S_0:

$$E_1 = \tfrac{1}{2}\dot{\theta}_{S_0}^T M \dot{\theta}_{S_0} \tag{7-13}$$

Lyapunov function on the switching surface S_2:

$$E_2 = \tfrac{1}{2}\dot{\theta}_{S_2}^T M \dot{\theta}_{S_2} \tag{7-14}$$

The total energy of the system:

$$E_{total} = E + E_p \tag{7-15}$$

where E_p = potential energy.

The above Lyapunov functions on the switching surfaces S_0 and S_2 can be considered the same as the total energy of the system. Because the potential energy on the surfaces S_0 and S_2 are the same, $E_2 - E_1$ is the same as the difference of the total energy on the surfaces S_0 and S_2, i.e. $E_{total}(S_2) - E_{total}(S_0)$.

The energy change is computed as,

$$\Delta E = E_2 - E_1 = \int_{t_0}^{t_1} \dot{E}_1 dt + \int_{t_1}^{t_2} \dot{E}_2 dt \tag{7-16}$$

where $\dot{E}_\alpha = \dot{\theta} D_\alpha U_\alpha$, $\alpha \in \{1,2\}$.

We can prove that when $E \rightarrow E^*$, equivalently we have

$$\| \Delta \| = \| \dot{\theta} - \dot{\theta}^* \| \rightarrow 0 \tag{7-17}$$

which implies that the dynamic motion converges to the stable limit cycle. The proof of (7-17) given $E \rightarrow E^*$ is provided in Appendix C.

7.5.2 Proof of limit cycle

The proof is constructured in two parts: First we analyze the local locomotion control schemes in double support and single support phase, and then we make necessary control adjustment to ensure that the surface Lyapunov functions contract to the minimum value E^* that is required for the nominal locomotion, $|E_2 - E^*| < |E_1 - E^*|$.

A. Deterministic dynamic mapping

We first look at the control and dynamics in double support phase (between switching surfaces S_0 and S_1). We can convert the equations in section 2 into a state space representation.

$$\begin{cases} \dot{x}_1 = x_2 \\ \dot{x}_2 = \dfrac{1}{Ml^2}(-Mgl\cos x_1 + \tau) \end{cases} \tag{7-18}$$

where $x_1 = \theta$, $x_1 = \dot{\theta}$. Substituting in the control term, $\tau = K_p(\dot{\theta}^* - \dot{\theta}) = K_p(\omega - \dot{\theta})$, we have

$$\begin{cases} \dot{x}_1 = x_2 \\ \dot{x}_2 = \dfrac{1}{Ml^2}(K_p\omega - K_p x_2 - Mgl\cos x_1) \end{cases} \tag{7-19}$$

Since the time interval for double support phase is usually very small (t_1 small), the state values do not change significantly, especially for the position variable $x_1 = \theta$. Therefore, local linearization allows us to find a closed form solution of the system dynamics in this period.

Let $x_1 = x_1(0) + \Delta x_1$, $x_2 = x_2(0) + \Delta x_2$. The linearized equation is

$$\begin{bmatrix} \Delta\dot{x}_1 \\ \Delta\dot{x}_2 \end{bmatrix} = \begin{bmatrix} 0 & 1 \\ -\frac{1}{l}g\sin x_1(0) & -\frac{K_p}{ml^2} \end{bmatrix} \begin{bmatrix} \Delta x_1 \\ \Delta x_2 \end{bmatrix} + \begin{bmatrix} x_2(0) \\ u_1 \end{bmatrix} \tag{7-20}$$

where $u_1 = -\dfrac{g}{l}\cos x_1(0) + \dfrac{K_p\omega}{Ml^2} - \dfrac{K_p x_2(0)}{Ml^2}$. (7-21)

The eigenvalues for the system are both negative. Then we conclude that this dynamic system is stable in double support phase, which means that we can increase the kinetic energy by pushing the robot body with the trailing leg. From equation (7-21), we can see that without the control input (the last two terms of (7-21)), the gravity (first term in (7-21)) will reduce the kinetic energy, thus reduce the angular velocity $\dot{\theta}$.

The state space representation of the dynamics in single support phase is

$$\begin{cases} \dot{x}_1 = x_2 \\ \dot{x}_2 = \frac{1}{\gamma_0}[mla\sin x_3 \cdot x_2 - mla\sin x_3 \cdot x_4 - \gamma_2 \cos x_1 + \tau_1 - \tau_2] \\ \dot{x}_3 = x_4 \\ \dot{x}_4 = \frac{1}{\gamma_0}[-\frac{l}{a}\gamma_1 \sin x_3 \cdot x_2 + mla\sin x_3 \cdot x_4 + \frac{g}{a}\cos(x_1 + x_3)\cdot\gamma_1 + \gamma_2 \cos x_1 \\ - mga\cos(x_1 + x_3) + \frac{\gamma_1}{ma^2}\tau_2 - \tau_1] \end{cases} \tag{7-22}$$

Two control schemes are used in toe-off period ($\phi_2 \geq 0$) and touch-down period ($\phi_2 < 0$).

When $\phi_2 \geq 0$, i.e. $\theta_1 + \theta_2 \geq \frac{\pi}{2}$, the control is,

$$\tau_1 = 0 \tag{7-23}$$

$$\tau_2 = K_p(\tfrac{\pi}{2} - \theta_1 - \theta_2) - K_d(\dot{\theta}_1 + \dot{\theta}_2). \tag{7-24}$$

When $\phi_2 < 0$, i.e. $\theta_1 + \theta_2 < \frac{\pi}{2}$,

$$\tau_1 = 0 \tag{7-25}$$

$$\tau_2 = K_p(-\pi + 2\theta_1 - \theta_2) - K_d(\dot{\theta}_1 + \dot{\theta}_2). \tag{7-26}$$

B. Contraction of Poincare map

From the above analysis, the mapping from S_0 to S_1 is determined by the dynamics (7-19). When the kinetic energy $E_{s_0} = E_1$ is not big enough, the switching surface S_2 may not be reached. In other words, it may not be transversal. However, if in a certain range of the initial state $\dot{\theta}(S_0)$, E_{s_0} will be big enough so that S_2 can be reached. In that case, further energy tuning (or contraction tuning) can be applicable. The following control adjustments are based on this condition.

1) Adjusting switching surface S_1.

New switching surface of S_1:

$$\theta^{(k+1)} = \theta^{(k)} + \Delta\theta \tag{7-27}$$

$$\Delta\theta + \lambda(E - E^*) = 0 \tag{7-28}$$

$$\Rightarrow \Delta E = Mgl(\sin\theta^{(k+1)} - \sin\theta^{(k)})$$

$$= 2Mgl\cos(\theta^{(k)} + \tfrac{\Delta\theta}{2})\sin(\tfrac{\Delta\theta}{2}) \tag{7-29}$$

From equation (7-29), we can see that when $E > E^*$, $\Delta\theta < 0$, $\Delta E < 0$. When $E < E^*$, the robot is pushed forward in double support phase, during which $\Delta E > 0$.

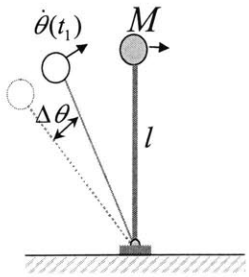

Figure 7-7: Adjustable switching surface S_1.

2) Adjusting control signal in single support phase.

$$\Delta u = -K_s \dot{\theta}(E - E^*), \quad K_s > 0. \tag{7-30}$$

$$u = U + \Delta u \tag{7-31}$$

where U is the nominal control described in section 7.3.2.

$$\Rightarrow \qquad \dot{E}_s = \dot{\theta}^T D u = \dot{\theta}^T D(U + \Delta u) \tag{7-32}$$

$$\Delta \dot{E}_s = \dot{\theta} D \Delta u = -K_s \dot{\theta}^T D \dot{\theta}(E - E^*)$$

Since $D = I$, $\Delta \dot{E}_s = -K_s(E - E^*)\dot{\theta}^T \dot{\theta}$ (7-33)

$$\Delta E_s = \int_{t_1}^{t_2} \Delta \dot{E}_s dt \tag{7-34}$$

Then $\Delta E_s < 0$, if $E > E^*$; $\Delta E_s \geq 0$, if $E \leq E^*$.

Therefore, with the above control adjustments, we see that $E \to E^*$ as $t \to \infty$. Then, the Poincare mapping from S_0 to S_1 is a contraction. Hence, a limit cycle of θ is constructed (realized).

7.6 Application to a Simulated Bipedal Walking Robot

We applied the switching control approach to a simulated 7-link planar bipedal walking robot (*Spring Flamingo*, a planar biped built by Jerry Pratt, MIT Leg Lab.; see Figure 2-3). The robot has a height of 1.2 meters, leg length 0.8 meters, foot length 0.18 meters, and body weight 14 kg. There are six joint actuators for the hip, knee, and ankle in each leg. In our simulation, several control sub-systems have been designed for single support phases and double support phases. The proposed switching control was implemented and achieved stable locomotion for the simulated planar bipedal walking robot.

Figures (7-8)~(7-11) show the results from a bipedal walking simulation. The simulation results show that the limit cycle was achieved very quickly. Hence a stable gait is also realized. Figure 7-8 shows the phase portrait of the global variable of the left leg. We

observe that the walking gait converged to a limit cycle quickly. Figure 7-9 shows the phase portraits of hip, knee and ankle joints of the left leg. The behaviors of the right leg are similar. Figure 7-10 shows the data profile of joint angular positions of the left leg and the stride length data profile during the simulation of bipedal walking. It shows that the stride length is almost constant in the control process, which is consistent with our assumption in the dynamics modeling of Chapter 4. A stick diagram (in Figure 7-11) shows that both the postural stability and gait stability are well maintained.

In the above switching control approach, bipedal gait stability is measured be means of two global gait variables. If the limit cycle of those global variables is reached, a periodic walking gait is realized for a bipedal walking robot. Provided that a proper height is well maintained during walking, the constant step length will be assured. In practical, gait stability is measured mostly by step length and time duration of a step, i.e. the step period [Todd (1985), Vukobratovic (1990)]. The measure (or the index for gait stability) used in this study gives stronger conditions for gait stability with respect to the practical one. However, they are weaker conditions than Vukobratovic's definition of bipedal gait stability.

Taga's demonstration with a simulated humanoid walking controlled by distributed neural oscillations [Taga (1995)] also generated periodic bipedal walking gait. However, considering the implementation, this switching control is much simpler for practical applications. In addition, the systematic analysis of the latter approach can be much easier.

Robustness tests have also been conducted with external force disturbances. We tested the simulated robot with two different types of force disturbances exerted on the robot body in forward (x-direction) and vertical direction (z-direction). Figure 7-12 shows the simulation results of the robustness test. It shows that the robot was pushed forward with10 lbs force for 0.5 seconds and it recovered quickly after the disturbance. We found that the robot is more robust in rejecting the disturbances in z-direction that in x-direction.

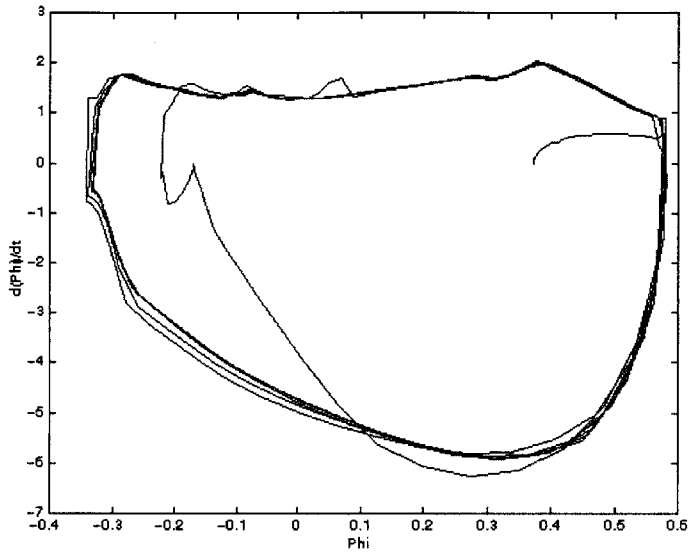

Figure 7-8: Simulation results of a planar biped robot. A phase plane diagram of global variable ϕ (left leg) is shown. The dark line represents the limit cycle of the global variable.

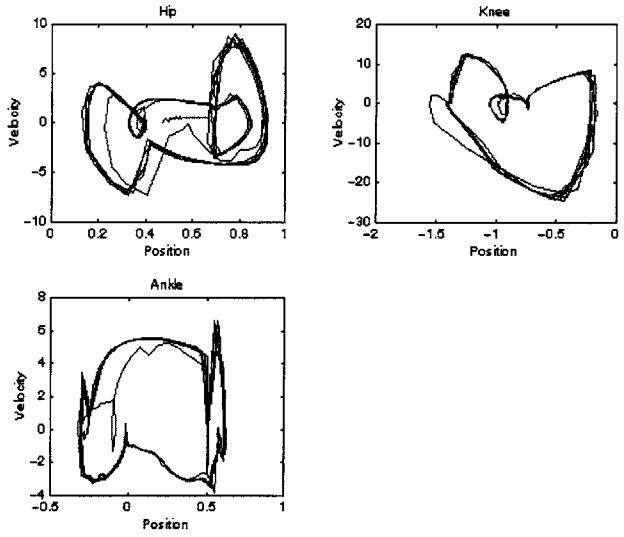

Figure 7-9: Phase plane portraits of hip, knee, and ankle joints of the left leg in the simulation.

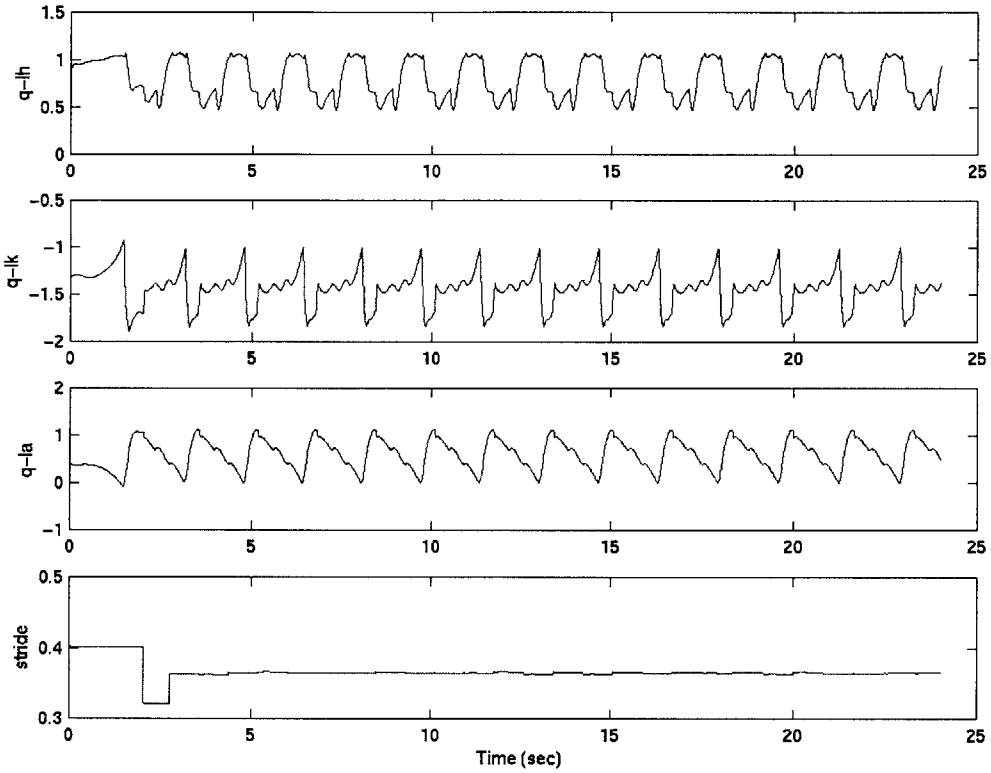

Figure 7-10: Simulation data profile of left leg joints. The responses (q.lh, q.lk, and q.la) are angular positions of hip, knee and ankle joints respectively. The figure at the bottom is the responses of the stride length, which is almost constant in the control process. The periodic property is shown in the responses.

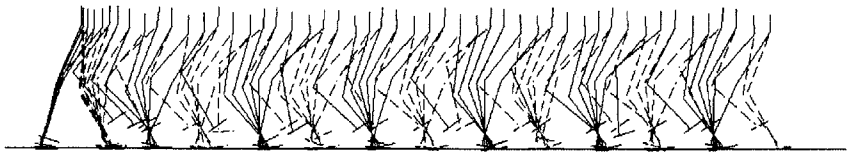

Figure 7-11: Stick diagram of bipedal walking. Solid lines are stick plots of the left leg and dashed lines are the stick plots of the right leg.

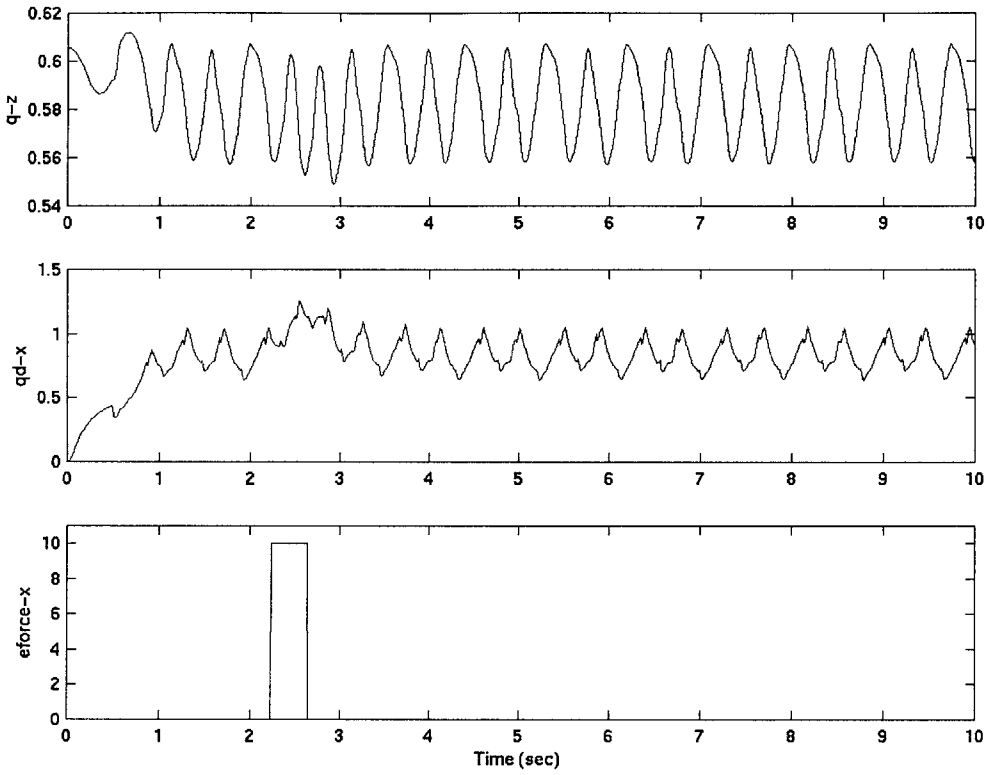

Figure 7-12: Robustness test of the simulated biped with switching control. The external force disturbance is 10 lbs exerted on the robot body in the forward direction.

7.7 Summary

A nonlinear switching control approach for a stable biped locomotion was presented. With this control technique, one can obtain gait stability and postural stability. Gait stability was proved using nonlinear system theory.

Simulation results have shown the effectiveness of this switching control approach. The simulated planar bipedal walking robot achieved postural stability and gait stability.

Robustness tests have been conducted with external forces exerted on the robot body. It has been shown that the simulated biped with switching control has good robustness in rejecting the external forces disturbances.

Chapter 8

Control of 3-D Bipedal Walking Robot

The control of a 3-D bipedal walking robot is implemented in this chapter. A frontal plane controller is developed here and combined with the sagittal plane controller of the previous chapters, disregarding the coupling between frontal and sagittal plane dynamics. Simulations of the resulting 3-D control are presented.

8.1 Dynamic Control of a 3-D Bipedal Walking Robot

In this chapter we will extend our previous analysis of the control of 2-D walking robots to the case of a 3-D bipedal walking robot with 12 degrees of freedom. The 3-D robot is provided with pitch joints (hip, knee, ankle), roll joints (hip and ankle) and a yaw joint (hip) in each leg.

The complexity of the dynamics of 3-D bipeds makes analysis of their control designs extremely difficult. The use of simplified dynamics models offers a great advantage in this case. We will extend the simplified dynamics models described in Chapters 4 and 7 for the 2-D biped's dynamics to the 3-D case by inclusion of a universal joint at the hip. Thus the leg of the 3-D biped is modeled as having a point mass, a linear slider joint for varying the leg length, and a universal joint at the hip.

The complexity of the control design may also be reduced by assuming that the frontal plane dynamics and sagittal plane dynamics are not coupled or are only weakly coupled during 3-D walking. This assumption is more plausible for straight line walking, which is the only case we shall consider here. Other researchers who have taken this approach include Pratt (1999), Chew (2000), Parseghian (2000). In more general walking, a dynamic compensation may be useful to accommodate the ignored coupling between frontal and sagittal dynamics, although we do not implement such compensation here.

In the following two sections, the separate control systems are presented for the frontal and sagittal plane.

8.2 Switching Control for Frontal Plane Dynamics

Several researchers discussed 3-D control recently. Kuo (1999) analyzed frontal dynamic control and stability by resolving the sagittal dynamics in a discrete control process. Chew (2000) proposed a linear inverted pendulum model for analyzing a stable control approach of frontal dynamics.

Similar to Chapter 7, a switching control approach is developed in this section for 3-D frontal dynamics. In the frontal plane, there are four switching surfaces, which are similar to those described in the sagittal plane control of the 2-D biped, provided that double support phases exist. Therefore, the control techniques used in Chapter 7 can be used in frontal plane:

1) Switching from double support to single support phase, the knee joint is extended when more energy is needed to push the robot from side to middle.

2) The following control law can be used for the dynamic control in single support phase:

$$u_{total} = u + \Delta u \tag{8-1}$$

where u is the regular control for maintaining the proper posture of the robot and Δu is the additional switching control term.

$$\Delta u = -K_f (E - E^*)\dot{\theta} \tag{8-2}$$

where E, E^* are the actual kinetic energy and desired kinetic energy measured at the switching surface respectively, $\dot{\theta}$ is the joint angular velocity, and $K_f > 0$.

3) The foot placement approach [Jerry (1999), Parseghian (2000), Chew (2000)] is also applied. The desired hip angular position of the swing leg is computed as

$$\theta^*_{roll} = \theta_n - K_r \dot{y} \tag{8-3}$$

where θ_n is the nominal position for the hip joint of swing leg before striking ground and $K_r > 0$.

The proof that a stable periodic motion in the frontal dynamic plane can be achieved by means of the above switching control methods can be carried out in the same way as in Chapter 7.

8.3 Control in the Sagittal Plane

The control approaches developed for a 2-D bipedal walking robot can be applied in the sagittal control of a 3-D. The switching control technique of the 2-D biped has been applied in this study. In this simulation of the M2 3-D biped, the switching control of the sagittal plane is given higher priority in control switching actions. Therefore, the

switching from double support phase to single support phase is dictated by the control of the sagittal plane.

8.4 Example

A test of the control system of the 3-D biped robot, M2, is provided by the following simulation, in which M2 is tasked to step in place without any forward motion. This test focuses on the frontal plane controller, but it is a 3-D simulation.

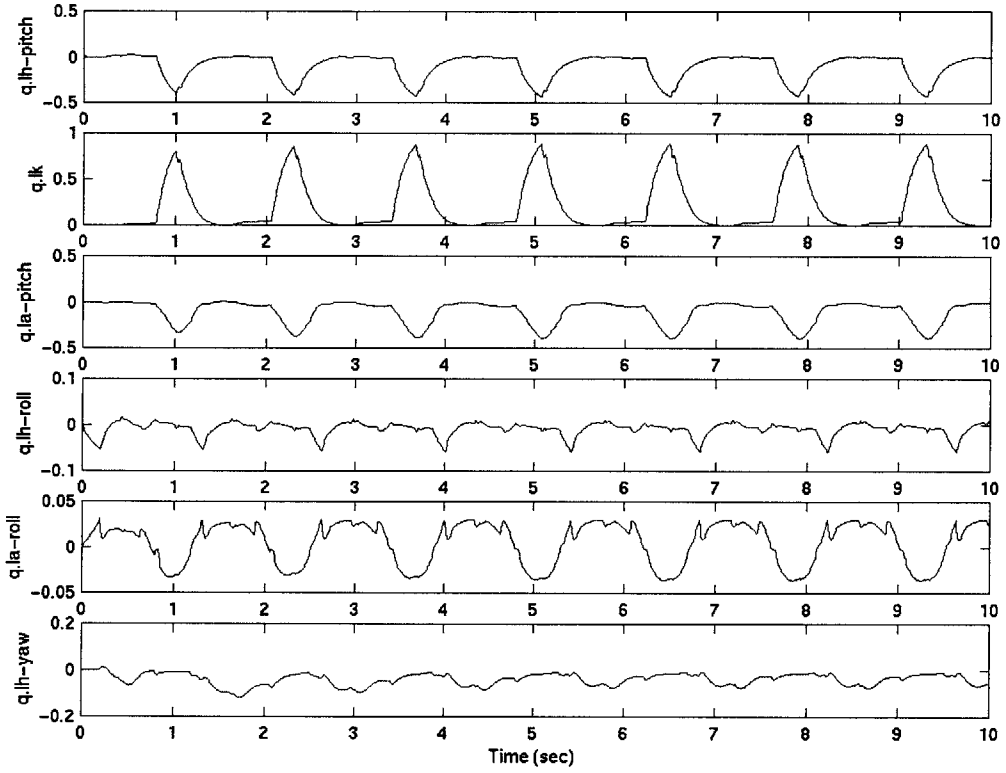

Figure 8-1: Dynamics responses of the joint angles in left leg. The responses from the top are angular position of hip pitch, knee, ankle pitch, hip roll, ankle roll and hip yaw joints in the left leg of the biped.

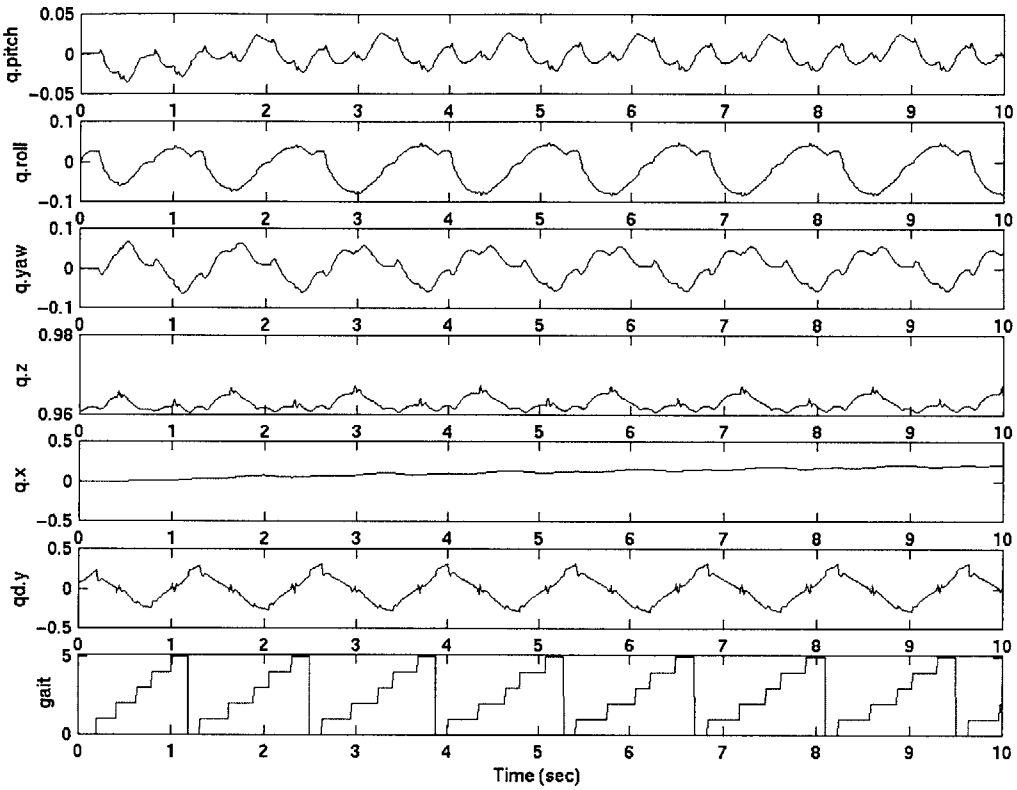

Figure 8-2: Dynamic responses of the robot posture variables and the gait variable. The responses (from the top) are body pitch, body roll, body yaw, body height, body forward position, body lateral velocity and robot gait.

Figure 8-1 shows the dynamic responses of the joints in the robot's left leg. Figure 8-2 shows the dynamics of the robot body. The 3-D biped was stabilized in the frontal plane with the switching control method described in section 8.2.

8.5 Discussions

From our study in 3-D biped control, we have shown that the frontal switching control can provide stability in lateral motion. Also, we have observed that there are some difficulties in coordination the dynamic control of the frontal plane and sagittal plane when combining the two switching control sub-systems (for sagittal plane and frontal plane) together. Further study is needed for the forward bipedal walking task, which requires the synchronization of the dynamics in frontal plane and sagittal plane.

Chapter 9

Conclusions

9.1 Summary of Thesis Research

Two control approaches have been proposed in this thesis, which will help in better understanding bipedal locomotion and motor-sensory control. Also they can provide systematic control schemes for walking robotic systems, in which the control design process is simplified.

(a) Neural oscillator based locomotion control. A design method for neural oscillator based locomotion control is developed with local dynamics shaping and appropriate sensory feedback, which is realized by a global state based sensory signal selection scheme. A systematic analysis of neuro-skeletal dynamics in a bipedal walking robot is provided. The intrinsic robustness of neural dynamics is achieved by means of the dynamics entrainment in bipedal robots.

(b) Contraction tuning based switching control. A contraction tuning based switching control approach can achieve gait stability for a bipedal walking robot. The existence of a limit cycle is proved by means of nonlinear system theory.

(c) Control applications are simulated for a planar bipedal walking robot, *Spring Flamingo*, and a 3-D biped, *M2*. Both neural-oscillator control and switching control approaches are demonstrated in the simulations of *Spring Flamingo* successfully. The switching controller is demonstrated in the frontal plane control of M2 successfully for a stepping in place task.

(d) Analytic tools are applied in the design and analysis of control systems for the bipedal walking robots.

9.2 Future Work

(a) Neural oscillator driven control of M2. By adding lateral control, the control algorithm for the planar biped (*Spring Flamingo*) with neural oscillators can be further extended to the locomotion control of *M2*. Secondly, a complete theoretic study of the neuro-skeletal dynamics of the 3-D biped is worthy of further investigation. The proof of entrainment between the neural dynamics and the skeletal (structural) dynamics and the environment can be accomplished by means of simplified dynamics model.

(b) Switching control of the 3-D biped, *M2*. Further efforts are needed to determine how to combine the switching control techniques in the frontal plane and the sagittal plane to achieve stable forward walking in 3-D. This requires the synchronization of two switching control processes in different dynamic planes, which can be viewed as a coordination task.

(c) Adaptive control of bipedal walking. Based on the two control frameworks, further study of adaptation and robustness can be executed with the expectations of performance enhancement.

Appendix A

Dynamics Models of a Biped

The dynamics models of a biped for single support phases and double support phase are derived by means of the Lagrangian equation. Reasonable approximations are made in the following dynamic models. Basically we assume:

a) *The robot legs are very light. The legs of such a biped are approximated with a lumped mass attached with a linear slider joint and a linkage (as shown in Figure A-1).*
b) *There is no slip between the feet and the ground.*
c) *In single support phase, the length of stance leg is fixed.*
d) *In double support phase, the leading leg has a constant leg length, and the distance between two feet (step length) is also fixed.*
e) *During walking, the step length λ in consecutive cycles is assumed to be constant.*

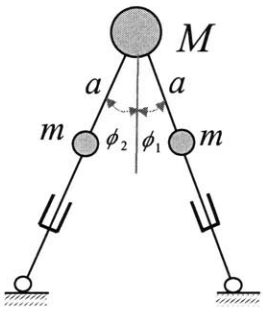

Figure A-1: A general dynamic model.

With the above assumptions, simplified dynamics models are derived as follows. Figure A-1 shows a general dynamic model for a biped, where the leg is approximated as a rotating hip joint and a sliding linear joint, which represents the function of a knee and an ankle joint.

A1 Model in double support phase

The leg mass (3~5% of body mass in *Spring Flamingo* shown in Figure 1-3) is ignored in the model of double support for simplicity of analysis. In Figure A-2, the leg length of the leading leg is fixed. Only the trailing leg can be extended so that the robot can propel forward. The length of leading leg is fixed in this control scheme. Therefore, there is only one degree of freedom in the model. For convenience, we choose θ as a state variable instead of x. The relationship between θ and x is expressed as

$$\cos\theta = \frac{l^2 + \lambda^2 - x^2}{2l\lambda} \tag{A-1}$$

$$\sin\theta = \sqrt{1 - \cos^2\theta}$$

where λ is the step length measuring the distance between two feet.

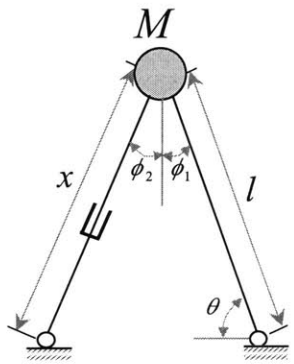

Figure A-2: Diagram for the dynamic model in doubles support phase.

We can derive the dynamics equation by means of the Lagrangian equation as follows,
Let

$$\vec{r} = (-l\cos\theta, l\sin\theta)$$

$$\dot{\vec{r}} = (l\sin\theta\cdot\dot{\theta}, l\cos\theta\cdot\dot{\theta})$$

$$v^2 = \dot{\vec{r}}\cdot\dot{\vec{r}} = l^2\dot{\theta}^2$$

$$\Rightarrow\ T^* = \tfrac{1}{2}Mv^2 = \tfrac{1}{2}Ml^2\dot{\theta}^2$$

$$V = Mgl\sin\theta$$

$$L = T^* - V = \tfrac{1}{2}Ml^2\dot{\theta}^2 - Mgl\sin\theta$$

$$\frac{d}{dt}\left(\frac{\partial L}{\partial\dot{\theta}}\right) - \frac{\partial L}{\partial\theta} = \tau$$

Then the system equation can be obtained, which is the same as an inverted pendulum except the actuator force f exerted by the slider joint in the trailing leg:

$$\Rightarrow \qquad Ml^2\ddot{\theta} + Mgl\cos\theta = \tau \tag{A-2}$$

where $\tau = \vec{f} \times \vec{r} = f \cdot l\sin\alpha$

$$\sin\alpha = \frac{\lambda}{x}\sin\theta$$

$$f = \tau \cdot \frac{x}{\lambda l \sin\theta} \tag{A-3}$$

Plugging (3) into (2), we can derive the dynamic equation about variable x:

$$m(x)\ddot{x} + n(x,\dot{x})\dot{x} + g(x) = c(x)\cdot f \tag{A-4}$$

We can also express ϕ_1 and ϕ_2 in term of θ:

$$\phi_1 = \frac{\pi}{2} - \theta \tag{A-5}$$

$$\phi_2 = tg^{-1}\frac{\lambda - l\cos\theta}{l\sin\theta} \tag{A-6}$$

A2 Model in single support phase

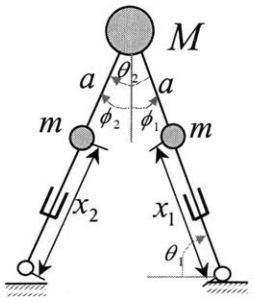

Figure A-3: Diagram for a dynamic model in single support.

The leg length of the stance leg is constant in this model (Figure A-3). The choosing variables θ_1, θ_2, the gait variables ϕ_1, ϕ_2 are expressed:

$$\begin{cases} \phi_1 = -(\frac{\pi}{2} - \theta_1) \\ \phi_2 = \theta_2 + \phi_1 = \theta_2 - \frac{\pi}{2} + \theta_1 \end{cases} \tag{A-7}$$

With the Lagrangian equation, we can derive the dynamic model for the single support phase below.

Let $\vec{r}_1 = (-x_1\cos\theta_1, x_1\sin\theta_1)$.

$$\dot{\vec{r}}_1 = (x_1\sin\theta_1\cdot\dot{\theta}_1, x_1\cos\theta_1\cdot\dot{\theta}_1)$$

$$v^2 = \dot{\vec{r}}_1\cdot\dot{\vec{r}}_1 = x_1^2\dot{\theta}_1^2$$

$$\vec{R} = (-l\cos\theta_1, l\sin\theta_1).$$

$$\dot{\vec{R}} = (l\sin\theta_1\cdot\dot{\theta}_1, l\cos\theta_1\cdot\dot{\theta}_1)$$

$$v^2 = \dot{\vec{R}}\cdot\dot{\vec{R}} = l^2\dot{\theta}_1^2$$

$$\vec{r}_2 = (-l\cos\theta_1 - a\sin(\theta_1+\theta_2-\tfrac{\pi}{2}), l\sin\theta_1 - a\cos(\theta_1+\theta_2-\tfrac{\pi}{2})).$$

$$\dot{\vec{r}}_2 = (l\sin\theta_1\cdot\dot{\theta}_1 - a\sin(\theta_1+\theta_2)\cdot(\dot{\theta}_1+\dot{\theta}_2), l\cos\theta_1\cdot\dot{\theta}_1 - a\cos(\theta_1+\theta_2)\cdot(\dot{\theta}_1+\dot{\theta}_2))$$

$$v_2^2 = \dot{\vec{r}}_2\cdot\dot{\vec{r}}_2)^2$$

$$v_2^2 = (l\sin\theta_1\cdot\dot{\theta}_1 - a\sin(\theta_1+\theta_2)\cdot(\dot{\theta}_1+\dot{\theta}_2))^2 + (l\cos\theta_1\cdot\dot{\theta}_1 - a\cos(\theta_1+\theta_2)\cdot(\dot{\theta}_1+\dot{\theta}))^2$$

$$\Rightarrow\quad v_2^2 = l^2\dot{\theta}_1^2 + a^2(\dot{\theta}_1+\dot{\theta}_2)^2 - 2la(\dot{\theta}_1+\dot{\theta}_2)\cos\theta_2$$

$$\Rightarrow\quad T^* = \tfrac{1}{2}mv_1^2 + \tfrac{1}{2}Mv^2 + \tfrac{1}{2}mv_2^2$$

$$\Rightarrow\quad T^* = \tfrac{1}{2}[mx_1^2 + (M+m)l^2]\dot{\theta}_1^2 + \tfrac{1}{2}ma^2(\dot{\theta}_1+\dot{\theta}_2)^2 - mla(\dot{\theta}_1+\dot{\theta}_2)\cos\theta_2$$

$$V = mgx_1\sin\theta_1 + Mgl\sin\theta_1 + mg(l\sin\theta_1 - a\cos(\theta_2+\theta_1-\tfrac{\pi}{2})$$

$$\Rightarrow\quad V = mgx_1\sin\theta_1 + Mgl\sin\theta_1 + mgl\sin\theta_1 - mga\sin(\theta_2+\theta_1)$$

$$L = T^* - V$$

$$L = \tfrac{1}{2}[mx_1^2 + (M+m)l^2]\dot{\theta}_1^2 + \tfrac{1}{2}ma^2(\dot{\theta}_1+\dot{\theta}_2)^2 - mla(\dot{\theta}_1+\dot{\theta}_2)\cos\theta_2$$

$$= -[mgx_1 + (m+M)gl]\sin\theta_1 + mga\cdot\sin(\theta_1+\theta_2) \qquad \text{(A-8)}$$

$$\Rightarrow\quad \begin{cases} \dfrac{d}{dt}\left(\dfrac{\partial L}{\partial\dot{\theta}_1}\right) - \dfrac{\partial L}{\partial\theta_1} = \tau_1 \\ \dfrac{d}{dt}\left(\dfrac{\partial L}{\partial\dot{\theta}_2}\right) - \dfrac{\partial L}{\partial\theta_2} = \tau_2 \end{cases}$$

$$\Rightarrow\ [mx_1^2 + (M+m)l^2 + ma^2]\ddot{\theta}_1 + ma^2\ddot{\theta}_2 + mla\cdot\sin\theta_2\cdot\dot{\theta}_2 + [mgx_1 + (m+M)gl]\cos\theta_1 - mga\cdot\cos(\theta_1+\theta_2) = \tau_1 \qquad \text{(A-9)}$$

$$ma^2\ddot{\theta}_1 + ma^2\ddot{\theta}_2 - mla\dot{\theta}_1\cdot\sin\theta_2 - mga\cdot\cos(\theta_1+\theta_2) = \tau_2 \qquad \text{(A-10)}$$

Appendix B

Proof of Existence of a Limit Cycle for the Oscillator Unit

Figure B-1 shows the piece-wise linear dynamics with the state space partitioned by two switching surfaces, S_1 $(x_2 = 0)$ and S_2 $(x_1 = 0)$. As shown in the figure, t_1^*, t_2^*, t_3^*, t_4^* denote the transition time from x_0^* to x_1^*, from x_1^* to x_2^*, from x_2^* to x_3^*, from x_3^* to x_4^*, respectively.

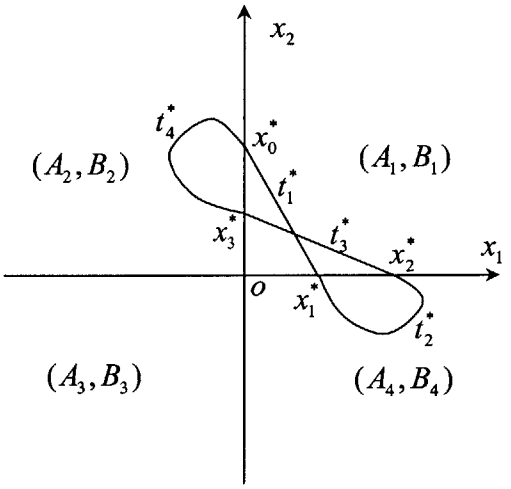

Figure B-1: Diagram for the piece-wise linear dynamic system, switching surfaces and limit cycle of neural oscillator (5-5).

The strategy of this proof is to first express x_i^* with time intervals t_1^*, t_2^*, t_3^*, t_4^*. Then we apply the switching surface equation to find the conditions for the existence of a limit cycle. Let $x_0 = x_0^* \in S_1$. In this oscillator, $B_i = B$, $i \in \{1,2,3,4\}$.

$$\Rightarrow\ x(t) = e^{A_1 t}(x_0 + A_1^{-1}Bu) - A_1^{-1}Bu$$

$$\Rightarrow\ x_1^* = e^{A_1 t_1^*}(x_0^* + A_1^{-1}Bu) - A_1^{-1}Bu\,,\ x_1^* \in S_2\,.$$

Similarly,

$$x_2^* = e^{A_4 t_2^*}(x_1^* + A_4^{-1}Bu) - A_4^{-1}Bu$$

$$x_3^* = e^{A_1 t_3^*}(x_2^* + A_1^{-1}Bu) - A_1^{-1}Bu$$

$$x_4^* = e^{A_2 t_4^*}(x_3^* + A_2^{-1}Bu) - A_2^{-1}Bu$$

Let $E_1 = e^{A_1 t_1^*}$, $E_2 = e^{A_4 t_2^*}$, $E_3 = e^{A_1 t_3^*}$, $E_4 = e^{A_2 t_4^*}$, $Z_i = A_i^{-1}Bu$, $i \in \{1,2,3,4\}$.

$$\Rightarrow \quad x_1^* = E_1(x_0^* + Z_1) - Z_1$$

$$x_2^* = E_2(x_1^* + Z_4) - Z_4$$

$$x_3^* = E_3(x_2^* + Z_1) - Z_1$$

$$x_0^* = x_4^* = E_4(x_3^* + Z_2) - Z_2$$

$$\Rightarrow \quad x_0^* = E_4\{Z_2 + E_3[Z_1 + E_2(Z_4 + E_1(x_0^* + Z_1) - Z_1) - Z_4] - Z_1\} - Z_2$$

$$x_0^* = E_4Z_2 + E_4E_3Z_1 + E_4E_3E_2Z_4 + E_4E_3E_2E_1x_0^* + E_4E_3E_2E_1Z_1 - E_4E_3E_2Z_1 - E_4E_3Z_4 - E_4Z_1 - Z_2$$

$$\Rightarrow \quad x_0^* = (1 - E_4E_3E_2E_1)^{-1}I_0$$

$$I_0 = E_4Z_2 + E_4E_3Z_1 + E_4E_3E_2Z_4 + E_4E_3E_2E_1Z_1 - E_4E_3E_2Z_1 - E_4E_3Z_4 - E_4Z_1 - Z_2$$

Repeating the same procedure, we can solve for x_1^*, x_2^*, x_3^*:

$$\Rightarrow \quad x_1^* = E_1\{Z_1 + E_4[Z_2 + E_3(Z_1 + E_2(x_1^* + Z_4) - Z_4) - Z_1] - Z_2\} - Z_1$$

$$x_1^* = E_1Z_1 + E_1E_4Z_2 + E_1E_4E_3Z_1 + E_1E_4E_3E_2x_1^* + E_1E_4E_3E_2Z_4 - E_1E_4E_3Z_4 - E_1E_4Z_1 - E_1Z_2 - Z_1$$

$$x_1^* = (1 - E_1E_4E_3E_2)^{-1}I_1$$

$$I_1 = E_1Z_1 + E_1E_4Z_2 + E_1E_4E_3Z_1 + E_1E_4E_3E_2Z_4 - E_1E_4E_3Z_4 - E_1E_4Z_1 - E_1Z_2 - Z_1$$

$$\Rightarrow \quad x_2^* = E_2\{Z_4 + E_1[Z_1 + E_4(Z_2 + E_3(x_0^* + Z_1) - Z_1) - Z_2] - Z_1\} - Z_4$$

$$x_2^* = E_2Z_4 + E_2E_1Z_1 + E_2E_1E_4Z_2 + E_2E_1E_4E_3x_0^* + E_2E_1E_4E_3Z_1 - E_2E_1E_4Z_1 - E_2E_1Z_2 - E_1Z_1 - Z_4$$

$$x_2^* = (1 - E_2E_1E_4E_3)^{-1}I_2$$

$$I_2 = E_2Z_4 + E_2E_1Z_1 + E_2E_1E_4Z_2 + E_2E_1E_4E_3Z_1 - E_2E_1E_4Z_1 - E_2E_1Z_2 - E_1Z_1 - Z_4$$

$$\Rightarrow \quad x_3^* = E_3\{Z_1 + E_2[Z_4 + E_1(Z_1 + E_4(x_3^* + Z_2) - Z_2) - Z_1] - Z_4\} - Z_1$$

$$x_3^* = E_3Z_1 + E_3E_2Z_4 + E_3E_2E_1Z_1 + E_3E_2E_1E_4x_3^* + E_3E_2E_1E_4Z_2 - E_3E_2E_1Z_2 - E_3E_2Z_1 - E_3Z_4 - Z_1$$

$$x_3^* = (1 - E_3E_2E_1E_4)^{-1} I_3$$

$$I_3 = E_3Z_1 + E_3E_2Z_4 + E_3E_2E_1Z_1 + E_3E_2E_1E_4Z_2 - E_3E_2E_1Z_2 - E_3E_2Z_1 - E_3Z_4 - Z_1$$

Considering $x_0^*,\ x_3^* \in S_1,\ x_1^*,\ x_2^* \in S_2$, we have

$$g_1(t_1^*, t_1^*, t_1^*, t_1^*) = C_1x_0^* = 0$$

$$g_2(t_1^*, t_1^*, t_1^*, t_1^*) = C_2x_1^* = 0$$

$$g_3(t_1^*, t_1^*, t_1^*, t_1^*) = C_2x_2^* = 0$$

$$g_4(t_1^*, t_1^*, t_1^*, t_1^*) = C_1x_3^* = 0$$

where $C_1 = [1 \quad 0 \quad 0 \quad 0]$, $C_2 = [0 \quad 1 \quad 0 \quad 0]$.

Q.E.D.

Appendix C

Contraction with Dynamics Constraint

Define a Lyapunov function (energy function) as

$$E = \tfrac{1}{2}\dot{\theta}^T \boldsymbol{M}\dot{\theta} \tag{C-1}$$

$$\boldsymbol{M} = \begin{bmatrix} \alpha & \beta \\ \beta & \beta \end{bmatrix}$$

$$\alpha = mx_1^2 + (M+m)l^2 + ma^2$$

$$\beta = ma^2$$

where θ is the state variable (refer to Appendix A), $\boldsymbol{M}$ is the inertia matrix measured on the switching surfaces (S_0 and S_2). Assume that $\dot{\theta}^*$ is the velocity vector at the fixed point on the limit cycle γ and the switching surfaces (S_0 and S_2).

Let $\dot{\theta} = \dot{\theta}^* + \Delta$, $\dot{\theta}^* = [\dot{\theta}_1^* \quad \dot{\theta}_2^*]^T$, $\Delta = [\Delta_1 \quad \Delta_2]^T$,

$$E = \tfrac{1}{2}(\dot{\theta}^* + \Delta)^T \boldsymbol{M}(\dot{\theta}^* + \Delta)$$

$$= \tfrac{1}{2}\dot{\theta}^{*T}\boldsymbol{M}\dot{\theta}^* + \tfrac{1}{2}\Delta^T\boldsymbol{M}\Delta + \dot{\theta}^{*T}\boldsymbol{M}\Delta \tag{C-2}$$

Considering the dynamics constraint in the state space region before penetrating the switching surface (S_0 or S_2), we have the following relationship

$$\Delta_2 = f(\Delta_1) = -\Delta_1 - g(\Delta_1) \tag{C-3}$$

where the function $g(\Delta_1)$ represents the angular velocity variation of the swing leg with respect to the angular velocity variation Δ_1 of the stance leg in a bipedal walking robot. In this case where the control law described in Chapter 7 is applied,

$$\Delta_2 \cong -2\Delta_1 \tag{C-4}$$

Then substituting (C-4) into (C-2), we get

$$E - E^* = \tfrac{1}{2}\Delta^T\boldsymbol{M}\Delta + \dot{\theta}^{*T}\boldsymbol{M}\Delta \tag{C-5}$$

$$E - E^* = \tfrac{1}{2}(\alpha\Delta_1^2 + \tfrac{1}{2}\beta\Delta_2^2 + \beta\Delta_1\Delta_2 + \Delta_1(\alpha\dot{\theta}_1^* + \beta\dot{\theta}_2^*) + \Delta_2\beta(\dot{\theta}_1^* + \dot{\theta}_2^*) \qquad \text{(C-6)}$$

Noticing that $\dot{\theta}_2^* = -2\dot{\theta}_1^*$ with the given control law, we can combine (C-4) and (C-6) and get

$$E - E^* = \tfrac{1}{2}\alpha\Delta_1^2 + \Delta_1\alpha\dot{\theta}_1^* = \Delta_1\alpha(\tfrac{1}{2}\Delta_1 + \dot{\theta}_1^*) \qquad \text{(C-7)}$$

When $E - E^* \to 0$, since $(\tfrac{1}{2}\Delta_1 + \dot{\theta}_1^*) \neq 0$, we get $\Delta_1 \to 0$. Then from (C-4), we know $\Delta \to 0$ as $E - E^* \to 0$.

References

Alexander, R.M. (1990), Three uses for springs in legged locomotion, *International Journal of Robotics Research*, Vol.9, No.2.

Astrom, K.J. (1995), Oscillations in Systems with relay Feedback. *The IMA Volumes in Mathematics and Its Applications: Adaptive Control, Filtering, and Signal Processing*, 74-: 1-25.

Bay, J.S. and Hemami, H. (1987), Modeling of a Neural Pattern Generator with Coupled Nonlinear Oscillators, *IEEE Transaction on Biomedical Engineering*, Vol. BME-34, No.4.

Benbrahim, H. and Franklin, J.A. (1997), Bipedal Dynamic Walking Using Reinforcement Learning, *International Journal of Robotics and Autonomous Systems*, 22 (283-302).

Chew, C.M. (2000), *Dynamic Bipedal walking Assisted by Learning*, Ph.D. Thesis of Mechanical Engineering, MIT, Cambridge, MA.

Dahleh, M. (1996), Dynamic Systems and Control, Lecture notes of MIT EECS Course 6.241.

Dunn, E. and Howe, R. (1996), Foot placement and velocity control in smooth bipedal walking, *IEEE International Conference on Robotics and Automation*, Minneapolis.

Furusho, J. and Masubuchi, M. (1987), A theoretically motivated reduced order model for the control of dynamic biped locomotion, *ASME Journal of Dynamic Systems, Measurement, and Control*, 109, 155-163.

Golliday, C.L. and Hemami, H. (1977), An approach to analyzing biped locomotion dynamics and designing robot locomotion control, *IEEE Trans. on Automatic Control*, AC-22-6, 963-972.

Gonçalves, J.M. (1999), *Analysis of Switching Systems*, Ph.D. Thesis Proposal of Electrical Engineering & Computer Science Dept., MIT, Cambridge, MA.

Gonçalves, J.M., Megretski, A. and Dahleh, M. (2000a), Global Stability of Relay Feedback Systems, *American Control Conference*.

Gonçalves, J.M. (2000b), Surface Lyapunov Functions in Global Stability Analysis of Saturation Systems, *IEEE International Conference on Decisions and Control.*

Gonçalves, J.M. (2000c), Global Stability Analysis of On/Off Systems, *IEEE International Conference on Decisions and Control.*

Goswami, A., Espiau, B. and Keramane, A. (1996), Limit Cycles and Their Stability in a Passive Biped Gait, *IEEE International Conference on Robotics & Automation,* Minneapolis, Minnesota.

Grillner, S. (1976), Some Aspects on the Descending Control of the Spinal Circuits Generating Locomotor Movements, in Herman, R.N., Grillner, S., Stein, P.S. & Stuart, D.G. eds. *'Neural Control of Locomotion'*, Plenum Press, New York, NY.

Grillner, S. (1985), Neurobiological bases of rhythmic motor acts in vertebrates, *Science* 228: 143-149.

Grinllner, S., Stein, P.S.G., Stuart, D.G., Forssberg, H. and Herman, R.M. (1986), *Neurobiology of Vertebrate Locomotion,* McMillan Press Ltd..

Guckenheimer, J. and Holmes, P. (1983), *Nonlinear Oscillations, Dynamical Systems, and Bifurcations of Vector Fields,* Spring-Verlag.

Hayashi, C. (1985), *Nonlinear Oscillations in Physical Systems,* Princeton University Press, Princeton, New Jersey, USA.

Hirai, K., Hirose, M., Haikawa, Y., and Takenaka, T.(1998), The Development of Honda Humanoid Robot, *IEEE International Conference on Robotics & Automation,* Leuven, Belgium.

Hu, J., Pratt, J., Chew, C.M., Herr, H. and Pratt, G. (1998a), Adaptive Virtual Model Control of a Bipedal Walking Robot, *IEEE Symposium on Intelligence in Automation and Robotics,* Washington D.C.

Hu, J., Pratt, J. and Pratt, G. (1998b), Adaptive Dynamic Control of a Bipedal Walking Robot with Radial Basis Function Neural Networks, *IEEE International Conference on Intelligent Robots and Systems,* Victor, Canada.

Hu, J., Williamson, M. and Pratt, G. (1999a), Bipedal Locomotion Control with Rhythmic Neural Oscillators, *IEEE International Conference on Intelligent Robots and Systems,* Kyongju, Korea.

Hu, J. (1999b), Stable Control with Rhythmic Neural Oscillators, *Term Project Report for Course 6.243 -Theory for Nonlinear Systems,* EECS Dept., MIT, Cambridge, MA.

Hu, J., and Pratt, G. (2000), Stable Locomotion Control of a Bipedal Walking Robot by Means of Switching Control Theory, *Technical Report* No. LL00101, MIT Leg Lab..

Jalics, I., Hemami, H. and Zheng, Y.F. (1997), Pattern Generation Using Coupled Oscillators for Robotic and Biorobotic Adaptive Periodic Movement, *IEEE International Conference on Robotics and Automation,* Albuquerque, New Mexico.

Johansson, K.H., Rantzer, A. and Astrom, K.J. (1996), Fast Switches in relay Feedback Systems, *Automatica.*

Kajita, S. and Tani, K. (1995), Experimental Study of Bipedal Dynamic Walking in the Linear Inverted Pendulum Mode, *IEEE International Conference on Robotics and Automation.*

Katayama, O. and Kurematsu, Y. (1995), Theoretical Studies on Neuro Oscillator for Application of Biped Locomotion, *IEEE International Conference on Robotics and Automation.*

Katoh, R, and Mori, M. (1984), Control Method of Biped Locomotion Giving Asymptotic Stability of Trajectory, *Automatica,* Vol.20, No.4.

Khalil, H.K. (1996), Nonlinear Systems, Prentice Hall, Upper Saddle River, NJ 07458.

Kun, A.L. and Miller, W.T. (1996), Adaptive Dynamic Balance of a Biped Robot Using Neural Networks, *IEEE International Conference on Robotics and Automation,* Vol. 1, pp 240-245.

Kun, A.L. and Miller, W.T. (1999), Control of Variable-speed Gaits for a Biped Robot, *IEEE Robotics & Automation Magazine,* Vol. 6, No.3, pp19-29.

Kuo, A.D. (1999), Stabilization of Lateral Motion in Passive Dynamic Walking, *International Journal of Robotics Research,* Vol. 18, No.9, pp917-930.

Lewis, M.A. (1996), *Self-organization of Locomotory Controllers in Robots and Animals,* Ph.D. Thesis of Electrical Engineering, University of Southern California. Los Angles, CA, USA.

Li, Q., Takanish, A., and Kato, I. (1992), Learning Control of Compensative Trunk Motion for Biped Walking Robot Based on ZMP Stability Criterion, *IEEE/RSJ International Workshop on Intelligent Robots and Systems,* Raleigh, NC.

Matsuoka, K., (1985), Sustained Oscillators Generated by Mutually Inhibiting Neurons with Adaptation, *Biological Cybernetics,* 52: 367-376.

McGeer, T. (1990), Passive Dynamic Walking, *International Journal of Robotics Research,* Vol. 9, No.2.

McMahon, T.A., (1984), Mechanics of Locomotion, *International Journal of Robotics Research,* Vol. 3, No. 2.

Megretski, A. (1996), Global Stability of Oscillations Induced by a Relay Feedback, *IFAC World Congress,* Budapest, Hungary, E:49-54.

Menzel, P. and D'Aluisio, F. (2000), *Robo Sapiens: Evolution of a New Spieces*, MIT Press, Cambridge, MA, USA.

Miller, S. and Scott, P.D. (1977), The spinal locomotor generator, *Exp. Brain Res.* 30:387-403.

Miller, W.T. (1994), Real-time Neural Network Control of Bipedal Walking Robot, *IEEE Control System Magazine.*

Miura, H. and Shimoyama, I., (1984), Dynamic walk of a biped, *International Journal of Robotics Research,* Vol. 3, No. 2.

Miyakoshi, S., Taga, G., Kuniyoshi, Y. and Nagakubo, A. (1998), Three Dimensional Bipdeal Stepping Motion Using Neural Oscillators - Towards Humanoid Motion in the Real World, *IEEE/RJS International Conference on Intelligent Robots and Systems,* Victoria, BC, Canada.

Miyazaki, F., and Arimoto, S. (1980), A control theoretic study on dynamical biped locomotion, *ASME Journal of Dynamic Systems, Measurement, and Control,* Vol. 102, 223-239.

Miyazaki, F., and Arimoto, S. (1983), A hierarchical control for biped robots, *IEEE International Conference on Robotics and Automation,* 299-306.

Nicola, E. (1995), Lecture Notes for MIT EECS Course 6.243 -Nonlinear Systems, No.9.

Orlovdky, G.N., Deliagina, T.G. and Grinllner, S. (1999) *Neural Control of Locomotion: From Mollusc to Man,* Oxford University Press.

Ozawa, N., (1995), Locomotion Control System for Mobile Robot, United States Patent #5,402,050, Honda Motor Company.

Parseghian, A. (2000), *Control of a Simulated, Three-Dimensional Bipedal Robot to Initiate Walking, Continue Walking, Rock side-to-side, and Balance,* Master Degree Thesis of Electrical Engineering and Computer Science, MIT, Cambridge, MA.

Pettit, N.B. (1997), The Analysis of Piece-wise Linear Dynamical Systems, *Control Using Logic-Based Switching,* pp49-58.

Pratt, G., Matthew M.W., (1995), Series Elastic Actuators, *IEEE International Conference on Intelligent Robots and Systems,* Pittsburgh.

Pratt, J., Torres, A., Dilworth, P. and Pratt, G. (1996), Virtual Model Control, *IEEE International Conference on Intelligent Robots and Systems,* Osaka, Japan.

Pratt, J., Dilworth, P. and Pratt, G. (1997), Virtual Model Control of a Bipedal Walking Robot, *IEEE International Conference on Robotics and Automation*, Albuquerque, NM.

Pratt, J and Pratt G. (1998), Intuitive control of a planar biped walking robot, *IEEE International Conference on Robotics and Automation*, Belgium.

Pratt, J. and Pratt, G. (1999), Exploiting Natural Dynamics in the Control of a 3D Bipedal Walking Simulation, *International Conference on Climbing and Walking Robots (CLAWAR99)*, Portsmouth, UK.

Pratt, J. (2000), *Exploring Inherent Robustness and Natural Dynamics in the Control of Bipedal Walking Robots*, Ph.D. Thesis of Electrical Engineering and Computer Science, MIT, Cambridge, MA.

Raibert, M.H. (1986), *Legged Robots That Balance*, Cambridge, Mass: MIT Press.

Salatian, A.W. and Zheng, Y.F. (1992), Gait Synthesis for a Bipedal Robot Climbing Sloping Surface Using Neural Networks -II, Dynamic Learning, *IEEE International Conference on Robotics & Automation*, Nice, France.

Slotine, J.E. and Li, W. (1991) *Applied Nonlinear Control*, Englewood Cliffs, NJ: Prentice Hall.

Taga, G., Yamaguchi, Y. and Shimizu, H. (1991), Self-organized control of biped locomotion by neural oscillators in unpredictable environments, *Biological Cybernetics*, 65: 147-159.

Taga, G., (1995), A model of the Neuro-musculo-skeletal System for Human Locomotion: I. Emergence of Basic Gait, *Biological Cybernetics*, 73: 97-111.

Taga, G. (1998), A model of the neural musculo-skeletal system for anticipatory adjustment of human locomotion during obstacle avoidance, *Biological Cybernetics*, 78: 9-17.

Todd, D.J. (1985), *Walking Machines: An Introduction to Legged Robots*, Kogan Page Ltd., London.

Vakakis, A.F. and Burdick, J.W. (1990), Chaotic Motions in the Dynamics of a Hoping Robot, *IEEE International Conference on Robotics & Automation*, Vol. 3.

Van der Linde, R.Q. (1999), Passive Bipedal Walking with Phasic Muscle Contraction, *Biological Cybernetics*, 81, 227-237.

Vidyasagar, M. (1993), *Nonlinear Systems Analysis*, Prentice Hall, Englewood Cliffs, New Jersey, USA.

Vukobratovic, M. (1973), Legged locomotion robots: mathematical models, control

algorithms, and realizations, In 5th *IFAC Symposium on Automatic Control in Space*, Genoa.

Vukobratovic, M., Borovac, B., Surla, D. and Stokic, D. (1990), *Biped Locomotion: Dynamics, Stability, Control and Application*, Berlin-Heidelberg, Germany: Springer-Verlag.

Wang, D. (1995), Emergent Synchrony in Locally Coupled Neural Oscillators, *IEEE Transactions on Neural Networks*, Vol.6, No.4.

Wiener, N. (1948), *Cybernetics: Control and Communication in the Animal and the machine*, Technology Press, Cambridge, MA.

Williamson, M. (1998), Rhythmic Robot Control Using Oscillators, *IEEE International Conference on Intelligent Robots and Systems (IROS'98)*.

Williamson, M. (1999a), Designing Rhythmic Motion Using Neural Oscillators, *IEEE/RJS International Conference on Intelligent Robots and Systems*, Kyongju, Korea.

Williamson, M. (1999b), *Robot Arm Control Exploiting Natural Dynamics*, Ph.D. Thesis of Electrical Engineering and Computer Science, MIT, Cambridge, MA.

Winter, D.A., (1990), *Biomechanics and Motor Control of Human Movement*, John Wiley & Sons, Inc.

Yamaguchi, J., Soga, E., Inoue, S. and Takanish, A. (1999), Development of a Biped Humanoid Robot - Control Method of Whole Body Cooperative Dynamic Bipedal Walking, *IEEE International Conference on Robotics & Automation*, pp368-374.

Yuasa, H. Ito, M., (1990), Coordination of many oscillators and generation of locomotory patterns, *Biological Cybernetics*, 63: 177-184.

Zielinska, T. (1996), Coupled oscillators utilized as gait rhythmic generators of a two-legged walking machine, *Biological Cybernetics*: 74, 263-273.